



Submitted to: JHEP



CERN-EP-2023-174

13th October 2023

Search for direct production of electroweakinos in final states with one lepton, jets and missing transverse momentum in pp collisions at $\sqrt{s} = 13$ TeV with the ATLAS detector

The ATLAS Collaboration

Searches for electroweak production of chargino pairs, $\tilde{\chi}_1^+ \tilde{\chi}_1^-$, and of chargino and next-to-lightest neutralino, $\tilde{\chi}_1^\pm \tilde{\chi}_2^0$, are presented. The models explored assume that the charginos decay into a W boson and the lightest neutralino, $\tilde{\chi}_1^\pm \rightarrow W^\pm \tilde{\chi}_1^0$. The next-to-lightest neutralinos are degenerate in mass with the chargino and decay to $\tilde{\chi}_1^0$ and either a Z or a Higgs boson, $\tilde{\chi}_2^0 \rightarrow Z \tilde{\chi}_1^0$ or $h \tilde{\chi}_1^0$. The searches exploit the presence of a single isolated lepton and missing transverse momentum from the W boson decay products and the lightest neutralinos, and the presence of jets from hadronically decaying Z or W bosons or from the Higgs boson decaying into a pair of b -quarks. The searches use 139 fb^{-1} of $\sqrt{s} = 13$ TeV proton–proton collisions data collected by the ATLAS detector at the Large Hadron Collider between 2015 and 2018. No deviations from the Standard Model expectations are found, and 95% confidence level exclusion limits are set. Chargino masses ranging from 260 to 520 GeV are excluded for a massless $\tilde{\chi}_1^0$ in chargino pair production models. Degenerate chargino and next-to-lightest neutralino masses ranging from 260 to 420 GeV are excluded for a massless $\tilde{\chi}_1^0$ for $\tilde{\chi}_2^0 \rightarrow Z \tilde{\chi}_1^0$. For decays through an on-shell Higgs boson and for mass-splitting between $\tilde{\chi}_1^\pm / \tilde{\chi}_2^0$ and $\tilde{\chi}_1^0$ as small as the Higgs boson mass, mass limits are improved by up to 40 GeV in the range of 200–260 GeV and 280–470 GeV compared to previous ATLAS constraints.

1 Introduction

The Standard Model (SM) is a strongly predictive effective theory, however it is not able to explain some observed phenomena, such as the abundance of dark matter and its nature, the matter–antimatter asymmetry, and the hierarchy problem [1–4]. The ATLAS and CMS discovery of the SM Higgs boson [5–8] confirmed the mechanism of electroweak symmetry breaking and heightened attention on the hierarchy problem. Supersymmetric (SUSY) [9–14] extensions to the SM can solve the hierarchy problem by introducing a new symmetry that predicts bosonic (fermionic) partners for the fermions (bosons) of the SM. In an R -parity [15] conserving model, the SUSY particles are produced in pairs and the lightest SUSY particle (LSP) is a viable dark-matter candidate [16, 17], as it is stable and weakly interacting.

The SUSY partners of the Higgs bosons and the SM electroweak gauge bosons, collectively called electroweakinos, are the higgsinos, winos (partners of the $SU(2)_L$ gauge fields), and bino (partner of the $U(1)$ gauge field). The electroweakino mass eigenstates are referred to as charginos $\tilde{\chi}_i^\pm$ ($i = 1, 2$), linear combinations of higgsino and wino fields, and neutralinos $\tilde{\chi}_j^0$ ($j = 1, 2, 3, 4$), linear combinations of higgsino, wino and bino fields. These are ordered in increasing value of their masses.

Natural SUSY scenarios [18, 19] predict that the lightest electroweakino mass be close to the electroweak scale. Squarks and sleptons (partners of the quarks and leptons) are heavier than a few TeV and hence decoupled since they cannot be produced at the Large Hadron Collider (LHC). The dominant SUSY production mechanism at the LHC may be the direct production of electroweakinos. SUSY models with light electroweakinos can also explain the observed discrepancy in the $g - 2$ measurement compared to the SM predictions [20, 21]. In the models considered in this paper, the compositions of the lightest chargino ($\tilde{\chi}_1^\pm$) and next-to-lightest neutralino ($\tilde{\chi}_2^0$) are wino-like and the two particles are nearly mass degenerate, while the lightest neutralino ($\tilde{\chi}_1^0$) is assumed to be a bino-like particle and the LSP. Two different SUSY processes are targeted in this paper: $\tilde{\chi}_1^+ \tilde{\chi}_1^-$ and $\tilde{\chi}_1^\pm \tilde{\chi}_2^0$ pair production.

Three searches performed by the ATLAS Collaboration for the direct production of electroweakinos in proton–proton (pp) collisions produced at the LHC at $\sqrt{s} = 13$ TeV are presented. The first analysis is designed to be sensitive to the direct pair-production of two charginos, referred to as the C1C1-WW model, where the charginos decay via $\tilde{\chi}_1^\pm \rightarrow W^\pm \tilde{\chi}_1^0$; the other two analyses are designed to be sensitive to the associated production of nearly mass-degenerate charginos and next-to-lightest neutralinos, latter decaying into the $\tilde{\chi}_1^0$ and either a Z boson ($\tilde{\chi}_2^0 \rightarrow Z \tilde{\chi}_1^0$) or a SM-like Higgs boson ($\tilde{\chi}_2^0 \rightarrow h \tilde{\chi}_1^0$) [22–24], referred to as the C1N2-WZ and C1N2-Wh models, respectively.

The target signature, in all scenarios, is a single isolated light lepton (electron or muon) produced by one of the W decays, or by τ -leptons produced in W decays, and missing transverse momentum ($\mathbf{p}_T^{\text{miss}}$) from LSPs and neutrinos. In the C1C1-WW and C1N2-WZ scenarios, due to the large momentum carried by the intermediate bosons, the jets are expected to be semi-boosted, or fully boosted. Thus up to three jets are required for these two models, which are produced by the hadronic decay of either a W (in the $\tilde{\chi}_1^+ \tilde{\chi}_1^-$ case) or a Z (in the $\tilde{\chi}_1^\pm \tilde{\chi}_2^0$ case), and the hadronic radiation. In the C1N2-Wh model, the Higgs boson candidates are identified through their decay into a pair of b -quarks ($h \rightarrow b\bar{b}$) and two jets originating from the fragmentation of b -quarks, called b -jets, are required. A set of simplified SUSY models [25, 26] is used to optimise the search and interpret the results. In these models the branching ratios of $\tilde{\chi}_1^\pm \rightarrow W \tilde{\chi}_1^0$ and $\tilde{\chi}_2^0 \rightarrow Z \tilde{\chi}_1^0$ or $\tilde{\chi}_2^0 \rightarrow h \tilde{\chi}_1^0$ are assumed to be 100%. The branching ratios of W , Z and Higgs bosons follow the SM predictions. Feynman diagrams of the processes under consideration are shown in Figure 1.

Previous searches for electroweakino production at the LHC targeting WW , WZ and intermediate states, and different lepton multiplicity in the final states, have been reported by the ATLAS [27–31] and CMS [32–34]

collaborations. This analysis is the first ATLAS search targeting final states with exactly one lepton, and profiting from the use of jet-substructure information for W and Z boson identification in large- R jets to target boosted regimes. The kinematic configurations where the decay products are boosted provide a handle to reduce the background. In the case of decays via Wh , stringent constraints have been set by the ATLAS [35] and CMS [36] collaborations exploiting the $h \rightarrow b\bar{b}$ decay mode and multiple decay modes of the Higgs boson, respectively. This analysis targets final states with mass-splitting between the chargino and the LSP, $\Delta m(\tilde{\chi}_1^\pm, \tilde{\chi}_1^0)$, between m_h and around 250 GeV, exploiting the $h \rightarrow b\bar{b}$ decay mode and the usage of dedicated boosted decision tree (BDT) discriminants. The BDT-based approach improves the sensitivity in the complex compressed phase-space where cut-and-count analyses suffer due to the similar kinematics of signal and SM backgrounds, especially from $t\bar{t}$ and Wt events.

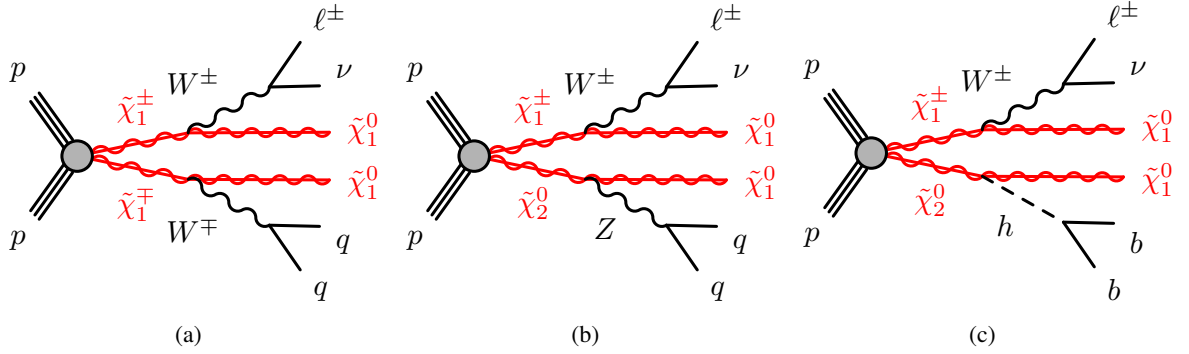


Figure 1: Feynman Diagrams for (a) electroweakino $\tilde{\chi}_1^+\tilde{\chi}_1^-$ and (b, c) $\tilde{\chi}_1^+\tilde{\chi}_2^0$ pair-production. One $\tilde{\chi}_1^\pm$ decays into a $\tilde{\chi}_1^0$ and a W boson that further decays leptonically. The other $\tilde{\chi}_1^\pm$ decays into a $\tilde{\chi}_1^0$ and a W boson that further decays hadronically (a). The $\tilde{\chi}_2^0$ decays into a $\tilde{\chi}_1^0$ and either a Z boson that further decays hadronically (b), or into a Higgs boson decaying into a pair of b -quarks (c).

2 ATLAS detector

The ATLAS detector [37] at the LHC covers nearly the entire solid angle around the collision point.¹ It consists of an inner tracking detector surrounded by a thin superconducting solenoid, electromagnetic and hadron calorimeters, and a muon spectrometer incorporating three large superconducting air-core toroidal magnets.

The inner-detector system (ID) is immersed in a 2 T axial magnetic field and provides charged-particle tracking in the range $|\eta| < 2.5$. The high-granularity silicon pixel detector covers the vertex region and typically provides four measurements per track, the first hit normally being in the insertable B-layer (IBL) installed before Run 2 [38, 39]. It is followed by the silicon microstrip tracker (SCT), which usually provides eight measurements per track. These silicon detectors are complemented by the transition radiation tracker (TRT), which enables radially extended track reconstruction up to $|\eta| = 2.0$. The TRT also provides

¹ ATLAS uses a right-handed coordinate system with its origin at the nominal interaction point in the centre of the detector. The positive x -axis is defined by the direction from the interaction point to the centre of the LHC ring, with the positive y -axis pointing upwards, while the beam direction defines the z -axis. Cylindrical coordinates (r, ϕ) are used in the transverse plane, ϕ being the azimuthal angle around the z -axis. The pseudorapidity η is defined in terms of the polar angle θ by $\eta = -\ln \tan(\theta/2)$. Rapidity is defined as $y = 0.5 \ln[(E + p_z)/(E - p_z)]$ where E denotes the energy and p_z is the component of the momentum along the beam direction. The angular distance ΔR is defined as $\sqrt{(\Delta\eta)^2 + (\Delta\phi)^2}$.

electron identification information based on the fraction of hits (typically 30 in total) above a higher energy-deposit threshold corresponding to transition radiation.

The calorimeter system covers the pseudorapidity range $|\eta| < 4.9$. Within the region $|\eta| < 3.2$, electromagnetic calorimetry is provided by barrel and endcap high-granularity lead/liquid-argon (LAr) calorimeters, with an additional thin LAr presampler covering $|\eta| < 1.8$ to correct for energy loss in material upstream of the calorimeters. Hadron calorimetry is provided by the steel/scintillator-tile calorimeter, segmented into three barrel structures within $|\eta| < 1.7$, and two copper/LAr hadron endcap calorimeters. The solid angle coverage is completed with forward copper/LAr and tungsten/LAr calorimeter modules optimised for electromagnetic and hadronic energy measurements respectively.

The muon spectrometer (MS) comprises separate trigger and high-precision tracking chambers measuring the deflection of muons in a magnetic field generated by the superconducting air-core toroidal magnets. The field integral of the toroids ranges between 2.0 and 6.0 T m across most of the detector. Three layers of precision chambers, each consisting of layers of monitored drift tubes, cover the region $|\eta| < 2.7$, complemented by cathode-strip chambers in the forward region, where the background is highest. The muon trigger system covers the range $|\eta| < 2.4$ with resistive-plate chambers in the barrel, and thin-gap chambers in the endcap regions.

Interesting events are selected by the first-level trigger system implemented in custom hardware, followed by selections made by algorithms implemented in software in the high-level trigger [40]. The first-level trigger accepts events from the 40 MHz bunch crossings at a rate below 100 kHz, which the high-level trigger further reduces in order to record events to disk at about 1 kHz.

An extensive software suite [41] is used in data simulation, in the reconstruction and analysis of real and simulated data, in detector operations, and in the trigger and data acquisition systems of the experiment.

3 Data and simulated events

The analyses presented in this paper use 139 fb^{-1} of pp collision data provided by the LHC and collected between 2015 and 2018 by the ATLAS detector, at a centre-of-mass energy of 13 TeV and with an interval of 25 ns between consecutive crossings of proton bunches. The average number of interactions per bunch crossing (pile-up) was $\langle \mu \rangle = 20$ in 2015–2016, $\langle \mu \rangle = 38$ in 2017 and $\langle \mu \rangle = 37$ in 2018. The uncertainty in the combined 2015–2018 integrated luminosity is 1.7% [42], obtained using the LUCID-2 detector [43] for the primary luminosity measurements.

Signal selection efficiencies and SM backgrounds are evaluated using Monte Carlo (MC) simulated event samples. The signal Monte Carlo samples were processed with a complete simulation of the response of the detector provided by GEANT 4 [44], or fast simulation [45] which relies on a parameterisation of the calorimeter response [46]. A varying number of inelastic pp interactions was overlaid on the hard-scattering event for all simulated events to model the multiple proton–proton interactions in the same and nearby bunch crossings. The pile-up events were generated with PYTHIA 8.186 [47] using the NNPDF2.3LO parton distribution function (PDF) set [48] and the A3 set of tuned parameters (tune) [49]. The simulated events were processed with the same trigger, reconstruction and identification algorithms used for data. Dedicated correction factors are applied to simulation to account for differences between data and MC simulated events.

The simulated backgrounds considered in the analyses are: $t\bar{t}$ pair production; single-top production (s -channel, t -channel, and associated Wt production); W/Z +jets production; $t\bar{t}$ production with an electroweak boson ($t\bar{t} + V$); Higgs boson production ($t\bar{t} + h$, Vh); diboson (WW , WZ , ZZ) and multiboson (VVV where $V = W, Z$) production. The simulated ggF and VBF Higgs samples are not used as these processes are taken into account in the diboson samples. A further overlap removal is applied to avoid double counting between Vh and diboson samples. Different MC event generators were used depending on the simulated processes. All simulated background processes were normalised to the best available theoretical calculation of their respective cross-sections. The samples for W and Z boson production associated with jets (W/Z +jets) were simulated using SHERPA. The modelling includes up to two partons at next-to-leading order (NLO), normalised to next-to-next-to-leading order (NNLO) for the inclusive cross-section, and five partons at leading order (LO) using Comix [50] and OpenLoops [51, 52] and merged with the SHERPA parton shower [53] according to the ME+PS@NLO prescription [54–57] using the set of tuned parameters developed by the SHERPA authors. SHERPA 2.2.1 is used in the C1N2-Wh analysis and SHERPA 2.2.11 is used in the C1N2-WZ and C1C1-WW analyses. The event generators, the parton shower and hadronisation routines, and the underlying-event parameter tunes and PDF sets used in simulating the SM background processes, along with the accuracy of the theoretical cross-sections, are all summarised in Table 1.

For all MC samples showered with PYTHIA, the EvtGen v1.2.0 [58] program was used to simulate the properties of the bottom- and charm-hadron decays. Systematic uncertainties associated with the different background-specific configurations of the MC generators are estimated by using MC samples produced without detector simulation. The uncertainties include variations of the renormalisation and factorisation scales, the CKKW-L [59] matching scale, and different PDF sets and fragmentation/hadronisation models. A detailed discussion of the uncertainties related to the MC modelling is presented in Section 7.

The SUSY signal samples were simulated using MADGRAPH5_aMC@NLO v2.6.2 [60] and PYTHIA 8.230 with the A14 [61] set of tuned parameters for the modelling of the parton showering (PS), hadronisation and underlying event. The matrix element (ME) calculation was performed at tree level and includes the emission of up to two additional partons. The ME–PS matching was performed using the CKKW-L prescription, with a matching scale set to one quarter of the chargino and next-to-lightest neutralino mass. The NNPDF2.3LO [48] PDF set was used.

Signal cross-sections are calculated at NLO accuracy in the strong coupling constant, adding the resummation of soft gluon emission at next-to-leading-logarithmic accuracy (NLO+NLL) [62–65]. The nominal cross-section and its uncertainty are taken as the midpoint and half-width of an envelope of cross-section predictions using different PDF sets and factorisation and renormalisation scales, as described in Ref. [66]. The simplified models considered for electroweakinos production rely on two parameters: for $\tilde{\chi}_1^+ \tilde{\chi}_1^-$, they are the masses of the $\tilde{\chi}_1^\pm$ and the $\tilde{\chi}_1^0$; for $\tilde{\chi}_1^\pm \tilde{\chi}_2^0$, they are the masses of $\tilde{\chi}_1^\pm / \tilde{\chi}_2^0$ (considered to be degenerate) and $\tilde{\chi}_1^0$. They also depend on the branching ratio \mathcal{B} of the SUSY particles decays: $\tilde{\chi}_1^+$ decays into $W\tilde{\chi}_1^0$ with $\mathcal{B} = 100\%$ whilst two separate sets of signal samples were produced for the $\tilde{\chi}_1^\pm \tilde{\chi}_2^0$ process, with $\tilde{\chi}_2^0$ decaying into a $\tilde{\chi}_1^0$ and either a Z boson or a Higgs boson. In each case, a 100% branching ratio was assumed for the $\tilde{\chi}_2^0$ decay. The production cross-section of the process $\tilde{\chi}_1^+ \tilde{\chi}_1^-$ ($\tilde{\chi}_1^\pm \tilde{\chi}_2^0$) decreases from 903 fb (1807 fb) to 0.62 fb (1.34 fb) with increasing $m(\tilde{\chi}_1^\pm / \tilde{\chi}_2^0)$ from 200 to 1000 GeV.

4 Event reconstruction

Events are selected if they have at least one reconstructed vertex with two or more associated tracks each with the transverse momentum $p_T > 500$ MeV. If multiple vertices are associated with an event the primary

Table 1: Simulated background MC samples used in this analysis with the corresponding matrix element and parton shower generators, underlying-event tune, PDF set, and cross-section order in α_s .

Process	Generator	Parton shower and hadronisation	Tune	PDF	Cross-section
$t\bar{t}$	POWHEG BOX v2 [67–70]	PYTHIA 8.230 [47]	A14 [61]	NNPDF2.3LO [48]	NNLO+NNLL [71]
Single top	POWHEG BOX v2 [72–74]	PYTHIA 8.230	A14	NNPDF2.3LO	NLO+NNLL [75]
W/Z +jets	SHERPA 2.2.1 & 2.2.11 [76]	SHERPA 2.2.1 & 2.2.11	SHERPA standard	NNPDF3.0NNLO	NNLO [77]
Diboson	SHERPA 2.2.1 [76] & 2.2.2	SHERPA 2.2.1 & 2.2.2	SHERPA standard	NNPDF3.0NNLO	NLO [77]
Multiboson	SHERPA 2.2.1 & 2.2.2	SHERPA 2.2.1 & 2.2.2	SHERPA standard	NNPDF3.0NNLO	NLO [77]
$t\bar{t} + V$	MADGRAPH5_aMC@NLO v2.3.3	PYTHIA 8.210	A14	NNPDF2.3LO	NLO [78]
$t\bar{t} + h$	POWHEG BOX v2	PYTHIA 8.230	AZNLO [79]	CTEQ6L1 [80]	NLO [81]
Vh	POWHEG BOX v2	PYTHIA 8.212	A14	NNPDF2.3LO	NLO [81]

vertex (PV) is defined as the one with the highest scalar sum of the squared transverse momenta of the associated tracks [82]. A set of baseline quality criteria are applied to reject events with non-collision backgrounds or detector noise [83].

Candidate jets and leptons have two levels of classification: ‘baseline’ and ‘signal’. Baseline objects have a lower purity but higher acceptance and are used for the computation of the missing transverse momentum and solving possible reconstruction ambiguities. Signal objects are a subset of baseline objects and are used in the definition of the regions of interest of the searches.

All electron candidates are reconstructed from energy deposits in the electromagnetic calorimeter that are matched to charged-particle tracks in the ID [84]. Baseline electron candidates are required to have $p_T > 7$ GeV and $|\eta| < 2.47$, excluding the transition region between the barrel and endcap calorimeters ($1.3 < |\eta| < 1.52$), and satisfy the identification requirements of the ‘loose’ operating point provided by a likelihood-based algorithm, described in Ref. [84]. The longitudinal impact parameter z_0 relative to the PV is required to satisfy $|z_0 \sin \theta| < 0.5$ mm. Discrimination between electrons and converted photons is achieved by observing the number of hits in the innermost pixel layer. Signal electrons are required to satisfy stricter identification criteria: they are required to satisfy a ‘tight’ likelihood operating point selection and the significance of the transverse impact parameter d_0 must satisfy $|d_0/\sigma(d_0)| < 5$. Signal electron candidates are further refined using a multivariate likelihood discriminant, in order to discriminate against electron candidates coming from hadronic jets, photon conversions and heavy-flavor hadron decays. Electron candidates with $p_T < 75$ GeV use a looser selection on the likelihood output value (*PLVLoose* working point), otherwise the candidates are required to satisfy more stringent selection (*PLVTight* isolation working point), an analogue procedure has been used in Ref. [85].

Muon candidates are reconstructed from matching tracks in the ID and muon spectrometer, refined through a global fit that uses the hits from both subdetectors [86]. Baseline muon candidates are required to have $p_T > 6$ GeV and $|\eta| < 2.7$, z_0 is required to satisfy $|z_0 \sin \theta| < 0.5$ mm and the ‘medium’ identification criteria. Signal muon candidates are required to satisfy stricter requirements on pseudorapidity and impact parameter, $|\eta| < 2.5$ and $|d_0/\sigma(d_0)| < 3$. Signal muon candidates are required to satisfy the *PLVLoose* isolation working point if they have $p_T < 75$ GeV, and the *PflowTightVarRad* isolation working point otherwise [87]. Finally a veto is applied on signal muons to reject events with a poorly measured charge-to-momentum ratio $\frac{\sigma(q/p)}{(q/p)} > 0.4$.

Jets are reconstructed from three-dimensional topological energy clusters [88] in the calorimeters using the anti- k_t algorithm with a radius parameter $R = 0.4$ [89]. Baseline jet candidates are required to have $|\eta| < 4.5$ and $p_T > 20$ GeV. Signal jets are required to have $|\eta| < 2.8$ and $p_T > 30$ GeV. To suppress jets

from pile-up interactions, signal jet candidates with $|\eta| < 2.4$ and $p_T < 60$ GeV are required to be matched to the PV through the jet vertex tagger (JVT), a tagging algorithm that identifies jets originating from the PV using track information [90, 91], using the *tight* working point. Additionally, jets are calibrated following the criteria in Ref. [92], which, among other things, includes corrections to the jet energy and resolution.

To exploit the high p_T phase space, large-R jets are used for the C1C1-WW and C1N2-WZ models to reconstruct highly boosted W and Z bosons by utilising the substructure of collimated objects. Large-R jets are reconstructed with the same algorithm (anti- k_r) as standard jets, but with a large radius parameter of $R = 1.0$. To reduce the pile-up contributions to the large-R jets, a jet trimming algorithm [93] is employed, with the R_{sub} and f_{cut} parameters set to 0.2 and 0.05, respectively, to refine the jet reconstruction, removing low p_T radiation and allowing the parton sub-jets inside the large-R jets to be identified. Large-R jets with $p_T > 200$ GeV and $|\eta| < 2.0$ are calibrated using ATLAS prescriptions [94], and are identified as possible W or Z candidates using dedicated taggers designed to identify W and Z bosons at 50% tagging efficiency [95, 96].

Jets originating from the hadronisation of a b -quark are identified (b -tagged) via a multivariate algorithm that combines information from the impact parameters of displaced tracks and topological properties of secondary and tertiary decay vertices reconstructed within the jet. The b -tagging relies on the *DL1r* tagger [97]. The full distribution of the tagger score is used in a procedure referred to as pseudo-continuous b -tagging, allowing a more fine-grained calibration of the b -tagged jets. The score is divided into five bins defined by fixed b -tagging efficiency working points and the distribution edge points (interpreted as the working points at 100% and 0% efficiency). The b -tagged jets are defined using a working point providing a 77% efficiency for b -hadron identification in $t\bar{t}$ simulated events. The variable quantifying the likelihood of a jet to be b -tagged (b -*quantile*) according to the pseudo-continuous b -tagging procedure is used in the analysis targeting the C1N2-Wh model.

To resolve the reconstruction ambiguities between electrons, muons, and jets, an overlap removal procedure is applied to baseline objects. First, any electron sharing the same ID track with a muon is rejected. If it shares the same ID track with another electron, the one with lower p_T is discarded. Next, jets are rejected if they lie within $\Delta R = 0.2$ of a muon or if the muon is matched to the jet through ghost association [98]. Subsequently, electrons within a cone of size $\Delta R = \min(0.4, 0.04 + 10 \text{ GeV} / p_T)$ around a jet are removed. Lastly, muons within a cone, defined in the same way as for electrons, around any remaining jet are removed.

The missing transverse momentum $\mathbf{p}_T^{\text{miss}}$, and its magnitude E_T^{miss} , are reconstructed by using the set of reconstructed and fully calibrated baseline objects, i.e., electrons, muons, photons and jets described above. Baseline photons [99] are defined as those that satisfy $p_T > 25$ GeV, $|\eta| < 2.37$, and the *tight* identification criteria. The determination of the missing transverse momentum also includes a soft term consisting of tracks that are not associated with any reconstructed object. In the searches described here, the *tight* working point is used for the missing transverse momentum [100, 101].

5 Analysis strategy and event selection

Three sets of signal regions (SRs) are defined in the analyses, with each set targeting one of the three models considered for electroweakinos production and decay. All event selections defined for these regions require that the events were recorded with single lepton (electron and muon) triggers [102, 103]. The offline

lepton p_T thresholds are set to ensure that the selected events are in the plateau region of the corresponding trigger efficiency distribution. The offline trigger p_T threshold values increased over the years due to the increase in luminosity, going from 25 (21) GeV to 27 (27.3) GeV for electron (muon) events.

Signal signatures have one leptonically decaying W boson, one hadronically decaying W or Z boson or a Higgs boson decaying into b -quarks, and missing transverse momentum due to the $\tilde{\chi}_1^0$ and neutrinos escaping detection. Hence events are required to have exactly one signal electron or muon, one to three (two to three) signal jets, allowing for an additional jet from initial- or final-state radiation and large (moderate) E_T^{miss} , for the C1C1-WW and C1N2-WZ (C1N2-Wh) scenarios.

A main feature of this analysis is that in the C1C1-WW and C1N2-WZ cases all events are additionally required to contain at least one large-R jet. This complements previous results [27] and allows boosted W or Z boson decays to be probed. Different boson tagging schemes are employed for different signal scenarios: W tagging is applied for the $\tilde{\chi}_1^+ \tilde{\chi}_1^-$ scenario, while Z tagging is applied for the $\tilde{\chi}_1^\pm \tilde{\chi}_2^0$ scenario. On the other hand, final states with small mass-splitting between the chargino and the LSP (still above the Higgs boson mass) are targeted in the case of the C1N2-Wh models. This complements the analysis presented in Ref. [35], optimised for large mass-splittings and small LSP masses. No significant boost is expected for the Higgs boson, and two b -tagged jets are required to identify the Higgs boson candidate. A BDT, described in the following, is used as the final discriminant.

The SRs for the three analyses are defined through selections that suppress background contributions and maximize the sensitivity to signal. The numbers of residual SM events are then estimated with the aid of MC simulated samples and using a profile likelihood fit [104] as detailed in Section 6. Normalisation factors of the MC samples corresponding to the SM processes expected to contribute the most to the event yields in the SRs are left free to float. A set of control regions (CR), specific for each analysis, are designed to aid in the SM backgrounds evaluation. The likelihood (one for each analysis) is finally built as the product of Poissonian terms for each CR and, when assessing the discovery (model-independent) or exclusion (model-dependent) sensitivity to new physics model, SR.

A set of kinematic variables is built from the physics objects introduced in the previous section and used to define the event selection for the SRs and CRs. They are described in the following.

- The transverse mass, m_T , is defined from the lepton transverse momentum \mathbf{p}_T^ℓ and the missing transverse momentum $\mathbf{p}_T^{\text{miss}}$ as

$$m_T = \sqrt{2p_T^\ell E_T^{\text{miss}} (1 - \cos[\Delta\phi(\mathbf{p}_T^\ell, \mathbf{p}_T^{\text{miss}})])},$$

where $\Delta\phi(\mathbf{p}_T^\ell, \mathbf{p}_T^{\text{miss}})$ is the azimuthal angle between \mathbf{p}_T^ℓ and $\mathbf{p}_T^{\text{miss}}$. For W +jets and semileptonic $t\bar{t}$ events in which one on-shell W boson decays leptonically, this observable has an upper endpoint at the W boson mass, while for signal events the m_T distribution extends significantly above m_W . A requirement is placed on the upper value of $\Delta\phi(\mathbf{p}_T^\ell, \mathbf{p}_T^{\text{miss}})$ for the analysis targeting the C1C1-WW and C1N2-WZ models to reject background with a high momentum lepton and soft jets, where the angle between lepton and $\mathbf{p}_T^{\text{miss}}$ can be large in ϕ .

- The missing transverse energy significance, $\sigma_{E_T^{\text{miss}}}$ [105], is defined as the log-likelihood (\mathcal{L}) ratio of measuring the total observed transverse momentum to the likelihood of the null hypothesis,

$$\sigma_{E_T^{\text{miss}}} = \sqrt{2 \ln \left[\frac{\max_{\mathbf{p}_T^{\text{inv}} \neq 0} \mathcal{L}(E_T^{\text{miss}} | \mathbf{p}_T^{\text{inv}})}{\max_{\mathbf{p}_T^{\text{inv}} = 0} \mathcal{L}(E_T^{\text{miss}} | \mathbf{p}_T^{\text{inv}})} \right]}. \quad (1)$$

A high value indicates that the measured E_T^{miss} value is not compatible with resolution effects alone and suggests that the event is more likely to contain objects escaping detection, which happens more in the signal events than the background events.

- Throughout the analyses, variables denoted by $m_{\alpha\beta}$ are invariant masses of particles α and β . In particular, the invariant mass of the two leading (highest p_T) jets, m_{jj} , is required to be in a range around the W or Z mass as signal events are expected to emit an on-shell W or Z boson and have a mass peak in the m_{jj} distribution. The invariant mass of the two jets with highest b -tag weight and consistent with being a b -jet, $m_{b\bar{b}}$, is required to be close to the Higgs boson mass for C1N2-Wh models. The invariant mass of the lepton and the jets with highest b -tag weight is denoted by $m_{\ell b_i}$, with $i = 1, 2$ and referring to the first, second leading b -jet, respectively. This observable provides good discrimination against $t\bar{t}$ and single-top background events.
- The effective mass, m_{eff} , is defined as the scalar sum of the lepton transverse momentum, the signal jets' transverse momenta, and the missing transverse momentum,

$$m_{\text{eff}} = p_T^\ell + \sum_{\text{jets}} p_T + E_T^{\text{miss}}. \quad (2)$$

In the design of SRs targeting exclusion sensitivity for the C1C1-WW and C1N2-WZ models, two m_{eff} regions are constructed to target low and high signal mass differences between the $\tilde{\chi}_1^\pm/\tilde{\chi}_2^0$ and the $\tilde{\chi}_1^0$.

- The am_{T2} [106] is referred to as the asymmetric transverse mass. The transverse mass, m_{T2} is a generalization of the transverse mass applied to signatures where pair-produced parent particles decay semi-invisibly. The am_{T2} is used if the parent particles decay with different (asymmetric) masses of the invisible particles. For the C1N2-Wh models, where the visible parts of the signal decay are the two b -jets and the lepton and the invisible parts are the neutralinos and the neutrino, am_{T2} is used as a discriminant to reject $t\bar{t}$ contributions. The jets are ordered by their b -tag weight as j_1 and j_2 , so that the am_{T2} is defined as:

$$am_{T2} = \min(m_{T2}(\ell + j_1, j_2), m_{T2}(\ell + j_2, j_1)), \quad (3)$$

where m_{T2} is defined as $\min[\max(m_T^2(p_\alpha, p), m_T^2(p_\beta, q))]$, with p_α either $p_\ell + p_{j_1}$ or $p_\ell + p_{j_2}$ and p_β either $p_{j_2} + p_\ell$ or $p_{j_1} + p_\ell$, as the momenta of the visible parts of the decay branches, and p and q are the possible transverse momenta of the invisible particles in the branches. The minimisation is conducted by selecting values for p and q such that their vector sum is equal to the missing transverse momentum.

- The variable m_{CT} [107], referred as contranverse mass, has similar properties to the transverse mass and is defined as:

$$m_{CT}^2 = (E_T(\alpha) + E_T(\beta))^2 - (p_T(\alpha) - p_T(\beta))^2, \quad (4)$$

where α and β are defined as above and $p_T(\alpha)$ and $p_T(\beta)$ are their transverse components. Similarly to am_{T2} , the m_{CT} variable is also used for the C1N2-Wh models to reject top-quark SM background contributions, since for signal, the two b -jets arise from the same particle (the Higgs boson), while for $t\bar{t}$ and single top-quark production they arise from two different particles.

SRs are then constructed through selections on these quantities or, for the C1N2-Wh models, using a BDT. Their definition follows two approaches: the exclusion SRs are designed for setting model-dependent exclusion limits (‘excl.’); the discovery SRs are constructed for model-independent limits and null-hypothesis tests (‘disc.’ for discovery). Once SRs are defined, the signal and background yield estimates are computed. The strategy is detailed in Section 6. The systematic uncertainties, fit and results are then discussed in the following sections.

5.1 C1C1-WW and C1N2-WZ SRs definition

An overview of the SR definitions targeting the C1C1-WW and C1N2-WZ models is provided in Table 2. The main difference between chargino–chargino and chargino–neutralino signal scenarios is the large-R jet boson-tagging type. Three separate classes of SRs are defined for each scenario, using m_T to target regions sensitive to the increasing mass differences between the $\tilde{\chi}_1^\pm$ (and its mass-degenerate $\tilde{\chi}_2^0$ wino partner) and the $\tilde{\chi}_1^0$. These regions are labelled as SRLM, SRMM and SRHM to indicate low (LM), medium (MM) and high (HM) mass differences, respectively. The requirements on m_T make the three regions mutually exclusive.

For both the C1C1-WW and C1N2-WZ models, each LM, MM and HM exclusion SR is further split into two m_{eff} bins, thus providing six exclusion SR bins in total per model for a simultaneous two-dimensional fit in m_T and m_{eff} . The multi-bin approach enhances the sensitivity to a range of SUSY scenarios with different properties. The missing transverse energy significance is optimized separately for low and high m_{eff} bins. In the low m_{eff} bin, the m_{jj} reconstructed from two resolved jets is required to be close to the mass of the W or Z boson. This is to improve the sensitivity in a semi-boosted regime where the large-R jet would catch most of the boson decay products but often two jets are resolved. The high m_{eff} bin is to target a fully boosted topology hence there is no additional mass constraint on the resolved jets. For the $\tilde{\chi}_1^\pm \tilde{\chi}_2^0$ model, the acceptance times efficiency is 0.37% in SRHM for a 600 GeV $\tilde{\chi}_1^\pm/\tilde{\chi}_2^0$ mass and massless $\tilde{\chi}_1^0$. For the $\tilde{\chi}_1^+ \tilde{\chi}_1^-$ model, the acceptance times efficiency is 0.31% in SRMM for a 600 GeV $\tilde{\chi}_1^\pm$ mass and massless $\tilde{\chi}_1^0$.

The discovery SRs are defined such that the various m_{eff} bins are merged for each of the three SRs per model, and selections on m_{jj} and $\sigma_{E_T^{\text{miss}}}$ are optimized for the best signal sensitivity at a benchmark point for each m_{eff} bin.

5.2 C1N2-Wh SR definition

The analysis targets scenarios characterised by $\Delta m(\tilde{\chi}_1^\pm, \tilde{\chi}_1^0)$ of at least m_h , where selections on individual variables are expected to be sub-optimal to separate the signal from SM production processes due to the similar kinematic properties of SUSY and SM background events. Consequently, a multivariate approach, where the discriminating power of multiple observables is exploited at once, is expected to increase the sensitivity. A BDT is implemented in the analysis by making use of the XGBoost (XGB) [108] framework. The training procedure uses events that satisfy an initial selection that requires exactly one signal lepton with $p_T > 27$ GeV, two to three jets with $p_T > 30$ GeV, exactly two b -tagged jets, $E_T^{\text{miss}} > 50$ GeV, $\sigma_{E_T^{\text{miss}}} > 5$ and $m_{b\bar{b}}$ in the range of 50–200 GeV. A set of object-based and event-based variables (30 in total) are used in the training. Object-based variables include the p_T , η and ϕ of the lepton and the jets, and the b -quantile of the jets. Event-based observables include $m_{b\bar{b}}$, am_{T2} , m_{CT} , m_T , $\sigma_{E_T^{\text{miss}}}$, $m_{\ell b_i, i=1,2}$ and radial distances between pairs of visible objects.

Table 2: Overview of the selection criteria for the exclusion SRs and the discovery SRs used in C1C1-WW and C1N2-WZ models. For exclusion SRs, they are further divided into two m_{eff} bins. The selection on m_{jj} and $\sigma_{E_{\text{T}}^{\text{miss}}}$ varies for low and high m_{eff} bins. For discovery SRs, one SR is defined per m_{T} region. The symbol ‘-’ indicates no additional requirement.

Variable	C1C1-WW model			C1N2-WZ model		
	SRLM	SRMM	SRHM	SRLM	SRMM	SRHM
$N_{\text{lep}} (p_{\text{T}} > 25 \text{ GeV})$	1					
$N_{\text{jet}} (p_{\text{T}} > 30 \text{ GeV})$	1–3					
$N_{\text{large-Rjet}} (p_{\text{T}} > 250 \text{ GeV})$	≥ 1					
$E_{\text{T}}^{\text{miss}} [\text{GeV}]$	> 200					
$\Delta\phi(\ell, E_{\text{T}}^{\text{miss}})$	< 2.6					
Large-R jet type	W tagged			Z tagged		
$m_{\text{T}} [\text{GeV}]$	120–200	200–300	> 300	120–200	200–300	> 300
Exclusion SR						
$m_{\text{eff}} [\text{GeV}]$ (excl.)	[600–850, > 850]			[600–850, > 850]		
$m_{\text{jj}} [\text{GeV}]$ (excl.)	[70–90, -]			[80–100, -]		
$\sigma_{E_{\text{T}}^{\text{miss}}} (\text{excl.})$	[> 12 , > 15]			[> 12 , > 12]		
Discovery SR						
$m_{\text{eff}} [\text{GeV}]$ (disc.)	> 600	> 600	> 850	> 600	> 850	> 850
$m_{\text{jj}} [\text{GeV}]$ (disc.)	-	-	-	80–100	-	-
$\sigma_{E_{\text{T}}^{\text{miss}}} (\text{disc.})$	> 15	> 15	> 15	> 12	> 12	> 12

Events are classified in five different categories: three corresponding to the main background processes ($t\bar{t}$, single-top and W +jets), one including all remaining minor background processes (Z +jets, diboson, rare processes), and one grouping together the signal samples in the region $m_h < \Delta m(\tilde{\chi}_1^\pm, \tilde{\chi}_1^0) < 200 \text{ GeV}$. The grouping of multiple signal samples increases the statistical power and is enabled by the similarity of the kinematic properties of the SUSY models of interest. A one-versus-rest multi-classification procedure was used, wherein each class is fitted against all the other classes producing output scores containing the predicted probability of an event being in that class. This method is more effective in discriminating the signal from the dominant backgrounds than using a binary signal versus background classifier. This also has the additional benefit of having background-processes classification scores that can be used to increase the purity of different backgrounds whilst building control and validation regions.

The output score w_{sig} denotes the signal class output score and is used in the definition of the SRs. The scores of the background classes are used in the definition of CRs and validation regions (VR). Tools to interpret the BDT learning process are used to identify the most relevant observables. The $m_{b\bar{b}}$ variable has the most predictive power for signal, as expected since it is used to identify the Higgs boson candidate. The m_{T} and the $am_{\text{T}2}$ are, on the other hand, the most predictive variables for W +jets and $t\bar{t}$ events, respectively.

The final selection for the analysis targeting the C1N2-Wh model requires $w_{\text{sig}} > 0.91$ (where the BDT score is defined between 0 and 1) and more stringent requirements on the invariant mass of the two b -tagged jets, $95 < m_{b\bar{b}} < 140 \text{ GeV}$, and on the missing transverse energy significance, $\sigma_{E_{\text{T}}^{\text{miss}}} > 8$. As an example, the acceptance times efficiency is around 0.1% for a 350 GeV $\tilde{\chi}_1^\pm/\tilde{\chi}_2^0$ mass and a 150 GeV $\tilde{\chi}_1^0$ mass. When

assessing the exclusion sensitivity for the signal-plus-background hypothesis, four w_{sig} bins are used in the likelihood fit: [0.91, 0.928), [0.928, 0.948), [0.948, 0.964), [0.964, 1], referred to as SRXGB Bin 1–4. Three discovery signal regions are defined, integrated over the signal score with increasing thresholds on it, namely [0.928,1], [0.948,1] and [0.964, 1].

6 Background estimation

Dominant SM background sources in the SRs depend on the analysis. For analyses targeting the C1C1-WW and C1N2-WZ models, W +jets and diboson production events constitute the main background (46%–73% and 16%–39%, respectively, depending on the SR). Subdominant SM background contributions originate from Z +jets, single-top, multiboson, $t\bar{t} + V$, $t\bar{t} + h$ and Vh . For the analysis targeting C1N2-Wh models, $t\bar{t}$ and single-top (almost exclusively Wt production) processes are dominant (about 30%–35% each across all bins), followed by W +jets (15%–20%). Remaining contributions originate from Z +jets, diboson, $t\bar{t} + V$ and Higgs boson production processes.

The main background contributions are estimated by using partially data-driven techniques through the set of CRs designed to be mutually exclusive and non-overlapping with the SRs (across and within the three analyses), and characterised by negligible expected signal contributions for the models of interest. The expected background yield in each SR is determined in the profile likelihood fit using the ‘background-only fit’ approach [104]. With this fit, the normalisation of the major backgrounds is adjusted to match the data in CRs with negligible signal contamination. A probability density function is defined for each CR. The inputs are the observed event yield and the predicted background yield from simulation, with Poisson statistical uncertainties and systematic uncertainties (detailed in Section 7) as nuisance parameters. The nuisance parameters are constrained by Gaussian distributions with widths corresponding to the sizes of the uncertainties. Systematic uncertainties account for bin-to-bin correlations, with normalisation and nuisance parameters correlated in all regions. The product of all the probability density functions forms the likelihood, which is maximised by adjusting the normalisation and nuisance parameters. The resulting normalisation factors are then used to correct the expected yields of the corresponding backgrounds in the various SRs. The extrapolation of the adjusted normalisation and nuisance parameters to the SRs is checked in VRs, which kinematically resemble the SRs but are expected to have low signal contamination, and do not overlap with either CRs or SRs.

6.1 C1C1-WW and C1N2-WZ Control and Validation regions

For the diboson background, single-lepton processes ($\ell\nu\nu\nu$) and dilepton processes ($\ell\ell\nu\nu$) contribute equally to the backgrounds in the signal regions. The $\ell\nu\nu\nu$ ($\ell\ell\nu\nu$) process is marked as diboson1l (diboson2l) in the following yield tables and kinematic figures. The diboson $\ell\ell\nu\nu$ entering in the SRs are events with two real leptons present in the decay chain, where one lepton fails the signal lepton requirement, or escapes detection. The $\ell\ell\nu\nu$ background is estimated and validated in the two-lepton control and validation regions. The crucial variable to enrich the diboson background contribution in the corresponding CR is the dilepton invariant mass, which is required to be consistent with the SM Z boson mass. Further selection criteria for $E_{\text{T}}^{\text{miss}}$, $\sigma_{E_{\text{T}}^{\text{miss}}}$, and $\Delta\phi(\mathbf{p}_{\text{T}}^{\ell}, \mathbf{p}_{\text{T}}^{\text{miss}})$ are defined similarly to the SRs, but with less stringent bounds, to enhance the number of events. An additional veto on the m_{jj} variable minimizes the potential overlap with a complementary chargino and neutralino search with two leptons and two jets in the final states performed by ATLAS [28], to allow future statistical combinations of different channels targeting the same SUSY

production processes. In addition to these selections, the control region DB2LCR requires m_T in the range of 50–200 GeV and the validation region DB2LVR requires m_T in the range of 200–350 GeV.

The single-lepton diboson process $\ell\nu\nu\nu$ has one lepton and missing energy in the final state, the kinematic behaviour of which is identical to W +jets background. A set of shared control and validation regions, the WDB1L regions, are designed for these two processes. The CR is defined with a selection similar to the SRs, but with m_T in the range of 50–80 GeV and with inverted $\sigma_{E_T^{\text{miss}}}$ requirements. A b -jet veto is applied to reduce heavy flavour contamination. Two sets of VRs are defined: the VR1 validates the extrapolation from the CR to the SRs in m_T , and the VR2 validates the extrapolation from the CR to the SRs in $\sigma_{E_T^{\text{miss}}}$ and m_T . The control and validation regions share the same m_{eff} binning as the signal regions. The $t\bar{t}$ control and validation regions, namely TCR, TVR1, and TVR2, have the same selections as the WDB1L regions, except for the requirement of at least one b -tagged jet.

A summary of all CR and VR selection criteria is reported in Tables 3 and 4. The W +jets ($\ell\nu\nu\nu$) purity is 42%-56% (13%-21%) in WDB1LCR. The $t\bar{t}$ purity is 58%-77% in TCR and $\ell\nu\nu$ purity is 58% in DB2LCR.

Sub-dominant background processes, such as Z +jets, single-top, multiboson, $t\bar{t}+V$, $t\bar{t}+h$ and Vh , which have no dedicated control regions, are normalised to the cross-sections indicated in Table 1. Similarly to the dominant backgrounds, their expected yields in the SRs are subject to statistical and systematic uncertainties. Backgrounds with misidentified (fake) leptons such as jets misreconstructed as a lepton, and events with leptons originating from a jet produced by heavy-flavour quarks or from photon conversions, are estimated by using a matrix method as described in Ref. [109], and found to be negligible in all regions.

6.2 C1N2-Wh Control and Validation regions

The multi-class BDT approach results in a classifier-output score for each of the background categories. Only the three categories representing the dominant backgrounds ($t\bar{t}$, single-top, and W +jets associated production) are considered, and selections on their output scores ($w_{t\bar{t}}$, w_{st} and $w_{W+\text{jets}}$, respectively) are applied to define the CRs after the initial common selection. Table 5 shows the definition of the CRs. The selections on the output scores are defined to maximize the purity of the CR for the targeted background.

Table 3: Overview of the CR and VR definitions for diboson $\ell\nu\nu$ backgrounds. The N_{lep} variable provides the orthogonality to the SR.

Variable	DB2L	
	CR	VR
$N_{\text{lep}} (p_T > 25 \text{ GeV})$	2	
$N_{\text{jet}} (p_T > 30 \text{ GeV})$	1–3	
$N_{\text{b-jet}} (p_T > 30 \text{ GeV})$	0	
$E_T^{\text{miss}} [\text{GeV}]$	> 200	
$\Delta\phi(\ell, E_T^{\text{miss}})$	< 2.9	
$m_{\ell\ell} [\text{GeV}]$	70–100	
$m_{\text{jj veto}} [\text{GeV}]$	75–95	
$\sigma_{E_T^{\text{miss}}}$	> 12	> 10
$m_T [\text{GeV}]$	50–200	200–350

Table 4: Overview of the CR and VR definitions for W +jets, diboson $\ell\nu\nu\nu$ and $t\bar{t}$ backgrounds. They share the same CR and VR definitions except for number of b -tagged jets requirement. The m_T variable provides the orthogonality to the SR.

Variable	WDB1L and T		
	CR	VR1	VR2
$N_{\text{lep}} (p_T > 25 \text{ GeV})$	1		
$N_{\text{jet}} (p_T > 30 \text{ GeV})$	1–3		
$N_{b\text{-jet}} (p_T > 30 \text{ GeV})$	0 for WDB1L; > 0 for Top		
$N_{\text{large-Rjet}} (p_T > 250 \text{ GeV})$	≥ 1		
$E_T^{\text{miss}} [\text{GeV}]$	> 200		
$\Delta\phi(\ell, E_T^{\text{miss}})$	< 2.9		
Large-R jet type	W-tagged		
$m_{\text{eff}} [\text{GeV}]$	[600–850, > 850]		
$\sigma_{E_T^{\text{miss}}}$	< 12	< 12	> 12
$m_T [\text{GeV}]$	50–80	> 80	50–120

Table 5: Definition of the CRs and VRs used to estimate $t\bar{t}$, single-top and W +jets background processes.

Variable	Regions		
$E_T^{\text{miss}} [\text{GeV}]$	> 50		
$N_{\text{lep}} (p_T > 27 \text{ GeV})$	1		
$N_{\text{jet}} (p_T > 30 \text{ GeV})$	2–3		
$N_{b\text{-jet}} (p_T > 30 \text{ GeV})$	2		
$m_{bb} [\text{GeV}]$	$\in [50, 200]$		
$\sigma_{E_T^{\text{miss}}}$	> 5		
	CR $t\bar{t}$ (CRttXGB)	CR single-top (CRstXGB)	CR W +jets (CRWXGB)
w_{sig}	$\in [0.2, 0.3]$	$\in [0, 0.2]$	$\in [0.0, 0.2]$
$w_{t\bar{t}}$	> 0.73	–	–
w_{st}	< 0.2	> 0.45	< 0.2
$w_{W\text{+jets}}$	< 0.4	–	> 0.65
	VR $t\bar{t}$ (VRttXGB)	VR single-top (VRstXGB)	VR W +jets (VRWXGB)
w_{sig}	$\in [0.4, 0.9]$	$\in [0.2, 0.9]$	$\in [0.2, 0.9]$
$w_{t\bar{t}}$	> 0.4	–	–
w_{st}	< 0.2	> 0.2	< 0.2
$w_{W\text{+jets}}$	< 0.4	–	> 0.4

To reduce the contamination from signals of interest to a negligible level, the w_{sig} score is also required to be low. The purity of the CRs obtained with these selections are 95%, 56% and 72% for $t\bar{t}$, single-top and W +jets, respectively. In the case of the single-top CR, most of the remaining events arise from $t\bar{t}$ production.

VRs are defined to validate the extrapolation from CRs. Each have events selected with tightened scores towards their respective background class and a higher signal classification score that approaches the SRs range. The requirements on the signal score are such that the validation regions are orthogonal to both the

CRs (by the lower bound) and the SR (by the upper bound). A selection on the background classification scores is maintained in VRs to isolate the extrapolation from each of the control regions and to reduce potential signal contamination to reasonable levels ($<10\%$ for all models). The definition of the validation regions are also given in Table 5.

Similarly to the C1C1-WW and C1N2-WZ models analyses, sub-dominant background processes, such as Z +jets, diboson, multiboson, $t\bar{t}+V$, $t\bar{t}+h$ and Vh , are normalised to their respective cross-sections and their expected yields in the SRs are subject to statistical and systematic uncertainties. Background contributions from misidentified leptons are also evaluated with the matrix method and found negligible.

7 Systematic uncertainties

The background yield in the SRs is subject to theoretical and experimental systematic uncertainties. The source of these systematic uncertainties for all simulated signal and background processes are evaluated and presented in this section.

The experimental uncertainties are related to the jet energy scale (JES), jet energy resolution (JER), b -tagging, E_T^{miss} modelling, lepton reconstruction and identification, pile-up, and JVT. The dominant uncertainties across all analyses and SRs arise from JES and JER, which are parameterized as a function of the p_T and η of the jet, the pile-up conditions, and the jet flavour composition [110]. The uncertainties arising from the large-R jet-boson tagging are grouped into JES and JER systematic uncertainties, for the C1C1-WW and C1N2-WZ SRs. The impact of uncertainties on the efficiencies and mis-tag rates of the b -tagging algorithm is relevant for the C1N2-Wh SRs and is estimated by varying, as a function of p_T , η and jet flavour, the scale factors used to correct the MC simulation, in a range that reflects the uncertainty in their measurement [111, 112]. The E_T^{miss} modelling systematic uncertainties are estimated by propagating the uncertainties in the energy and momentum scale of each of the objects entering the calculation, and the uncertainties in the soft term's resolution and scale [101]. The evaluation of the lepton reconstruction and identification uncertainties is performed using $Z \rightarrow \ell^+\ell^-$, $J/\psi \rightarrow \ell^+\ell^-$ samples [86, 113]. The procedure of pile-up reweighting is applied to the simulation to match the number of reconstructed vertices to the data. The pile-up uncertainty is estimated by performing a reweighting in which $\langle\mu\rangle$ is varied by $\pm 4\%$.

Uncertainties in the modelling of the SM background processes from MC simulation are profiled for dominant backgrounds in dedicated control regions, where the systematic uncertainties only have an impact on the extrapolation factors, while for sub-dominant backgrounds they are entirely estimated from simulation and affect the inclusive cross-section for each process and the acceptance of the analysis selection in all regions. They are assumed to be fully correlated across signal regions within the same analysis, but uncorrelated between different processes.

Theoretical uncertainties in the $t\bar{t}$ and single-top backgrounds are dominant for the analysis targeting C1N2-Wh models, but also relevant for the others. They take into account uncertainties due to modelling of the hard-scattering, evaluated through a comparison between the nominal POWHEG BOX +PYTHIA 8 sample and the alternative aMC@NLO +PYTHIA 8 sample, and uncertainties arising from the parton shower and hadronisation models, derived from comparisons between samples generated with POWHEG BOX +PYTHIA 8 and POWHEG BOX +HERWIG 7 [114]. Variations of the renormalisation and factorisation scales (scaled up and down by a factor of two), the initial- and final-state radiation parameters and PDF sets are also considered. The uncertainty assigned to the interference between single-top Wt and $t\bar{t}$ production [115] is obtained by comparing diagram removal (DR) and diagram subtraction (DS) samples, modelled by

POWHEG BOX +PYTHIA 8 for the C1C1-WW and C1N2-WZ channels. In the case of the C1N2-Wh analysis, the Wt predictions of the DS sample in some of the CRs and VRs are significantly lower than those of the nominal sample and the data, such that a systematic uncertainty estimation by comparison is not possible. A conservative 35% uncertainty is assumed for the uncertainty in the interference between the Wt and $t\bar{t}$ processes, following studies reported in Ref.[35] and Ref.[116].

The diboson modelling uncertainties are among the dominant uncertainties in the C1C1-WW and C1N2-WZ channels, and are studied separately for the single-lepton and the dilepton processes. They are evaluated by studying the envelope of the variations of the renormalisation and factorisation scales. Variations of the renormalisation and factorisation scales are also applied to W/Z +jets, multiboson, $t\bar{t}+V$, $t\bar{t}+h$, and Vh . The PDF uncertainties are considered following the PDF4LHC15 recommendations [117].

For W/Z +jets, the resummation (QSF) and matching scale (CKKW-L) [118] for the W/Z +jets are estimated by varying the scale parameters up and down for the SHERPA generator. Further, for SHERPA 2.2.11 W/Z +jets samples, the electroweak NLO correction uncertainties are assigned to account for the impact of applying different correction methods. An overall 5% systematic uncertainty in the inclusive cross-section is assigned for the Z +jets samples [119] and similar cross-section uncertainties, 5%–10%, are also assigned for other sub-dominant background contributions.

The variations of the parameters corresponding to the factorisation, renormalisation and CKKW-L matching scales in aMC@NLO +PYTHIA 8 samples provide the uncertainties for the two simplified signal models considered.

The dominant systematic uncertainties in the background estimates for the signal regions are presented in Tables 6, 7 and 8. Theoretical and experimental uncertainties are shown for each of the dominant background contribution. The uncertainties in the scale factor fits to the control regions are listed as ‘Normalisation of dominant backgrounds’. For the SRs targeting the C1C1-WW and C1N2-WZ models, they contribute around 6%–7% across regions. For the analysis targeting the C1N2-Wh model, they are around 9%–16% and are dominated by $t\bar{t}$ and single-top backgrounds. The largest individual experimental uncertainty amounts to 4%–17% depending on the SR for C1C1-WW and C1N2-WZ. For the C1N2-Wh analysis, the dominant experimental uncertainty arises from the JER (12%–20%) followed by the JES and b -tagging. The MC statistical uncertainties contribute up to 19% depending on the SR and analysis.

Table 6: Breakdown of the dominant systematic uncertainties in background estimates in the various exclusion signal regions for the C1C1-WW model. The individual uncertainties can be correlated, and do not necessarily add up in quadrature to the total background uncertainty.

C1C1-WW model	SRLM	SRMM	SRHM
Total background expectation	22.0	9.2	15.7
Total background systematic uncertainty	± 3.2	± 2.5	± 3.0
Theoretical systematic uncertainties			
$t\bar{t}$	± 1.1	± 0.25	± 0.15
Single top	± 0.31	± 0.08	± 0.35
W+jets	± 0.4	± 0.15	± 0.32
Diboson	± 0.29	± 0.24	± 0.26
Other backgrounds	± 0.10	± 0.07	± 0.08
MC statistical uncertainties			
MC statistical uncertainty	± 2.1	± 1.6	± 2.1
Uncertainties in the background normalisation			
Normalisation of dominant backgrounds	± 1.5	± 0.6	± 1.1
Experimental systematic uncertainties			
Jet energy resolution	± 1.1	± 1.0	± 1.4
Jet energy scale	± 1.7	± 1.5	± 1.1
E_T^{miss}	± 0.5	± 0.26	± 0.6
Lepton uncertainties	± 0.4	± 0.10	± 0.5
Pile-up/JVT	± 0.10	± 0.21	± 0.23

Table 7: Breakdown of the dominant systematic uncertainties in background estimates in the various exclusion signal regions for the C1N2-WZ model. The individual uncertainties can be correlated, and do not necessarily add up in quadrature to the total background uncertainty.

C1N2-WZ model	SRLM	SRMM	SRHM
Total background expectation	29	12.7	17.0
Total background systematic uncertainty	± 4	± 2.5	± 2.9
Theoretical systematic uncertainties			
$t\bar{t}$	± 0.9	± 0.29	± 0.20
Single top	± 1.1	± 0.24	± 0.5
W+jets	± 0.6	± 0.22	± 0.4
Diboson	± 0.5	± 0.24	± 0.6
Other backgrounds	± 0.15	± 0.18	± 0.09
MC statistical uncertainties			
MC statistical uncertainty	± 2.5	± 1.4	± 2.1
Uncertainties in the background normalisation			
Normalisation of dominant backgrounds	± 2.0	± 0.8	± 1.2
Experimental systematic uncertainties			
Jet energy resolution	± 1.1	± 1.3	± 0.8
Jet energy scale	± 1.3	± 1.0	± 1.3
E_T^{miss}	± 0.5	± 0.6	± 0.07
Lepton uncertainties	± 0.34	± 0.23	± 0.20
Pile-up/JVT	± 0.06	± 0.8	± 0.11

Table 8: Breakdown of the dominant systematic uncertainties in background estimates in the various exclusion signal regions for the C1N2-Wh model. The individual uncertainties can be correlated, and do not necessarily add up in quadrature to the total background uncertainty. The category ‘Others’ refers to diboson, $t\bar{t}$ W/Z , Higgs boson and Z +jets events.

C1C1-Wh model	SRXGB Bin 1 [0.91, 0.928)	SRXGB Bin 2 [0.928, 0.948)	SRXGB Bin 3 [0.948, 0.964)	SRXGB Bin 4 [0.964, 1]
Total background expectation	9.4	5.7	4.2	2.2
Total background systematic uncertainty	± 2.1	± 2.0	± 1.4	± 0.7
Theoretical systematic uncertainties				
$t\bar{t}$	± 1.1	± 0.7	± 0.5	± 0.10
Single top	± 1.2	± 0.9	± 0.9	± 0.4
W +jets	± 0.17	± 0.14	± 0.12	± 0.04
Other backgrounds	± 0.14	± 0.13	± 0.13	± 0.10
MC statistical uncertainties				
MC statistical uncertainty	± 1.0	± 0.8	± 0.7	± 0.4
Uncertainties in the background normalisation				
Normalisation of dominant backgrounds	± 1.3	± 0.9	± 0.5	± 0.19
Experimental systematic uncertainties				
Jet energy resolution	± 1.1	± 1.2	± 0.6	± 0.4
Jet energy scale	± 0.5	± 0.31	± 0.33	± 0.07
b -tagging	± 0.12	± 0.8	± 0.05	± 0.06
Pile-up/JVT	± 0.4	± 0.5	± 0.29	± 0.09
Lepton and E_T^{miss} uncertainties	± 0.05	± 0.4	± 0.14	± 0.12

8 Results

The observed event yield in each of the exclusion signal regions for the three analyses is summarized in Tables 9, 10 and 11 for the C1C1-WW, C1N2-WZ and C1N2-Wh models, respectively. Yields in data are reported with the corresponding SM predictions obtained from the background-only fit, where the predicted post-fit level of background is compared with the observed yields in the corresponding VRs and SRs. Two distinct fits are run, one for the C1C1-WW and C1N2-WZ analyses, and one for the analysis targeting C1N2-Wh models. In the former case, the normalisation factors to be applied to the MC predictions of the main SM backgrounds are $0.81_{-0.09}^{+0.10}$ for $t\bar{t}$, $1.05_{-0.09}^{+0.09}$ for W +jets and diboson 1L, and $1.22_{-0.18}^{+0.18}$ for diboson 2L. In the latter case, the normalisation factors are found to be 1.00 ± 0.29 for $t\bar{t}$, 0.95 ± 0.19 for single top and 1.30 ± 0.05 for W +jets production. The large uncertainties in the $t\bar{t}$ and single top normalisation factors are related to their large theoretical systematic uncertainties. Overall the normalisation factors are found to be consistent across analyses for each background process within uncertainties. For the W +jets normalisation factors, differences are expected because of the different requirement on the number of b -tagged jets. MC predictions for the production of a W or Z boson and b -jets are consistently below data in SM cross-section measurements, and in agreement if no b -jets are required in the event [120].

The agreement between the observed and expected event yields in control, validation and exclusion signal regions is illustrated in Figures 2 and 3. No significant excesses are observed in data above the SM prediction.

Figures 4–5 present the post-fit m_T , $\sigma_{E_T^{\text{miss}}}$, and m_{eff} distributions for the C1C1-WW and C1N2-WZ analyses compared with the data in the selected control and validation regions. The data and the background expectation in all validation regions agree well within around two standard deviations. Therefore no further systematic uncertainty is applied to the background estimate in the signal regions. Figure 6 shows the post-fit m_{eff} distributions in SRLM, SRMM, and SRHM for both the C1C1-WW and C1N2-WZ models. The uncertainty bands include all statistical and systematic uncertainties. The dashed lines represent the benchmark signal points.

For the C1N2-Wh analysis, E_T^{miss} and output signal score distributions in $t\bar{t}$ and single top validation regions are shown in Figure 7. The data and the background expectation in all validation regions agree well within around one standard deviations. Figure 8 shows the post-fit distributions for E_T^{miss} , am_{T2} , $m_{b\bar{b}}$ and $\sigma_{E_T^{\text{miss}}}$ in the inclusive SR, i.e., considering all SR bins. Events selected by the BDT as compatible with the signal of interest (high w_{sig} score) have a moderate to large E_T^{miss} and am_{T2} , $m_{b\bar{b}}$ close to the Higgs boson mass and large $\sigma_{E_T^{\text{miss}}}$.

Table 9: Observed event yields and the background expectation obtained from a background fit in the C1C1-WW model SRs with an integrated luminosity of 139 fb^{-1} . The first column with numbers stands for the yields in all bins. The second and third columns correspond to the low and high bins in m_{eff} . Uncertainties reported for the fitted background estimates combine statistical and systematic uncertainties.

C1C1-WW model	SRLM	Bin 0 [600, 850] GeV	Bin 1 > 850 GeV
Observed events	23	16	7
Total SM background events	22.0 ± 3.2	15.8 ± 2.8	6.2 ± 1.0
$t\bar{t}$	2.6 ± 1.3	2.2 ± 1.2	0.36 ± 0.21
W +jets	13.6 ± 2.7	10.1 ± 2.3	3.5 ± 0.8
Z +jets	$0.10^{+0.16}_{-0.10}$	$0.04^{+0.13}_{-0.04}$	0.054 ± 0.034
Single-top	0.5 ± 0.4	$0.19^{+0.25}_{-0.19}$	0.26 ± 0.18
Diboson2l	1.7 ± 0.5	1.3 ± 0.4	0.43 ± 0.12
Diboson1l	3.0 ± 0.7	1.5 ± 0.5	1.41 ± 0.30
$t\bar{t} + V$	0.50 ± 0.14	0.30 ± 0.10	0.20 ± 0.06
$t\bar{t} + h$	0.008 ± 0.005	0.005 ± 0.005	0.003 ± 0.001
Multiboson	0.005 ± 0.002	–	0.005 ± 0.002
C1C1-WW model	SRMM	Bin 0 [600, 850] GeV	Bin 1 > 850 GeV
Observed events	11	7	4
Total SM background events	9.2 ± 2.5	6.4 ± 2.2	2.7 ± 0.9
$t\bar{t}$	0.60 ± 0.32	0.44 ± 0.25	0.16 ± 0.10
W +jets	5.3 ± 2.1	4.0 ± 1.9	1.3 ± 0.5
Z +jets	0.11 ± 0.04	0.09 ± 0.04	0.020 ± 0.010
Single-top	0.12 ± 0.09	0.09 ± 0.07	$0.03^{+0.03}_{-0.07}$
Diboson2l	1.4 ± 0.4	0.89 ± 0.32	0.49 ± 0.21
Diboson1l	1.4 ± 0.4	0.80 ± 0.28	0.64 ± 0.25
$t\bar{t} + V$	0.29 ± 0.12	0.16 ± 0.09	0.13 ± 0.07
$t\bar{t} + h$	0.004 ± 0.002	0.004 ± 0.002	–
Multiboson	–	–	–
C1C1-WW model	SRHM	Bin 0 [600, 850] GeV	Bin 1 > 850 GeV
Observed events	16	4	12
Total SM background events	15.7 ± 3.0	4.8 ± 1.3	10.8 ± 2.5
$t\bar{t}$	0.36 ± 0.18	0.19 ± 0.11	0.17 ± 0.09
W +jets	11.3 ± 2.5	3.3 ± 1.1	8.0 ± 2.2
Z +jets	0.17 ± 0.07	0.14 ± 0.06	0.029 ± 0.018
Single-top	0.49 ± 0.34	0.23 ± 0.17	0.26 ± 0.20
Diboson2l	1.5 ± 0.4	0.54 ± 0.17	0.99 ± 0.28
Diboson1l	1.5 ± 0.4	0.39 ± 0.14	1.09 ± 0.31
$t\bar{t} + V$	0.33 ± 0.12	0.037 ± 0.035	0.29 ± 0.11
$t\bar{t} + h$	0.003 ± 0.003	–	0.003 ± 0.003
Multiboson	0.004 ± 0.001	–	0.004 ± 0.001

Table 10: Observed event yields and the background expectation obtained from a background fit in the C1N2-WZ model SRs with an integrated luminosity of 139 fb^{-1} . The first column with numbers stands for the yields in all bins. The second and third columns correspond to the low and high bins in m_{eff} . Uncertainties reported for the fitted background estimates combine statistical and systematic uncertainties.

C1N2-WZ model	SRLM	Bin 0 [600, 850] GeV	Bin 1 > 850 GeV
Observed events	26	16	10
Total SM background events	29 ± 4	15.6 ± 2.8	13.0 ± 1.8
$t\bar{t}$	2.7 ± 1.0	1.6 ± 0.7	1.1 ± 0.4
W +jets	18.1 ± 2.8	10.6 ± 2.1	7.5 ± 1.2
Z +jets	$0.06^{+0.06}_{-0.06}$	$0.03^{+0.06}_{-0.03}$	$0.03^{+0.06}_{-0.03}$
Single-top	$0.6^{+1.0}_{-0.6}$	$0.16^{+0.34}_{-0.16}$	$0.5^{+0.8}_{-0.5}$
Diboson2l	2.4 ± 0.6	1.4 ± 0.4	0.96 ± 0.28
Diboson1l	3.9 ± 0.9	1.3 ± 0.4	2.5 ± 0.6
$t\bar{t} + V$	0.74 ± 0.22	0.37 ± 0.13	0.37 ± 0.11
$t\bar{t} + h$	0.021 ± 0.006	0.011 ± 0.004	0.010 ± 0.004
Multiboson	0.020 ± 0.005	–	0.020 ± 0.005
C1N2-WZ model	SRMM	Bin 0 [600, 850] GeV	Bin 1 > 850 GeV
Observed events	22	13	9
Total SM background events	12.7 ± 2.5	7.0 ± 2.2	5.7 ± 1.3
$t\bar{t}$	0.9 ± 0.4	0.52 ± 0.23	0.41 ± 0.20
W +jets	7.3 ± 2.0	4.4 ± 1.9	2.9 ± 0.8
Z +jets	0.30 ± 0.23	0.12 ± 0.12	0.18 ± 0.15
Single-top	$0.14^{+0.24}_{-0.14}$	$0.09^{+0.16}_{-0.09}$	$0.05^{+0.11}_{-0.05}$
Diboson2l	1.5 ± 0.4	0.66 ± 0.28	0.85 ± 0.25
Diboson1l	1.9 ± 0.5	0.94 ± 0.27	0.95 ± 0.30
$t\bar{t} + V$	0.54 ± 0.17	0.25 ± 0.10	0.28 ± 0.10
$t\bar{t} + h$	$0.026^{+0.029}_{-0.026}$	0.005 ± 0.004	$0.022^{+0.025}_{-0.022}$
Multiboson	0.008 ± 0.002	0.004 ± 0.001	0.004 ± 0.001
C1N2-WZ model	SRHM	Bin 0 [600, 850] GeV	Bin 1 > 850 GeV
Observed events	26	5	21
Total SM background events	17.0 ± 2.8	3.3 ± 1.4	13.7 ± 2.3
$t\bar{t}$	0.63 ± 0.28	0.23 ± 0.15	0.40 ± 0.19
W +jets	11.6 ± 2.1	2.3 ± 1.1	9.3 ± 1.6
Z +jets	0.045 ± 0.022	0.076 ± 0.021	–
Single-top	1.3 ± 0.7	$0.014^{+0.066}_{-0.014}$	1.2 ± 0.7
Diboson2l	1.5 ± 0.7	0.30 ± 0.18	1.2 ± 0.5
Diboson1l	1.6 ± 0.4	0.35 ± 0.15	1.22 ± 0.30
$t\bar{t} + V$	0.42 ± 0.14	$0.019^{+0.023}_{-0.019}$	0.40 ± 0.14
$t\bar{t} + h$	0.003 ± 0.003	–	0.003 ± 0.003
Multiboson	$0.006^{+0.011}_{-0.006}$	–	$0.006^{+0.011}_{-0.006}$

Table 11: Observed event yields and the background expectation obtained from a background fit in the C1N2-Wh model SR with an integrated luminosity of 139 fb^{-1} . Each column corresponds to a bin in w_{sig} score. Uncertainties reported for the fitted background estimates combine statistical and systematic uncertainties. The category ‘Others’ refers to Z+jets and multiboson events.

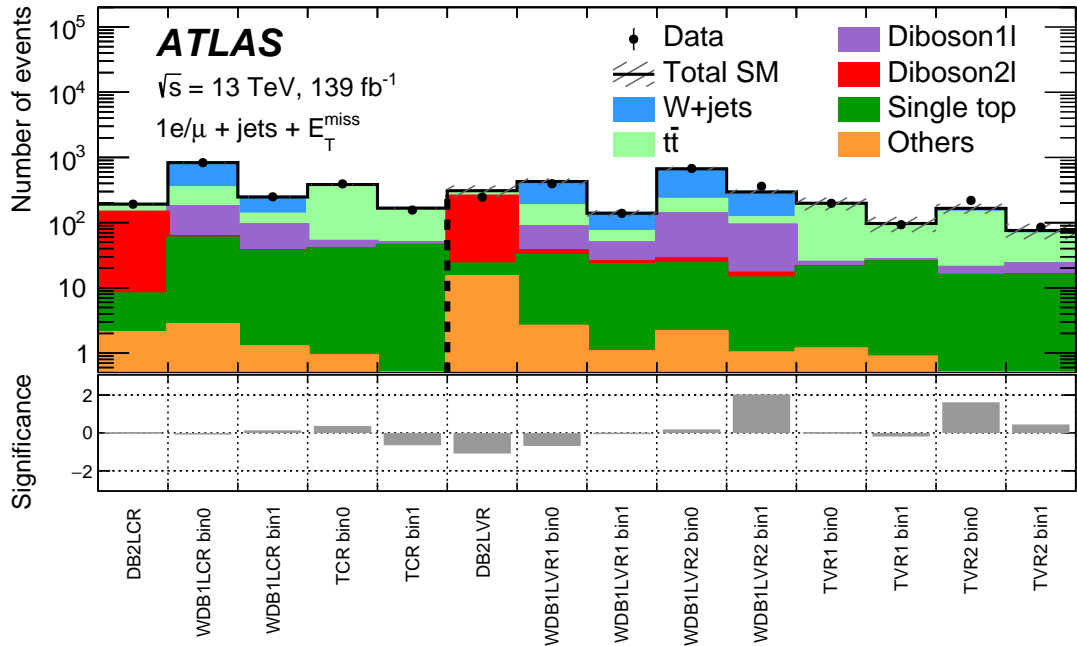
Yields	SRXGB Bin 1 [0.91, 0.928)	SRXGB Bin 2 [0.928, 0.948)	SRXGB Bin 3 [0.948, 0.964)	SRXGB Bin 4 [0.964, 1]
Observed events	5	9	6	5
Total SM background events	9.4 ± 2.1	5.7 ± 2.0	4.2 ± 1.4	2.2 ± 0.8
$t\bar{t}$	3.8 ± 1.1	2.3 ± 1.4	1.3 ± 0.7	$0.30^{+0.32}_{-0.30}$
Single-top	3.1 ± 1.6	2.5 ± 1.2	1.8 ± 1.0	0.8 ± 0.5
W+jets	1.7 ± 0.6	0.5 ± 0.4	0.8 ± 0.2	0.8 ± 0.2
Diboson	0.4 ± 0.2	0.14 ± 0.09	0.09 ± 0.07	0.05 ± 0.02
$t\bar{t} h, Wh$	0.24 ± 0.22	0.18 ± 0.05	0.14 ± 0.02	0.15 ± 0.03
$t\bar{t} +W/Z$	0.13 ± 0.06	$0.04^{+0.05}_{-0.04}$	0.08 ± 0.06	0.05 ± 0.02
Others	$0.04^{+0.05}_{-0.04}$	0.05 ± 0.04	0.01 ± 0.01	0.02 ± 0.01

Table 12: The number of observed events, total SM background, 95% CL upper limits on the visible cross-section ($\langle\epsilon\sigma\rangle_{obs}^{95}$) and on the number of signal events (S_{obs}^{95}). The fifth column (S_{exp}^{95}) shows the 95% CL upper limit on the number of signal events, given the expected number (with ± 1 standard deviation excursions on the expectation) of background events. The last three columns indicate the CL_B value that provides a measure of compatibility of the observed data with the 95% CL signal strength hypothesis relative to fluctuations of the background, the discovery p -value (p_0) that measures compatibility of the observed data with the background-only (zero signal strength) hypothesis relative to fluctuations of the background and the corresponding Gaussian significance (Z). Larger values indicate greater relative compatibility. The p_0 is not calculated in signal regions with a deficit relative to the nominal background prediction and here the p_0 value is capped at 0.50.

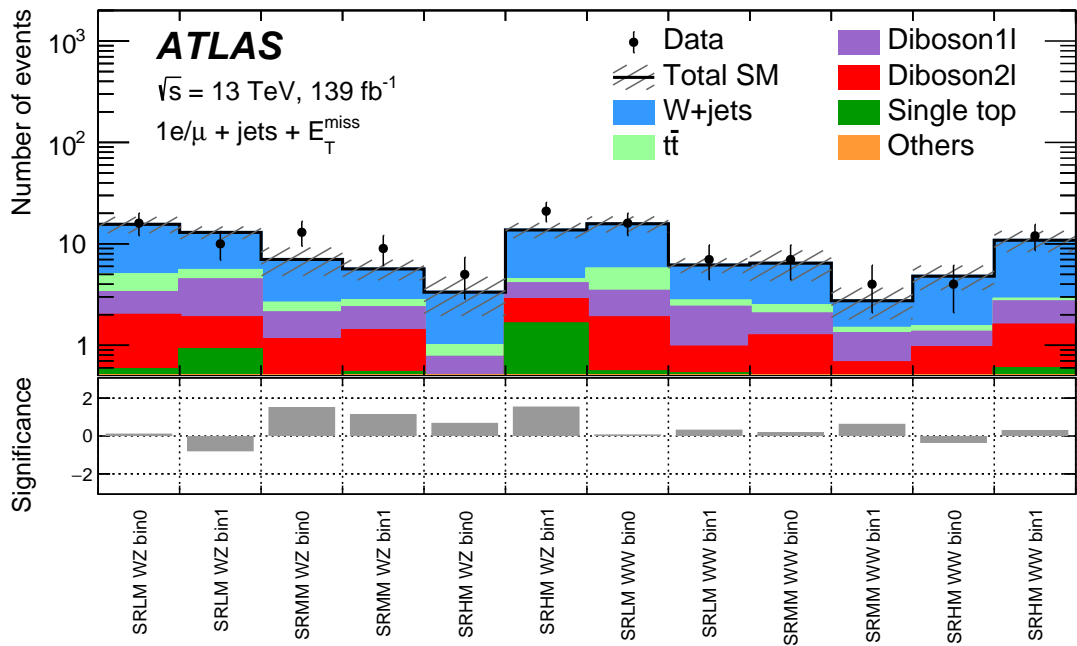
Signal channel	Observed events	Total SM background	$\langle\epsilon\sigma\rangle_{obs}^{95}$ [fb]	S_{obs}^{95}	S_{exp}^{95}	CL_B	p_0	Z
C1C1-WW model								
SRLM (disc.)	16	11.6 ± 1.6	0.09	13.0	$8.8^{+4.3}_{-1.5}$	0.84	0.14	1.09
SRMM (disc.)	9	9.8 ± 2.0	0.06	7.9	$9.0^{+5.4}_{-1.4}$	0.42	0.50	0.00
SRHM (disc.)	12	10.8 ± 2.5	0.07	10.4	$9.4^{+4.1}_{-3.0}$	0.60	0.39	0.29
C1N2-WZ model								
SRLM (disc.)	17	18.4 ± 2.9	0.08	11.5	$13.7^{+4.0}_{-4.5}$	0.40	0.50	0.00
SRMM (disc.)	9	5.7 ± 1.3	0.07	10.2	$6.8^{+3.1}_{-0.9}$	0.87	0.13	1.11
SRHM (disc.)	21	13.7 ± 2.3	0.13	17.5	$10.5^{+4.4}_{-2.4}$	0.92	0.06	1.54
C1N2-Wh model								
SR (inclusive)	25	21.4 ± 4.2	0.12	16.2	$13.4^{+5.5}_{-4.0}$	0.70	0.29	0.57
SR Bin 2–4	20	12.0 ± 3.0	0.13	17.9	$10.7^{+4.7}_{-3.1}$	0.92	0.06	1.58
SR Bin 3–4	11	6.3 ± 1.6	0.09	12.0	$7.4^{+3.5}_{-2.3}$	0.89	0.08	1.42
SR Bin 4	5	2.2 ± 1.0	0.06	8.0	$5.1^{+2.7}_{-1.6}$	0.86	0.08	1.37

Table 12 summarises the observed (S_{obs}^{95}) and expected (S_{exp}^{95}) 95% confidence level (CL) upper limits on the number of signal events and on the observed visible cross-section, $\langle\epsilon\sigma\rangle_{obs}^{95}$, for each SR(disc.). The discovery SRs are used to test for the presence of any beyond-the-Standard-Model (BSM) physics processes. Upper limits on contributions from new physics processes are estimated by using the ‘model-independent fit’, where a generic BSM process is assumed to contribute only to the SR and not to the CRs, thus giving a conservative background estimate in the SR. When normalised to the integrated luminosity of the data sample, the results can be interpreted as corresponding to observed upper limits $\langle\epsilon\sigma\rangle_{obs}^{95}$, defined as the product of the production cross-section, the acceptance, and the selection efficiency of a BSM signal. The p_0 value and the CL_B value are also provided. The former represents the probability of the SM background alone to fluctuate to the observed number of events or higher, and latter provides the confidence level observed for the background-only hypothesis. The limits are validated by comparing pseudo-experiments and using asymptotic formulae, and found to be comparable. All limits presented in this paper are calculated using asymptotic formulae.

Model-dependent exclusion limits at 95% CL are placed on the signal model. These limits are shown as a function of the masses of the SUSY particles in Figure 9 for C1C1-WW and C1N2-WZ models, and Figure 10 for C1N2-Wh models. A likelihood similar to the one used in the background-only fit, but with additional terms for the SRs, is used for the calculation. The exclusion SRs are included in the fit and are used to constrain normalisation and nuisance parameters. A signal is allowed in this likelihood in both the CRs and SRs. The VRs are not used in the fit. The CL_s method [122] is used to derive the CL of the exclusion for a particular signal model; signal models with a CL_s value below 0.05 are excluded at 95% CL. The uncertainties in the observed limit are calculated by varying the cross-section for the



(a)



(b)

Figure 2: Comparison of the observed and expected event yields in (a) the control and validation regions, and (b) the exclusion signal regions for the C1C1-WW and C1N2-WZ analyses. Uncertainties in the background estimates include both the statistical and systematic uncertainties. The bottom panel shows the significance [121] of the differences between the observed and expected yields.

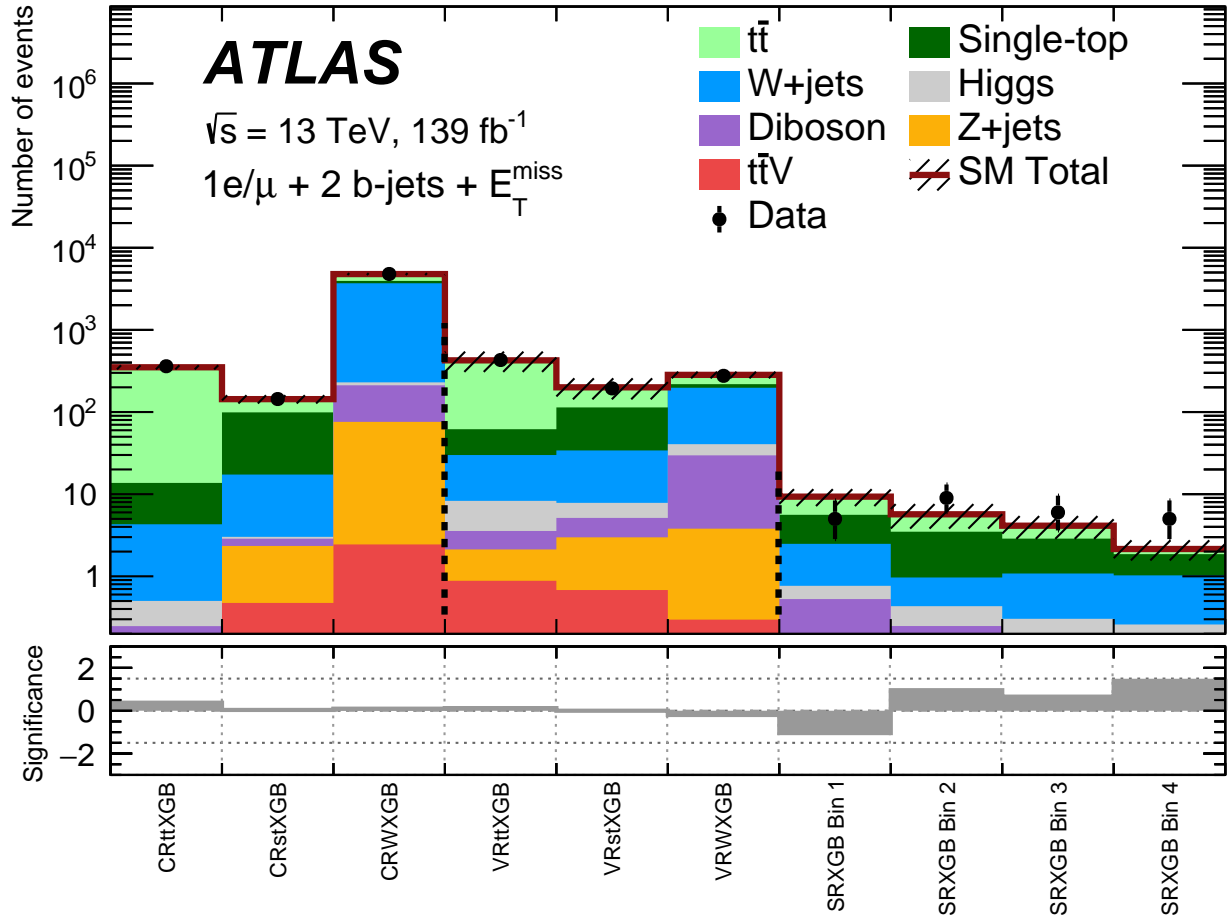


Figure 3: Comparison of the observed and expected event yields in control, validation regions, and exclusion SR bins for the C1N2-Wh analysis. Uncertainties in the background estimates include both the statistical and systematic uncertainties. The bottom panel shows the significance [121] of the differences between the observed and expected yields for control regions, validation regions and in the signal region in bins of w_{sig} .

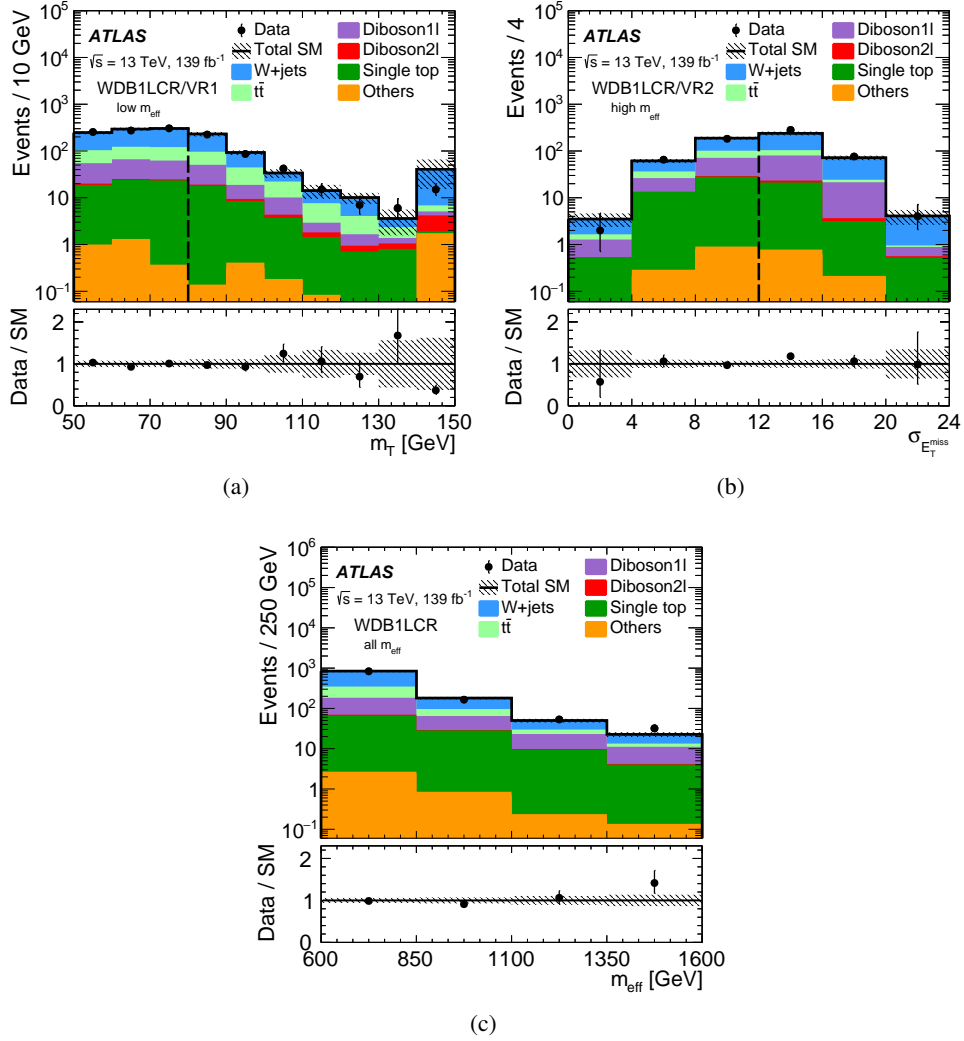


Figure 4: The post-fit (a) m_T distribution in WDB1L CR and VR1 for low m_{eff} bin, (b) $\sigma_{E_T^{\text{miss}}}$ distribution in WDB1L CR and VR2 for high m_{eff} bin and (c) m_{eff} distribution in WDB1L CR. The vertical dashed line separates the control and validation regions. The uncertainty bands plotted include all statistical and systematic uncertainties. The overflow events, where present, are included in the last bin. The lower panels of the plots show the ratio of the observed data to the total background prediction.

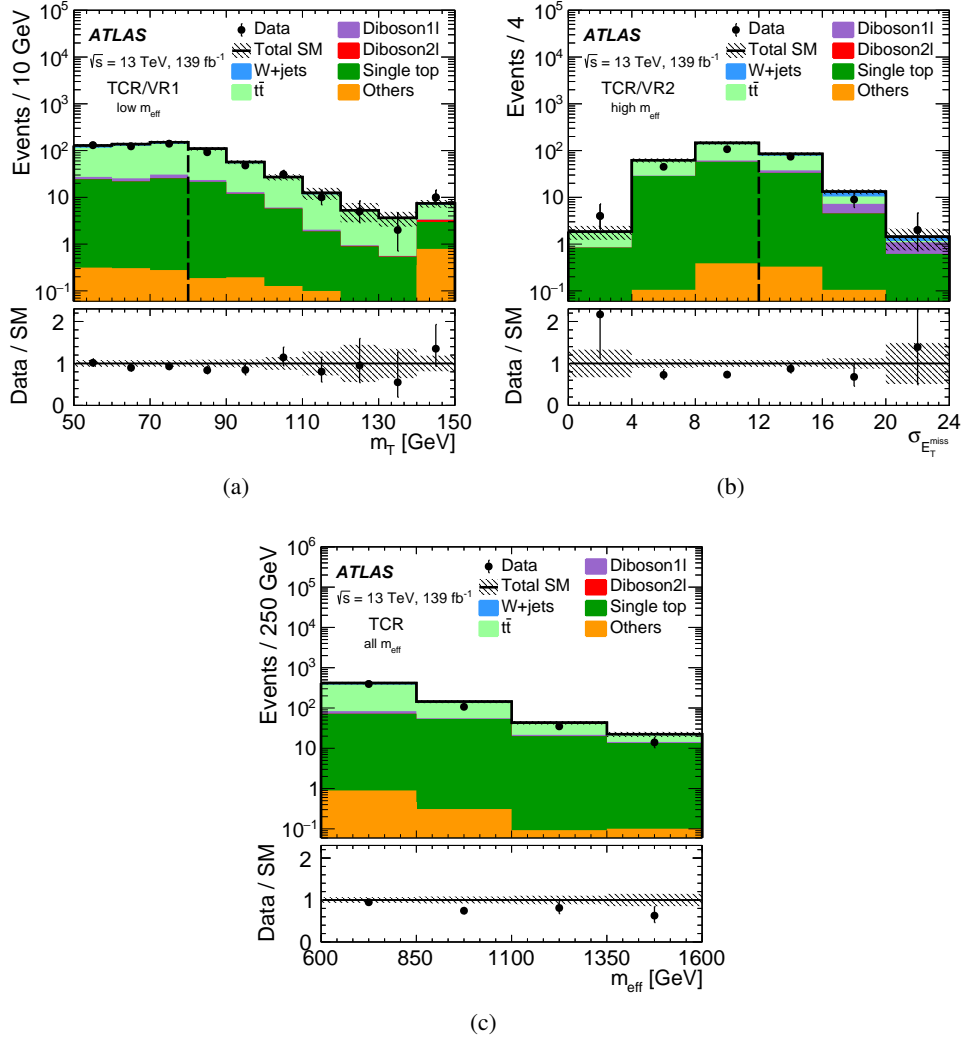


Figure 5: The post-fit (a) m_T distribution in $t\bar{t}$ CR and VR1 for low m_{eff} bin, (b) $\sigma_{E_T^{\text{miss}}}$ distribution in $t\bar{t}$ CR and VR2 for high m_{eff} bin and (c) m_{eff} distribution in $t\bar{t}$ CR. The vertical dashed line separates the control and validation regions. The uncertainty bands plotted include all statistical and systematic uncertainties. The overflow events, where present, are included in the last bin. The lower panels of the plots show the ratio of the observed data to the total background prediction.

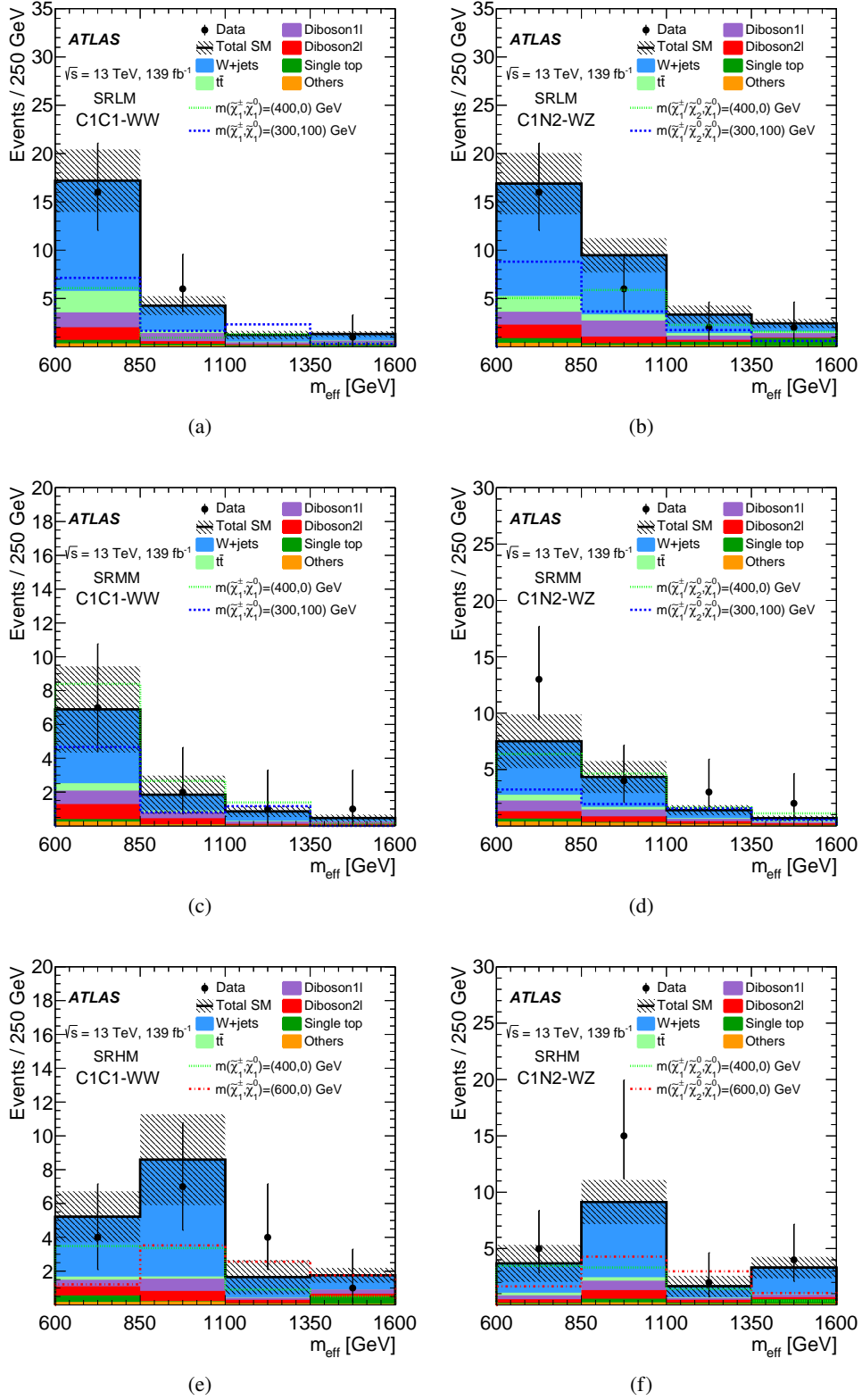


Figure 6: The post-fit m_{eff} distributions in the exclusion signal regions (a, b) SRLM, (c, d) SRMM, and (e, f) SRHM for the C1C1-WW and C1N2-WZ models. The uncertainty bands plotted include all statistical and systematic uncertainties. The dashed lines represent the benchmark signal samples. The overflow events, where present, are included in the last bin.

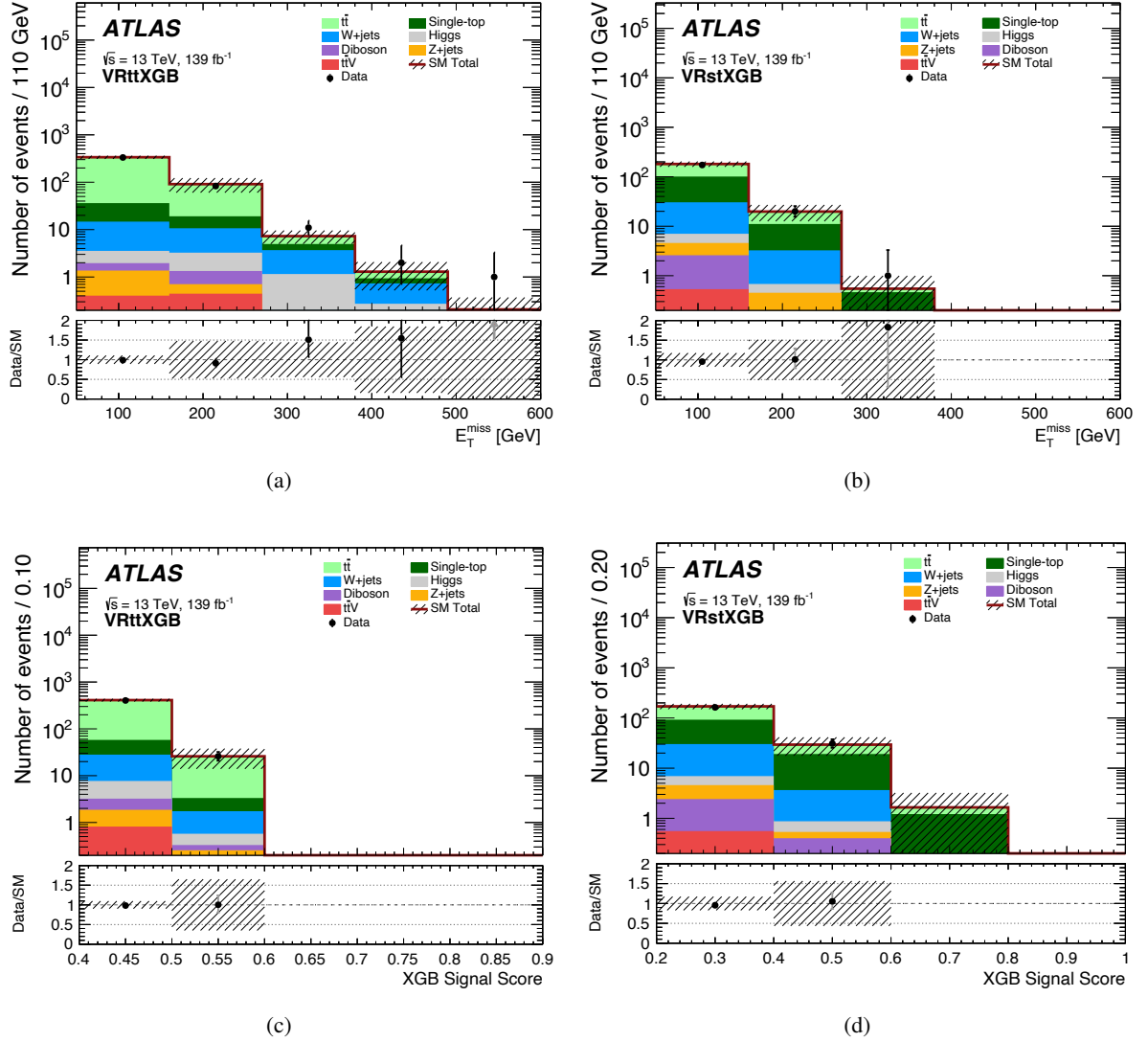


Figure 7: Post-fit E_T^{miss} and signal output score distributions: (a) and (c) in $t\bar{t}$, (b) and (d) in single-top VRs. The uncertainty bands plotted include all statistical and systematic uncertainties. The overflow events, where present, are included in the last bin. The lower panels of the plots show the ratio of the observed data to the total background prediction.

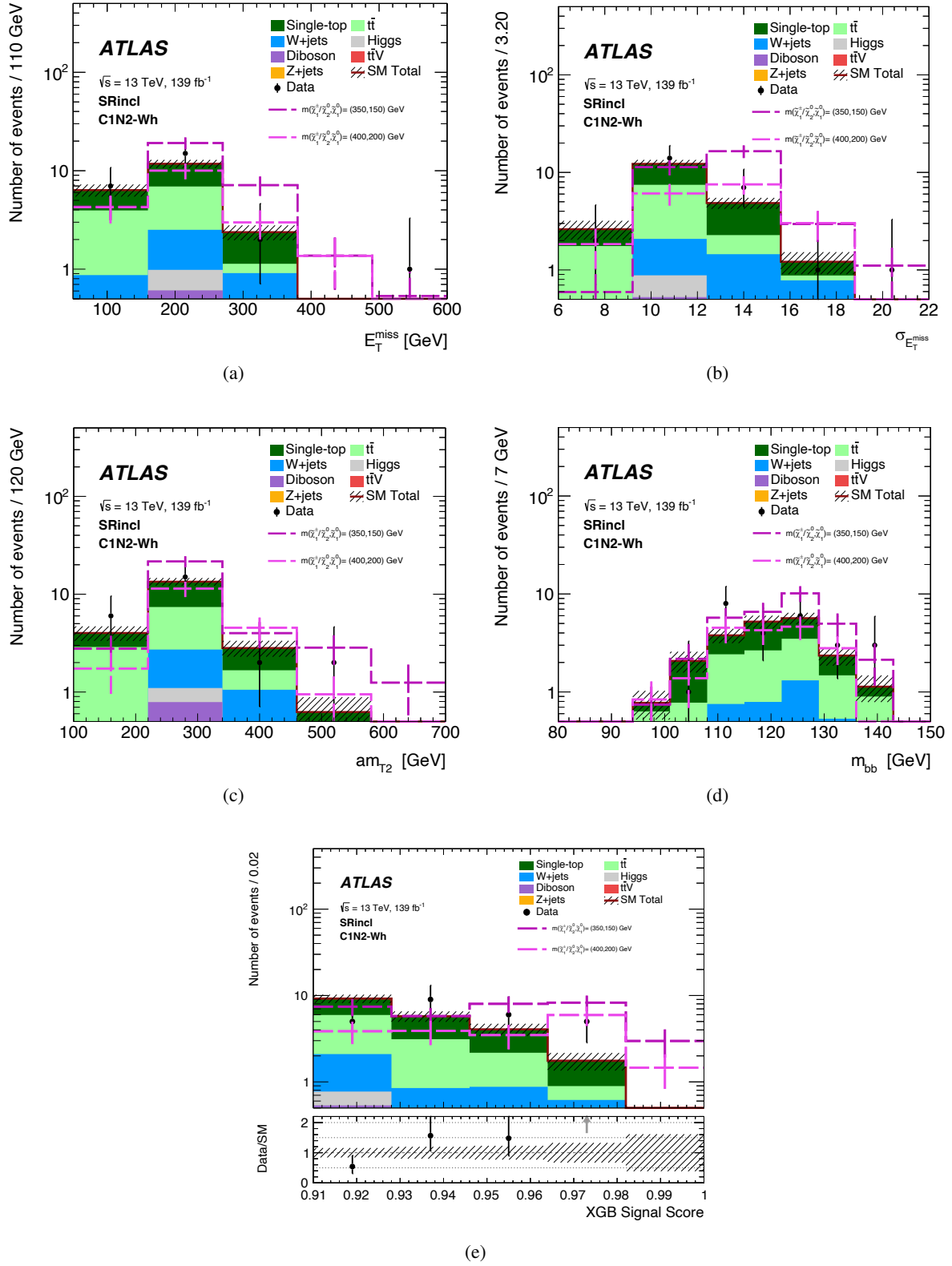
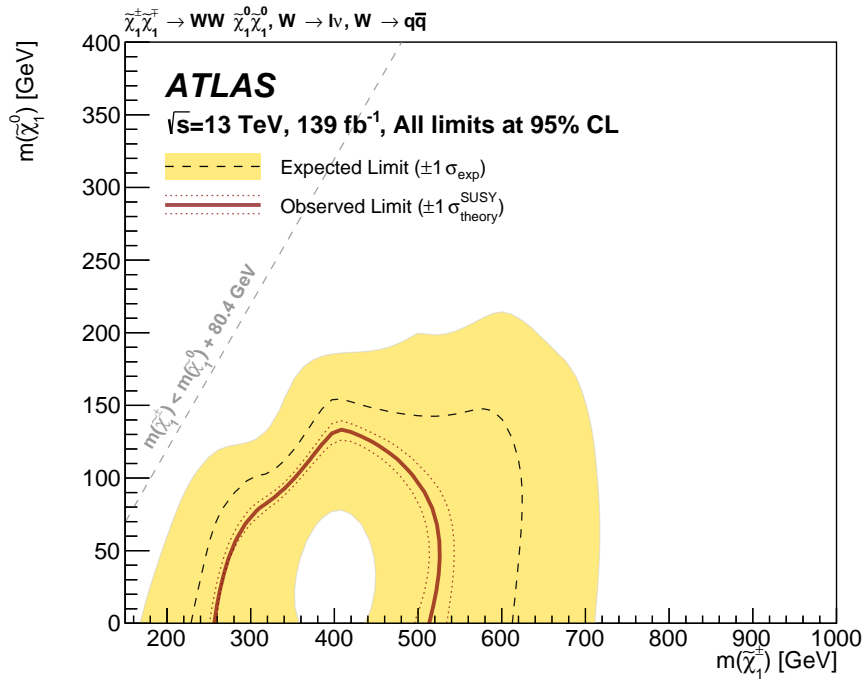
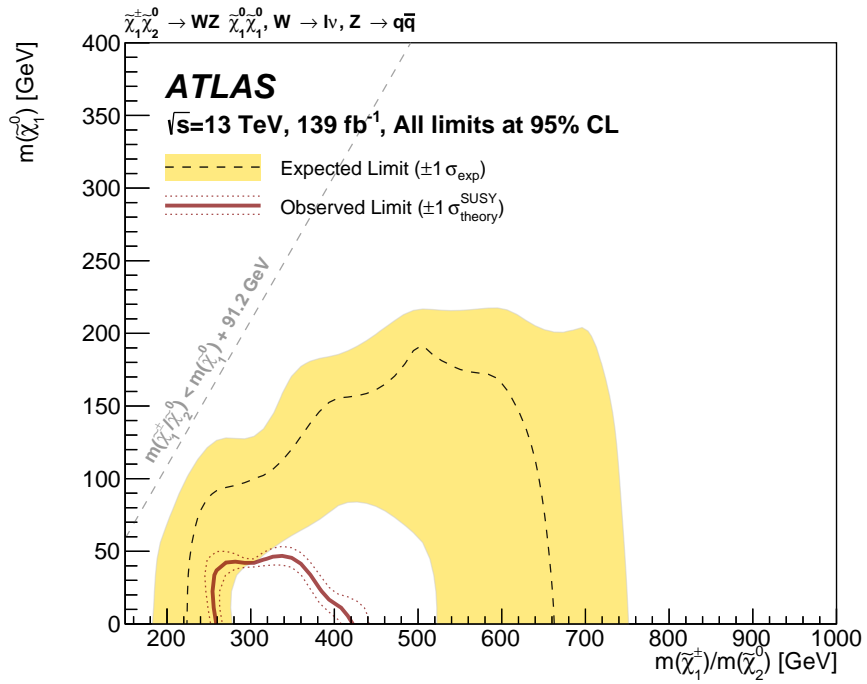


Figure 8: Post-fit distributions in the SRs (not binned in signal output score) for representative kinematic observables (a) E_T^{miss} , (b) $\sigma_{E_T^{\text{miss}}}$, (c) am_{T2} , (d) $m_{b\bar{b}}$ and (e) the signal output score. Two representative SUSY signal models are overlaid for illustration. The uncertainty bands plotted include all statistical and systematic uncertainties. The overflow events, where present, are included in the last bin.



(a)



(b)

Figure 9: Model-dependent exclusion contour at 95% CL on (a) the chargino pair production and (b) the production of a chargino and a next-to-lightest neutralino. The observed limit is given by the solid line with the signal cross-section uncertainties shown by the dotted lines as indicated in the text. Expected limits are given by the dashed line with uncertainties shown by the shaded band.

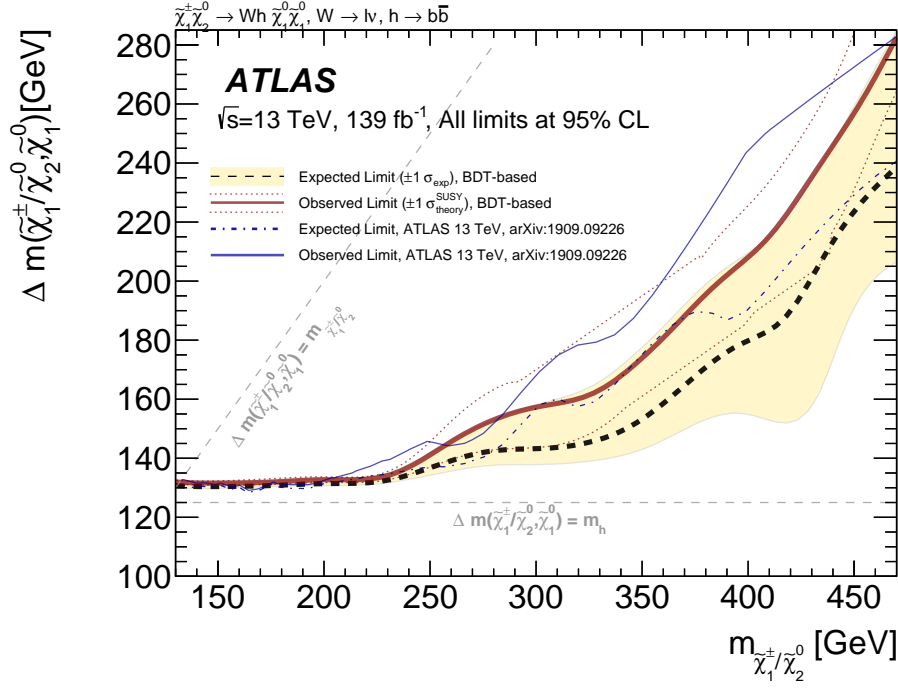


Figure 10: Model-dependent exclusion contour at 95% CL on the chargino and a next-to-lightest neutralino mass versus the mass difference between chargino and LSP in the C1N2-Wh model. The observed limit is given by the solid line with the signal cross-section uncertainties shown by the dotted lines as indicated in the text. Expected limits are given by the dashed line with uncertainties shown by the shaded band. The observed and expected limit contours from the previous ATLAS analysis of the same data sample using standard cut-and-count methods are also shown for comparison.

signal up and down by its uncertainty. For the C1C1-WW model, the $\tilde{\chi}_1^\pm$ mass of about 260–520 GeV is excluded for a massless $\tilde{\chi}_1^0$, which complements the previous ATLAS limits in a 0-lepton channel [30] and a 2-lepton channel [29]. For the C1N2-WZ model, the range of 260–420 GeV in $m(\tilde{\chi}_1^\pm/\tilde{\chi}_2^0)$ for a massless $\tilde{\chi}_1^0$ is excluded. The limit in the high $m(\tilde{\chi}_1^\pm/\tilde{\chi}_2^0)$ region is dominated by the high m_{eff} bin of SR-HM. Combining the low and high m_{eff} bins of SRMM for C1N2-WZ model leads to a signal significance of around 2.1 standard deviations. This differences between observed and expected events in bins with small numbers of events lead to an observed limit weaker than the expected one. Similar differences arise in the exclusion limit of C1N2-Wh models. In this case, limits are shown as a function of the mass of the chargino and next-to-lightest neutralino and the mass difference between that and the LSP, and are compared with previous ATLAS results on the same data sample. The presented mass range is chosen to illustrate the improved region only. While the low numbers of events and the large systematic uncertainties in the most constraining bins in w_{sig} reduce the expected sensitivity, the BDT approach exceed previous constraints at low $\Delta m(\tilde{\chi}_1^\pm/\tilde{\chi}_2^0/\tilde{\chi}_1^0)$ by up to 40 GeV in the range of 200–260 GeV and 280–470 GeV in $m(\tilde{\chi}_1^\pm/\tilde{\chi}_2^0)$.

9 Conclusion

The results of three searches for electroweakino pair production $pp \rightarrow \tilde{\chi}_1^\pm \tilde{\chi}_2^0/\tilde{\chi}_1^+ \tilde{\chi}_1^-$ in which the chargino ($\tilde{\chi}_1^\pm$) decays into a W boson and the lightest neutralino ($\tilde{\chi}_1^0$), while the heavier neutralino ($\tilde{\chi}_2^0$) decays into

either a Z or a Higgs boson and a second $\tilde{\chi}_1^0$ are presented. The searches are performed in events with one isolated lepton, jets and missing transverse momentum, using pp collisions provided by the LHC at a centre-of-mass energy of 13 TeV. Data collected with the ATLAS detector between 2015 and 2018 are used, corresponding to an integrated luminosity of 139 fb^{-1} . No significant deviation from the expected Standard Model background is observed, and limits are set on the direct production of the electroweakinos in simplified models. Searches exploiting large radius jets to identify hadronically decaying W and Z bosons complement the previous ATLAS limits. In the $\tilde{\chi}_1^+ \tilde{\chi}_1^-$ model, masses of $\tilde{\chi}_1^\pm$ ranging from 260 to 520 GeV are excluded at 95% confidence level for a massless $\tilde{\chi}_1^0$. In the $\tilde{\chi}_1^\pm \tilde{\chi}_2^0$ model with $\tilde{\chi}_2^0$ decaying via a Z boson, masses of $\tilde{\chi}_1^\pm / \tilde{\chi}_2^0$ ranging from 260 to 420 GeV are excluded at 95% CL for a massless $\tilde{\chi}_1^0$. Utilizing a BDT discriminant, the search targeting $\tilde{\chi}_1^\pm \tilde{\chi}_2^0$ models with $\tilde{\chi}_2^0$ decaying via a Higgs boson and mass-splitting between the mass-degenerate $\tilde{\chi}_1^\pm$ and $\tilde{\chi}_2^0$ as small as the Higgs boson mass and the LSP exceed previous constraints by up to 40 GeV in the range of 200–260 GeV and 280–470 GeV in $m(\tilde{\chi}_1^\pm / \tilde{\chi}_2^0)$.

Acknowledgements

We thank CERN for the very successful operation of the LHC, as well as the support staff from our institutions without whom ATLAS could not be operated efficiently.

We acknowledge the support of ANPCyT, Argentina; YerPhI, Armenia; ARC, Australia; BMWFW and FWF, Austria; ANAS, Azerbaijan; CNPq and FAPESP, Brazil; NSERC, NRC and CFI, Canada; CERN; ANID, Chile; CAS, MOST and NSFC, China; Minciencias, Colombia; MEYS CR, Czech Republic; DNRF and DNSRC, Denmark; IN2P3-CNRS and CEA-DRF/IRFU, France; SRNSFG, Georgia; BMBF, HGF and MPG, Germany; GSRI, Greece; RGC and Hong Kong SAR, China; ISF and Benoziyo Center, Israel; INFN, Italy; MEXT and JSPS, Japan; CNRST, Morocco; NWO, Netherlands; RCN, Norway; MEiN, Poland; FCT, Portugal; MNE/IFA, Romania; MESTD, Serbia; MSSR, Slovakia; ARRS and MIZŠ, Slovenia; DSI/NRF, South Africa; MICINN, Spain; SRC and Wallenberg Foundation, Sweden; SERI, SNSF and Cantons of Bern and Geneva, Switzerland; MOST, Taiwan; TENMAK, Türkiye; STFC, United Kingdom; DOE and NSF, United States of America. In addition, individual groups and members have received support from BCKDF, CANARIE, Compute Canada and CRC, Canada; PRIMUS 21/SCI/017 and UNCE SCI/013, Czech Republic; COST, ERC, ERDF, Horizon 2020 and Marie Skłodowska-Curie Actions, European Union; Investissements d’Avenir Labex, Investissements d’Avenir IDEX and ANR, France; DFG and AvH Foundation, Germany; Herakleitos, Thales and Aristeia programmes co-financed by EU-ESF and the Greek NSRF, Greece; BSF-NSF and MINERVA, Israel; Norwegian Financial Mechanism 2014-2021, Norway; NCN and NAWA, Poland; La Caixa Banking Foundation, CERCA Programme Generalitat de Catalunya and PROMETEO and GenT Programmes Generalitat Valenciana, Spain; Göran Gustafssons Stiftelse, Sweden; The Royal Society and Leverhulme Trust, United Kingdom.

The crucial computing support from all WLCG partners is acknowledged gratefully, in particular from CERN, the ATLAS Tier-1 facilities at TRIUMF (Canada), NDGF (Denmark, Norway, Sweden), CC-IN2P3 (France), KIT/GridKA (Germany), INFN-CNAF (Italy), NL-T1 (Netherlands), PIC (Spain), ASGC (Taiwan), RAL (UK) and BNL (USA), the Tier-2 facilities worldwide and large non-WLCG resource providers. Major contributors of computing resources are listed in Ref. [123].

References

- [1] N. Sakai, *Naturalness in supersymmetric GUTS*, *Z. Phys. C* **11** (1981) 153.
- [2] S. Dimopoulos, S. Raby and F. Wilczek, *Supersymmetry and the scale of unification*, *Phys. Rev. D* **24** (1981) 1681.
- [3] L. E. Ibáñez and G. G. Ross, *Low-energy predictions in supersymmetric grand unified theories*, *Phys. Lett. B* **105** (1981) 439.
- [4] S. Dimopoulos and H. Georgi, *Softly broken supersymmetry and SU(5)*, *Nucl. Phys. B* **193** (1981) 150.
- [5] ATLAS Collaboration, *Observation of a new particle in the search for the Standard Model Higgs boson with the ATLAS detector at the LHC*, *Phys. Lett. B* **716** (2012) 1, arXiv: 1207.7214 [hep-ex].
- [6] CMS Collaboration, *Observation of a new boson at a mass of 125 GeV with the CMS experiment at the LHC*, *Phys. Lett. B* **716** (2012) 30, arXiv: 1207.7235 [hep-ex].
- [7] ATLAS and CMS Collaborations, *Combined Measurement of the Higgs Boson Mass in pp Collisions at $\sqrt{s} = 7$ and 8 TeV with the ATLAS and CMS Experiments*, *Phys. Rev. Lett.* **114** (2015) 191803, arXiv: 1503.07589 [hep-ex].
- [8] ATLAS and CMS Collaborations, *Measurements of the Higgs boson production and decay rates and constraints on its couplings from a combined ATLAS and CMS analysis of the LHC pp collision data at $\sqrt{s} = 7$ and 8 TeV*, *JHEP* **08** (2016) 045, arXiv: 1606.02266 [hep-ex].
- [9] Y. A. Golfand and E. P. Likhtman, *Extension of the Algebra of Poincare Group Generators and Violation of P invariance*, *JETP Lett.* **13** (1971) 323, [*Pisma Zh. Eksp. Teor. Fiz.* **13** (1971) 452].
- [10] D. V. Volkov and V. P. Akulov, *Is the neutrino a goldstone particle?*, *Phys. Lett. B* **46** (1973) 109.
- [11] J. Wess and B. Zumino, *Supergauge transformations in four-dimensions*, *Nucl. Phys. B* **70** (1974) 39.
- [12] J. Wess and B. Zumino, *Supergauge invariant extension of quantum electrodynamics*, *Nucl. Phys. B* **78** (1974) 1.
- [13] S. Ferrara and B. Zumino, *Supergauge invariant Yang-Mills theories*, *Nucl. Phys. B* **79** (1974) 413.
- [14] A. Salam and J. A. Strathdee, *Super-symmetry and non-Abelian gauges*, *Phys. Lett. B* **51** (1974) 353.
- [15] G. R. Farrar and P. Fayet, *Phenomenology of the production, decay, and detection of new hadronic states associated with supersymmetry*, *Phys. Lett. B* **76** (1978) 575.
- [16] H. Goldberg, *Constraint on the Photino Mass from Cosmology*, *Phys. Rev. Lett.* **50** (1983) 1419, [Erratum: *Phys. Rev. Lett.* **103** (2009) 099905].
- [17] J. R. Ellis, J. S. Hagelin, D. V. Nanopoulos, K. A. Olive and M. Srednicki, *Supersymmetric relics from the big bang*, *Nucl. Phys. B* **238** (1984) 453.
- [18] R. Barbieri and G. F. Giudice, *Upper bounds on supersymmetric particle masses*, *Nucl. Phys. B* **306** (1988) 63.

- [19] B. de Carlos and J. A. Casas, *One-loop analysis of the electroweak breaking in supersymmetric models and the fine-tuning problem*, *Phys. Lett. B* **309** (1993) 320, arXiv: [hep-ph/9303291](#) [[hep-ph](#)].
- [20] J. L. Feng and T. Moroi, *Supernatural supersymmetry: Phenomenological implications of anomaly-mediated supersymmetry breaking*, *Phys. Rev. D* **61** (2000) 095004.
- [21] S. Heinemeyer, W. Hollik and G. Weiglein, *Electroweak precision observables in the minimal supersymmetric standard model*, *Physics Reports* **425** (2006) 265.
- [22] P. Fayet, *Supersymmetry and Weak, Electromagnetic and Strong Interactions*, *Phys. Lett. B* **64** (1976) 159.
- [23] P. Fayet, *Spontaneously broken supersymmetric theories of weak, electromagnetic and strong interactions*, *Phys. Lett. B* **69** (1977) 489.
- [24] J. F. Gunion et al., *Calculation and Phenomenology of Two Body Decays of Neutralinos and Charginos to W, Z, and Higgs Bosons*, *Int. J. Mod. Phys. A* **2** (1987) 1145.
- [25] J. Alwall, P. Schuster and N. Toro, *Simplified models for a first characterization of new physics at the LHC*, *Phys. Rev. D* **79** (2009) 075020, arXiv: [0810.3921](#) [[hep-ph](#)].
- [26] D. Alves et al., *Simplified models for LHC new physics searches*, *J. Phys. G* **39** (2012) 105005, arXiv: [1105.2838](#) [[hep-ph](#)].
- [27] ATLAS Collaboration, *Search for chargino and neutralino production in final states with a Higgs boson and missing transverse momentum at $\sqrt{s} = 13$ TeV with the ATLAS detector*, *Phys. Rev. D* **100** (2019) 012006, arXiv: [1812.09432](#) [[hep-ex](#)].
- [28] ATLAS Collaboration, *Searches for new phenomena in events with two leptons, jets, and missing transverse momentum in 139 fb^{-1} of $\sqrt{s} = 13$ TeV pp collisions with the ATLAS detector*, *Eur. Phys. J. C* **83** (2022) 515, arXiv: [2204.13072](#) [[hep-ex](#)].
- [29] ATLAS Collaboration, *Search for electroweak production of charginos and sleptons decaying into final states with two leptons and missing transverse momentum in $\sqrt{s} = 13$ TeV pp collisions using the ATLAS detector*, *Eur. Phys. J. C* **80** (2020) 123, arXiv: [1908.08215](#) [[hep-ex](#)].
- [30] ATLAS Collaboration, *Search for charginos and neutralinos in final states with two boosted hadronically decaying bosons and missing transverse momentum in pp collisions at $\sqrt{s} = 13$ TeV with the ATLAS detector*, *Phys. Rev. D* **104** (2021) 112010, arXiv: [2108.07586](#) [[hep-ex](#)].
- [31] ATLAS Collaboration, *Search for chargino–neutralino pair production in final states with three leptons and missing transverse momentum in $\sqrt{s} = 13$ TeV pp collisions with the ATLAS detector*, *Eur. Phys. J. C* **81** (2021) 1118, arXiv: [2106.01676](#) [[hep-ex](#)].
- [32] CMS Collaboration, *Search for electroweak production of charginos and neutralinos in proton–proton collisions at $\sqrt{s} = 13$ TeV*, *JHEP* **04** (2021) 147, arXiv: [2106.14246](#) [[hep-ex](#)].
- [33] CMS Collaboration, *Search for supersymmetry in final states with two oppositely charged same-flavor leptons and missing transverse momentum in proton–proton collisions at $\sqrt{s} = 13$ TeV*, *JHEP* **04** (2020) 123, arXiv: [2012.08600](#) [[hep-ex](#)].

- [34] CMS Collaboration, *Search for electroweak production of charginos and neutralinos at $\sqrt{s} = 13$ TeV in final states containing hadronic decays of WW, WZ, or WH and missing transverse momentum*, *Phys. Lett. B* **842** (2022) 137460, arXiv: 2205.09597 [hep-ex].
- [35] ATLAS Collaboration, *Search for direct production of electroweakinos in final states with one lepton, missing transverse momentum and a Higgs boson decaying into two b-jets in pp collisions at $\sqrt{s} = 13$ TeV with the ATLAS detector*, *Eur. Phys. J. C* **80** (2020) 691, arXiv: 1909.09226 [hep-ex].
- [36] CMS Collaboration, *Search for chargino-neutralino production in events with Higgs and W bosons using 137 fb^{-1} of proton-proton collisions at $\sqrt{s} = 13$ TeV*, *JHEP* **10** (2021) 045, arXiv: 2107.12553 [hep-ex].
- [37] ATLAS Collaboration, *The ATLAS Experiment at the CERN Large Hadron Collider*, *JINST* **3** (2008) S08003.
- [38] ATLAS Collaboration, *ATLAS Insertable B-Layer Technical Design Report*, ATLAS-TDR-19, 2010, URL: <https://cds.cern.ch/record/1291633>, *ATLAS Insertable B-Layer Technical Design Report Addendum*, ATLAS-TDR-19-ADD-1, 2012, URL: <https://cds.cern.ch/record/1451888>.
- [39] B. Abbott et al., *Production and integration of the ATLAS Insertable B-Layer*, *JINST* **13** (2018) T05008, arXiv: 1803.00844 [physics.ins-det].
- [40] ATLAS Collaboration, *Performance of the ATLAS trigger system in 2015*, *Eur. Phys. J. C* **77** (2017) 317, arXiv: 1611.09661 [hep-ex].
- [41] ATLAS Collaboration, *The ATLAS Collaboration Software and Firmware*, ATL-SOFT-PUB-2021-001, 2021, URL: <https://cds.cern.ch/record/2767187>.
- [42] ATLAS Collaboration, *Luminosity determination in pp collisions at $\sqrt{s} = 13$ TeV using the ATLAS detector at the LHC*, ATLAS-CONF-2019-021, 2019, URL: <https://cds.cern.ch/record/2677054>.
- [43] G. Avoni et al., *The new LUCID-2 detector for luminosity measurement and monitoring in ATLAS*, *JINST* **13** (2018) P07017.
- [44] S. Agostinelli et al., *GEANT4 - a simulation toolkit*, *Nucl. Instrum. Meth. A* **506** (2003) 250.
- [45] ATLAS Collaboration, *The ATLAS Simulation Infrastructure*, *Eur. Phys. J. C* **70** (2010) 823, arXiv: 1005.4568 [physics.ins-det].
- [46] ATLAS Collaboration, *The simulation principle and performance of the ATLAS fast calorimeter simulation FastCaloSim*, ATL-PHYS-PUB-2010-013, 2010, URL: <https://cds.cern.ch/record/1300517>.
- [47] T. Sjöstrand, S. Mrenna and P. Z. Skands, *A brief introduction to PYTHIA 8.1*, *Comput. Phys. Commun.* **178** (2008) 852, arXiv: 0710.3820 [hep-ph].
- [48] R. D. Ball et al., *Parton distributions with LHC data*, *Nucl. Phys. B* **867** (2013) 244, arXiv: 1207.1303 [hep-ph].
- [49] ATLAS Collaboration, *The Pythia 8 A3 tune description of ATLAS minimum bias and inelastic measurements incorporating the Donnachie–Landshoff diffractive model*, ATL-PHYS-PUB-2016-017, 2016, URL: <https://cds.cern.ch/record/2206965>.

- [50] T. Gleisberg and S. Höche, *Comix, a new matrix element generator*, *JHEP* **12** (2008) 039, arXiv: [0808.3674 \[hep-ph\]](#).
- [51] F. Cascioli, P. Maierhöfer and S. Pozzorini, *Scattering Amplitudes with Open Loops*, *Phys. Rev. Lett.* **108** (2012) 111601, arXiv: [1111.5206 \[hep-ph\]](#).
- [52] A. Denner, S. Dittmaier and L. Hofer, *COLLIER: A fortran-based complex one-loop library in extended regularizations*, *Comput. Phys. Commun.* **212** (2017) 220, arXiv: [1604.06792 \[hep-ph\]](#).
- [53] S. Schumann and F. Krauss, *A parton shower algorithm based on Catani–Seymour dipole factorisation*, *JHEP* **03** (2008) 038, arXiv: [0709.1027 \[hep-ph\]](#).
- [54] S. Höche, F. Krauss, M. Schönherr and F. Siegert, *A critical appraisal of NLO+PS matching methods*, *JHEP* **09** (2012) 049, arXiv: [1111.1220 \[hep-ph\]](#).
- [55] S. Höche, F. Krauss, M. Schönherr and F. Siegert, *QCD matrix elements + parton showers. The NLO case*, *JHEP* **04** (2013) 027, arXiv: [1207.5030 \[hep-ph\]](#).
- [56] S. Catani, F. Krauss, B. R. Webber and R. Kuhn, *QCD Matrix Elements + Parton Showers*, *JHEP* **11** (2001) 063, arXiv: [hep-ph/0109231](#).
- [57] S. Höche, F. Krauss, S. Schumann and F. Siegert, *QCD matrix elements and truncated showers*, *JHEP* **05** (2009) 053, arXiv: [0903.1219 \[hep-ph\]](#).
- [58] D. J. Lange, *The EvtGen particle decay simulation package*, *Nucl. Instrum. Meth. A* **462** (2001) 152.
- [59] L. Lönnblad and S. Prestel, *Merging multi-leg NLO matrix elements with parton showers*, *JHEP* **03** (2013) 166, arXiv: [1211.7278 \[hep-ph\]](#).
- [60] J. Alwall et al., *The automated computation of tree-level and next-to-leading order differential cross sections, and their matching to parton shower simulations*, *JHEP* **07** (2014) 079, arXiv: [1405.0301 \[hep-ph\]](#).
- [61] ATLAS Collaboration, *ATLAS Pythia 8 tunes to 7 TeV data*, ATL-PHYS-PUB-2014-021, 2014, URL: <https://cds.cern.ch/record/1966419>.
- [62] J. Debove, B. Fuks and M. Klasen, *Threshold resummation for gaugino pair production at hadron colliders*, *Nucl. Phys. B* **842** (2011) 51, arXiv: [1005.2909 \[hep-ph\]](#).
- [63] B. Fuks, M. Klasen, D. R. Lamprea and M. Rothering, *Gaugino production in proton-proton collisions at a center-of-mass energy of 8 TeV*, *JHEP* **1210** (2012) 081, arXiv: [1207.2159 \[hep-ph\]](#).
- [64] B. Fuks, M. Klasen, D. R. Lamprea and M. Rothering, *Precision predictions for electroweak superpartner production at hadron colliders with Resummino*, *Eur.Phys.J.* **C73** (2013) 2480, arXiv: [1304.0790 \[hep-ph\]](#).
- [65] J. Fiaschi and M. Klasen, *Neutralino-chargino pair production at NLO+NLL with resummation-improved parton density functions for LHC Run II*, *Phys. Rev. D* **98** (2018) 055014, arXiv: [1805.11322 \[hep-ph\]](#).

- [66] C. Borschensky et al.,
Squark and gluino production cross sections in pp collisions at $\sqrt{s} = 13, 14, 33$ and 100 TeV,
Eur. Phys. J. C **74** (2014) 3174, arXiv: [1407.5066 \[hep-ph\]](#).
- [67] S. Alioli, P. Nason, C. Oleari and E. Re, *A general framework for implementing NLO calculations in shower Monte Carlo programs: the POWHEG BOX*, *JHEP* **06** (2010) 043,
arXiv: [1002.2581 \[hep-ph\]](#).
- [68] S. Frixione, P. Nason and C. Oleari,
Matching NLO QCD computations with parton shower simulations: the POWHEG method,
JHEP **11** (2007) 070, arXiv: [0709.2092 \[hep-ph\]](#).
- [69] S. Frixione, P. Nason and G. Ridolfi,
A positive-weight next-to-leading-order Monte Carlo for heavy flavour hadroproduction,
JHEP **09** (2007) 126, arXiv: [0707.3088 \[hep-ph\]](#).
- [70] P. Nason, *A new method for combining NLO QCD with shower Monte Carlo algorithms*,
JHEP **11** (2004) 040, arXiv: [hep-ph/0409146](#).
- [71] M. Czakon and A. Mitov,
Top++: A program for the calculation of the top-pair cross-section at hadron colliders,
Comput. Phys. Commun. **185** (2014) 2930, arXiv: [1112.5675 \[hep-ph\]](#).
- [72] E. Re,
Single-top Wt-channel production matched with parton showers using the POWHEG method,
Eur. Phys. J. C **71** (2011) 1547, arXiv: [1009.2450 \[hep-ph\]](#).
- [73] R. Frederix, E. Re and P. Torrielli,
Single-top t-channel hadroproduction in the four-flavour scheme with POWHEG and aMC@NLO,
JHEP **09** (2012) 130, arXiv: [1207.5391 \[hep-ph\]](#).
- [74] S. Alioli, P. Nason, C. Oleari and E. Re,
NLO single-top production matched with shower in POWHEG: s- and t-channel contributions,
JHEP **09** (2009) 111, [Erratum: *JHEP*02,011(2010)], arXiv: [0907.4076 \[hep-ph\]](#).
- [75] M. Aliev et al., *HATHOR – HAdronic Top and Heavy quarks crOss section calculatoR*,
Comput. Phys. Commun. **182** (2011) 1034, arXiv: [1007.1327 \[hep-ph\]](#).
- [76] T. Gleisberg et al., *Event generation with SHERPA 1.1*, *JHEP* **02** (2009) 007,
arXiv: [0811.4622 \[hep-ph\]](#).
- [77] C. Anastasiou, L. J. Dixon, K. Melnikov and F. Petriello,
High precision QCD at hadron colliders: Electroweak gauge boson rapidity distributions at NNLO,
Phys. Rev. D **69** (2004) 094008, arXiv: [hep-ph/0312266](#).
- [78] P. Bärnreuther, M. Czakon and A. Mitov, *Percent Level Precision Physics at the Tevatron: First Genuine NNLO QCD Corrections to $q\bar{q} \rightarrow t\bar{t} + X$* , *Phys. Rev. Lett.* **109** (2012) 132001,
arXiv: [1204.5201 \[hep-ph\]](#).
- [79] ATLAS Collaboration, *Measurement of the Z/γ^* boson transverse momentum distribution in pp collisions at $\sqrt{s} = 7$ TeV with the ATLAS detector*, *JHEP* **09** (2014) 145,
arXiv: [1406.3660 \[hep-ex\]](#).
- [80] P. M. Nadolsky et al., *Implications of CTEQ global analysis for collider observables*,
Phys. Rev. D **78** (2008) 013004, arXiv: [0802.0007 \[hep-ph\]](#).

- [81] D. de Florian et al., *Handbook of LHC Higgs Cross Sections: 4. Deciphering the Nature of the Higgs Sector*, (2016), arXiv: [1610.07922](https://arxiv.org/abs/1610.07922) [hep-ph].
- [82] ATLAS Collaboration, *Vertex Reconstruction Performance of the ATLAS Detector at $\sqrt{s} = 13$ TeV*, ATL-PHYS-PUB-2015-026, 2015, URL: <https://cds.cern.ch/record/2037717>.
- [83] ATLAS Collaboration, *Selection of jets produced in 13 TeV proton–proton collisions with the ATLAS detector*, ATLAS-CONF-2015-029, 2015, URL: <https://cds.cern.ch/record/2037702>.
- [84] ATLAS Collaboration, *Electron and photon performance measurements with the ATLAS detector using the 2015-2017 LHC proton-proton collision data*, (2019), arXiv: [1908.00005](https://arxiv.org/abs/1908.00005) [hep-ex].
- [85] ATLAS Collaboration, *Evidence for the associated production of the Higgs boson and a top quark pair with the ATLAS detector*, *Phys. Rev. D* **97** (7 2018) 072003, URL: <https://link.aps.org/doi/10.1103/PhysRevD.97.072003>.
- [86] ATLAS Collaboration, *Muon reconstruction performance of the ATLAS detector in proton–proton collision data at $\sqrt{s} = 13$ TeV*, *Eur. Phys. J. C* **76** (2016) 292, arXiv: [1603.05598](https://arxiv.org/abs/1603.05598) [hep-ex].
- [87] ATLAS Collaboration, *Muon reconstruction and identification efficiency in ATLAS using the full Run 2 pp collision data set at $\sqrt{s} = 13$ TeV*, *Eur. Phys. J. C* **81** (2021) 578, arXiv: [2012.00578](https://arxiv.org/abs/2012.00578) [hep-ex].
- [88] ATLAS Collaboration, *Topological cell clustering in the ATLAS calorimeters and its performance in LHC Run 1*, *Eur. Phys. J. C* **77** (2017) 490, arXiv: [1603.02934](https://arxiv.org/abs/1603.02934) [hep-ex].
- [89] M. Cacciari, G. P. Salam and G. Soyez, *The anti- k_t jet clustering algorithm*, *JHEP* **04** (2008) 063, arXiv: [0802.1189](https://arxiv.org/abs/0802.1189) [hep-ph].
- [90] ATLAS Collaboration, *Performance of pile-up mitigation techniques for jets in pp collisions at $\sqrt{s} = 8$ TeV using the ATLAS detector*, *Eur. Phys. J. C* **76** (2016) 581, arXiv: [1510.03823](https://arxiv.org/abs/1510.03823) [hep-ex].
- [91] M. Cacciari, G. P. Salam and G. Soyez, *FastJet user manual*, *Eur. Phys. J. C* **72** (2012) 1896, arXiv: [1111.6097](https://arxiv.org/abs/1111.6097) [hep-ph].
- [92] ATLAS Collaboration, *Jet Calibration and Systematic Uncertainties for Jets Reconstructed in the ATLAS Detector at $\sqrt{s} = 13$ TeV*, ATL-PHYS-PUB-2015-015, 2015, URL: <https://cds.cern.ch/record/2037613>.
- [93] D. Krohn, J. Thaler and L.-T. Wang, *Jet trimming*, *JHEP* **02** (2010) 084, arXiv: [0912.1342](https://arxiv.org/abs/0912.1342) [hep-ph].
- [94] ATLAS Collaboration, *Jet mass reconstruction with the ATLAS Detector in early Run 2 data*, ATLAS-CONF-2016-035, 2016, URL: <https://cds.cern.ch/record/2200211>.
- [95] ATLAS Collaboration, *Performance of top-quark and W-boson tagging with ATLAS in Run 2 of the LHC*, *Eur. Phys. J. C* **79** (2019) 375, arXiv: [1808.07858](https://arxiv.org/abs/1808.07858) [hep-ex].
- [96] ATLAS Collaboration, *Boosted hadronic vector boson and top quark tagging with ATLAS using Run 2 data*, ATL-PHYS-PUB-2020-017, 2020, URL: <https://cds.cern.ch/record/2724149>.

- [97] ATLAS Collaboration, *ATLAS flavour-tagging algorithms for the LHC Run 2 pp collision dataset*, *Eur. Phys. J. C* **83** (2022) 681, arXiv: 2211.16345 [[physics.data-an](#)].
- [98] M. Cacciari, G. P. Salam and G. Soyez, *The catchment area of jets*, *JHEP* **04** (2008) 005, arXiv: 0802.1188 [[hep-ph](#)].
- [99] ATLAS Collaboration, *Measurement of the photon identification efficiencies with the ATLAS detector using LHC Run 2 data collected in 2015 and 2016*, *Eur. Phys. J. C* **79** (2019) 205, arXiv: 1810.05087 [[hep-ex](#)].
- [100] ATLAS Collaboration, *Performance of missing transverse momentum reconstruction with the ATLAS detector using proton–proton collisions at $\sqrt{s} = 13$ TeV*, *Eur. Phys. J. C* **78** (2018) 903, arXiv: 1802.08168 [[hep-ex](#)].
- [101] ATLAS Collaboration, *E_T^{miss} performance in the ATLAS detector using 2015–2016 LHC pp collisions*, ATLAS-CONF-2018-023, 2018, URL: <https://cds.cern.ch/record/2625233>.
- [102] ATLAS Collaboration, *Performance of the ATLAS muon triggers in Run 2*, *JINST* **15** (2020) P09015, arXiv: 2004.13447 [[hep-ex](#)].
- [103] ATLAS Collaboration, *Performance of electron and photon triggers in ATLAS during LHC Run 2*, *Eur. Phys. J. C* **80** (2020) 47, arXiv: 1909.00761 [[hep-ex](#)].
- [104] M. Baak et al., *HistFitter software framework for statistical data analysis*, *Eur. Phys. J. C* **75** (2015) 153, arXiv: 1410.1280 [[hep-ex](#)].
- [105] ATLAS Collaboration, *Object-based missing transverse momentum significance in the ATLAS Detector*, ATLAS-CONF-2018-038, 2018, URL: <https://cds.cern.ch/record/2630948>.
- [106] C. G. Lester and B. Nachman, *Bisection-based asymmetric M_{T2} computation: a higher precision calculator than existing symmetric methods*, *JHEP* **03** (2015) 100, arXiv: 1411.4312 [[hep-ph](#)].
- [107] D. R. Tovey, *On measuring the masses of pair-produced semi-invisibly decaying particles at hadron colliders*, *JHEP* **04** (2008) 034, arXiv: 0802.2879 [[hep-ph](#)].
- [108] T. Chen and C. Guestrin, *{XGBoost}: A Scalable Tree Boosting System*, *Proceedings of the 22nd ACM SIGKDD International Conference on Knowledge Discovery and Data Mining* (2016), arXiv: 1603.02754 [[cs.LG](#)].
- [109] ATLAS Collaboration, *Tools for estimating fake/non-prompt lepton backgrounds with the ATLAS detector at the LHC*, (2022), arXiv: 2211.16178 [[hep-ex](#)].
- [110] ATLAS Collaboration, *Jet energy scale measurements and their systematic uncertainties in proton–proton collisions at $\sqrt{s} = 13$ TeV with the ATLAS detector*, *Phys. Rev. D* **96** (2017) 072002, arXiv: 1703.09665 [[hep-ex](#)].
- [111] ATLAS Collaboration, *ATLAS b-jet identification performance and efficiency measurement with $t\bar{t}$ events in pp collisions at $\sqrt{s} = 13$ TeV*, *Eur. Phys. J. C* **79** (2019) 970, arXiv: 1907.05120 [[hep-ex](#)].
- [112] ATLAS Collaboration, *Calibration of the b-tagging efficiency on charm jets using a sample of $W + c$ events with $\sqrt{s} = 13$ TeV ATLAS data*, ATLAS-CONF-2018-055, 2018, URL: <https://cds.cern.ch/record/2652195>.

- [113] ATLAS Collaboration, *Electron and photon performance measurements with the ATLAS detector using the 2015–2017 LHC proton–proton collision data*, *JINST* **14** (2019) P12006, arXiv: [1908.00005 \[hep-ex\]](#).
- [114] J. Bellm et al., *Herwig 7.0/Herwig++ 3.0 release note*, *Eur. Phys. J.* **C76** (2016) 196, arXiv: [1512.01178 \[hep-ph\]](#).
- [115] ATLAS Collaboration, *Simulation of top-quark production for the ATLAS experiment at $\sqrt{s} = 13$ TeV*, ATL-PHYS-PUB-2016-004, 2016, URL: <https://cds.cern.ch/record/2120417>.
- [116] M. Aaboud et al., *Search for chargino and neutralino production in final states with a Higgs boson and missing transverse momentum at $\sqrt{s} = 13$ TeV with the ATLAS detector*, *Phys. Rev. D* **100** (2019) 012006, arXiv: [1812.09432 \[hep-ex\]](#).
- [117] J. Butterworth et al., *PDF4LHC recommendations for LHC Run II*, *J. Phys. G* **43** (2016) 023001, arXiv: [1510.03865 \[hep-ph\]](#).
- [118] L. Lönnblad and S. Prestel, *Matching tree-level matrix elements with interleaved showers*, *JHEP* **03** (2012) 019, arXiv: [1109.4829 \[hep-ph\]](#).
- [119] ATLAS Collaboration, *Multi-boson simulation for 13 TeV ATLAS analyses*, ATL-PHYS-PUB-2016-002, 2016, URL: <https://cds.cern.ch/record/2119986>.
- [120] ATLAS Collaboration, *Measurements of the production cross-section for a Z boson in association with b-jets in proton-proton collisions at $\sqrt{s} = 13$ TeV with the ATLAS detector*, *JHEP* **07** (2020) 044, arXiv: [2003.11960 \[hep-ex\]](#).
- [121] R. D. Cousins, J. T. Linnemann and J. Tucker, *Evaluation of three methods for calculating statistical significance when incorporating a systematic uncertainty into a test of the background-only hypothesis for a Poisson process*, *Nucl. Instrum. Meth. A* **595** (2008) 480, arXiv: [physics/0702156 \[physics.data-an\]](#).
- [122] A. L. Read, *Presentation of search results: the CL_s technique*, *J. Phys. G* **28** (2002) 2693.
- [123] ATLAS Collaboration, *ATLAS Computing Acknowledgements*, ATL-SOFT-PUB-2023-001, 2023, URL: <https://cds.cern.ch/record/2869272>.

The ATLAS Collaboration

G. Aad ¹⁰², B. Abbott ¹²⁰, K. Abeling ⁵⁵, N.J. Abicht ⁴⁹, S.H. Abidi ²⁹, A. Aboulhorma ^{35e}, H. Abramowicz ¹⁵¹, H. Abreu ¹⁵⁰, Y. Abulaiti ¹¹⁷, B.S. Acharya ^{69a,69b,q}, C. Adam Bourdarios ⁴, L. Adamczyk ^{86a}, S.V. Addepalli ²⁶, M.J. Addison ¹⁰¹, J. Adelman ¹¹⁵, A. Adiguzel ^{21c}, T. Adye ¹³⁴, A.A. Affolder ¹³⁶, Y. Afik ³⁶, M.N. Agaras ¹³, J. Agarwala ^{73a,73b}, A. Aggarwal ¹⁰⁰, C. Agheorghiesei ^{27c}, A. Ahmad ³⁶, F. Ahmadov ^{38,ak}, W.S. Ahmed ¹⁰⁴, S. Ahuja ⁹⁵, X. Ai ^{62a}, G. Aielli ^{76a,76b}, A. Aikot ¹⁶³, M. Ait Tamlihat ^{35e}, B. Aitbenchikh ^{35a}, I. Aizenberg ¹⁶⁹, M. Akbiyik ¹⁰⁰, T.P.A. Åkesson ⁹⁸, A.V. Akimov ³⁷, D. Akiyama ¹⁶⁸, N.N. Akolkar ²⁴, S. Aktas ^{21a}, K. Al Houry ⁴¹, G.L. Alberghi ^{23b}, J. Albert ¹⁶⁵, P. Albicocco ⁵³, G.L. Albouy ⁶⁰, S. Alderweireldt ⁵², M. Aleksa ³⁶, I.N. Aleksandrov ³⁸, C. Alexa ^{27b}, T. Alexopoulos ¹⁰, F. Alfonsi ^{23b}, M. Algren ⁵⁶, M. Alhroob ¹²⁰, B. Ali ¹³², H.M.J. Ali ⁹¹, S. Ali ¹⁴⁸, S.W. Alibocus ⁹², M. Aliev ¹⁴⁵, G. Alimonti ^{71a}, W. Alkakhri ⁵⁵, C. Allaire ⁶⁶, B.M.M. Allbrooke ¹⁴⁶, J.F. Allen ⁵², C.A. Allendes Flores ^{137f}, P.P. Allport ²⁰, A. Aloisio ^{72a,72b}, F. Alonso ⁹⁰, C. Alpigiani ¹³⁸, M. Alvarez Estevez ⁹⁹, A. Alvarez Fernandez ¹⁰⁰, M. Alves Cardoso ⁵⁶, M.G. Alvigi ^{72a,72b}, M. Aly ¹⁰¹, Y. Amaral Coutinho ^{83b}, A. Ambler ¹⁰⁴, C. Amelung ³⁶, M. Amerl ¹⁰¹, C.G. Ames ¹⁰⁹, D. Amidei ¹⁰⁶, S.P. Amor Dos Santos ^{130a}, K.R. Amos ¹⁶³, V. Ananiev ¹²⁵, C. Anastopoulos ¹³⁹, T. Andeen ¹¹, J.K. Anders ³⁶, S.Y. Andrean ^{47a,47b}, A. Andreazza ^{71a,71b}, S. Angelidakis ⁹, A. Angerami ^{41,ao}, A.V. Anisenkov ³⁷, A. Annovi ^{74a}, C. Antel ⁵⁶, M.T. Anthony ¹³⁹, E. Antipov ¹⁴⁵, M. Antonelli ⁵³, F. Anulli ^{75a}, M. Aoki ⁸⁴, T. Aoki ¹⁵³, J.A. Aparisi Pozo ¹⁶³, M.A. Aparo ¹⁴⁶, L. Aperio Bella ⁴⁸, C. Appelt ¹⁸, A. Apyan ²⁶, N. Aranzabal ³⁶, S.J. Arbiol Val ⁸⁷, C. Arcangeletti ⁵³, A.T.H. Arce ⁵¹, E. Arena ⁹², J-F. Arguin ¹⁰⁸, S. Argyropoulos ⁵⁴, J.-H. Arling ⁴⁸, O. Arnaez ⁴, H. Arnold ¹¹⁴, G. Artoni ^{75a,75b}, H. Asada ¹¹¹, K. Asai ¹¹⁸, S. Asai ¹⁵³, N.A. Asbah ⁶¹, J. Assahsah ^{35d}, K. Assamagan ²⁹, R. Astalos ^{28a}, S. Atashi ¹⁶⁰, R.J. Atkin ^{33a}, M. Atkinson ¹⁶², H. Atmani ^{35f}, P.A. Atlasiddha ¹²⁸, K. Augsten ¹³², S. Auricchio ^{72a,72b}, A.D. Auriol ²⁰, V.A. Austrup ¹⁰¹, G. Avolio ³⁶, K. Axiotis ⁵⁶, G. Azuelos ^{108,av}, D. Babal ^{28b}, H. Bachacou ¹³⁵, K. Bachas ^{152,w}, A. Bachi ³⁴, F. Backman ^{47a,47b}, A. Badea ⁶¹, T.M. Baer ¹⁰⁶, P. Bagnaia ^{75a,75b}, M. Bahmani ¹⁸, A.J. Bailey ¹⁶³, V.R. Bailey ¹⁶², J.T. Baines ¹³⁴, L. Baines ⁹⁴, O.K. Baker ¹⁷², E. Bakos ¹⁵, D. Bakshi Gupta ⁸, V. Balakrishnan ¹²⁰, R. Balasubramanian ¹¹⁴, E.M. Baldin ³⁷, P. Balek ^{86a}, E. Ballabene ^{23b,23a}, F. Balli ¹³⁵, L.M. Baltos ^{63a}, W.K. Balunas ³², J. Balz ¹⁰⁰, E. Banas ⁸⁷, M. Bandieramonte ¹²⁹, A. Bandyopadhyay ²⁴, S. Bansal ²⁴, L. Barak ¹⁵¹, M. Barakat ⁴⁸, E.L. Barberio ¹⁰⁵, D. Barberis ^{57b,57a}, M. Barbero ¹⁰², M.Z. Barel ¹¹⁴, K.N. Barends ^{33a}, T. Barillari ¹¹⁰, M-S. Barisits ³⁶, T. Barklow ¹⁴³, P. Baron ¹²², D.A. Baron Moreno ¹⁰¹, A. Baroncelli ^{62a}, G. Barone ²⁹, A.J. Barr ¹²⁶, J.D. Barr ⁹⁶, L. Barranco Navarro ^{47a,47b}, F. Barreiro ⁹⁹, J. Barreiro Guimarães da Costa ^{14a}, U. Barron ¹⁵¹, M.G. Barros Teixeira ^{130a}, S. Barsov ³⁷, F. Bartels ^{63a}, R. Bartoldus ¹⁴³, A.E. Barton ⁹¹, P. Bartos ^{28a}, A. Basan ^{100,af}, M. Baselga ⁴⁹, A. Bassalat ^{66,b}, M.J. Basso ^{156a}, C.R. Basson ¹⁰¹, R.L. Bates ⁵⁹, S. Batlamous ^{35e}, J.R. Batley ³², B. Batool ¹⁴¹, M. Battaglia ¹³⁶, D. Battulga ¹⁸, M. Bause ^{75a,75b}, M. Bauer ³⁶, P. Bauer ²⁴, L.T. Bazzano Hurrell ³⁰, J.B. Beacham ⁵¹, T. Beau ¹²⁷, J.Y. Beauchamp ⁹⁰, P.H. Beauchemin ¹⁵⁸, F. Becherer ⁵⁴, P. Bechtel ²⁴, H.P. Beck ^{19,u}, K. Becker ¹⁶⁷, A.J. Beddall ⁸², V.A. Bednyakov ³⁸, C.P. Bee ¹⁴⁵, L.J. Beemster ¹⁵, T.A. Beermann ³⁶, M. Begalli ^{83d}, M. Begel ²⁹, A. Behera ¹⁴⁵, J.K. Behr ⁴⁸, J.F. Beirer ³⁶, F. Beisiegel ²⁴, M. Belfkir ¹⁵⁹, G. Bella ¹⁵¹, L. Bellagamba ^{23b}, A. Bellerive ³⁴, P. Bellos ²⁰, K. Beloborodov ³⁷, D. Benckekroun ^{35a}, F. Bendebba ^{35a}, Y. Benhammou ¹⁵¹, M. Benoit ²⁹, J.R. Bensinger ²⁶,

S. Bentvelsen [ID114](#), L. Beresford [ID48](#), M. Beretta [ID53](#), E. Bergeaas Kuutmann [ID161](#), N. Berger [ID4](#),
 B. Bergmann [ID132](#), J. Beringer [ID17a](#), G. Bernardi [ID5](#), C. Bernius [ID143](#), F.U. Bernlochner [ID24](#),
 F. Bernon [ID36,102](#), A. Berrocal Guardia [ID13](#), T. Berry [ID95](#), P. Berta [ID133](#), A. Berthold [ID50](#),
 I.A. Bertram [ID91](#), S. Bethke [ID110](#), A. Betti [ID75a,75b](#), A.J. Bevan [ID94](#), N.K. Bhalla [ID54](#), M. Bhamjee [ID33c](#),
 S. Bhatta [ID145](#), D.S. Bhattacharya [ID166](#), P. Bhattarai [ID143](#), V.S. Bhopatkar [ID121](#), R. Bi [ID29,ay](#),
 R.M. Bianchi [ID129](#), G. Bianco [ID23b,23a](#), O. Biebel [ID109](#), R. Bielski [ID123](#), M. Biglietti [ID77a](#), M. Bindi [ID55](#),
 A. Bingul [ID21b](#), C. Bini [ID75a,75b](#), A. Biondini [ID92](#), C.J. Birch-sykes [ID101](#), G.A. Bird [ID20,134](#),
 M. Birman [ID169](#), M. Biros [ID133](#), S. Biryukov [ID146](#), T. Bisanz [ID49](#), E. Bisceglie [ID43b,43a](#), J.P. Biswal [ID134](#),
 D. Biswas [ID141](#), A. Bitadze [ID101](#), K. Bjørke [ID125](#), I. Bloch [ID48](#), A. Blue [ID59](#), U. Blumenschein [ID94](#),
 J. Blumenthal [ID100](#), G.J. Bobbink [ID114](#), V.S. Bobrovnikov [ID37](#), M. Boehler [ID54](#), B. Boehm [ID166](#),
 D. Bogavac [ID36](#), A.G. Bogdanchikov [ID37](#), C. Bohm [ID47a](#), V. Boisvert [ID95](#), P. Bokan [ID48](#), T. Bold [ID86a](#),
 M. Bomben [ID5](#), M. Bona [ID94](#), M. Boonekamp [ID135](#), C.D. Booth [ID95](#), A.G. Borbély [ID59,as](#),
 I.S. Bordulev [ID37](#), H.M. Borecka-Bielska [ID108](#), G. Borissov [ID91](#), D. Bortoletto [ID126](#), D. Boscherini [ID23b](#),
 M. Bosman [ID13](#), J.D. Bossio Sola [ID36](#), K. Bouaouda [ID35a](#), N. Bouchhar [ID163](#), J. Boudreau [ID129](#),
 E.V. Bouhova-Thacker [ID91](#), D. Boumediene [ID40](#), R. Bouquet [ID165](#), A. Boveia [ID119](#), J. Boyd [ID36](#),
 D. Boye [ID29](#), I.R. Boyko [ID38](#), J. Bracinek [ID20](#), N. Brahimi [ID62d](#), G. Brandt [ID171](#), O. Brandt [ID32](#),
 F. Braren [ID48](#), B. Brau [ID103](#), J.E. Brau [ID123](#), R. Brenner [ID169](#), L. Brenner [ID114](#), R. Brenner [ID161](#),
 S. Bressler [ID169](#), D. Britton [ID59](#), D. Britzger [ID110](#), I. Brock [ID24](#), G. Brooijmans [ID41](#), W.K. Brooks [ID137f](#),
 E. Brost [ID29](#), L.M. Brown [ID165,n](#), L.E. Bruce [ID61](#), T.L. Bruckler [ID126](#), P.A. Bruckman de Renstrom [ID87](#),
 B. Brüers [ID48](#), A. Bruni [ID23b](#), G. Bruni [ID23b](#), M. Bruschi [ID23b](#), N. Bruscinò [ID75a,75b](#), T. Buanes [ID16](#),
 Q. Buat [ID138](#), D. Buchin [ID110](#), A.G. Buckley [ID59](#), O. Bulekov [ID37](#), B.A. Bullard [ID143](#), S. Burdin [ID92](#),
 C.D. Burgard [ID49](#), A.M. Burger [ID40](#), B. Burghgrave [ID8](#), O. Burlayenko [ID54](#), J.T.P. Burr [ID32](#),
 C.D. Burton [ID11](#), J.C. Burzynski [ID142](#), E.L. Busch [ID41](#), V. Büscher [ID100](#), P.J. Bussey [ID59](#),
 J.M. Butler [ID25](#), C.M. Buttar [ID59](#), J.M. Butterworth [ID96](#), W. Buttinger [ID134](#), C.J. Buxo Vazquez [ID107](#),
 A.R. Buzykaev [ID37](#), S. Cabrera Urbán [ID163](#), L. Cadamuro [ID66](#), D. Caforio [ID58](#), H. Cai [ID129](#),
 Y. Cai [ID14a,14e](#), Y. Cai [ID14c](#), V.M.M. Cairo [ID36](#), O. Cakir [ID3a](#), N. Calace [ID36](#), P. Calafiura [ID17a](#),
 G. Calderini [ID127](#), P. Calfayan [ID68](#), G. Callea [ID59](#), L.P. Caloba [ID83b](#), D. Calvet [ID40](#), S. Calvet [ID40](#),
 T.P. Calvet [ID102](#), M. Calvetti [ID74a,74b](#), R. Camacho Toro [ID127](#), S. Camarda [ID36](#), D. Camarero Munoz [ID26](#),
 P. Camarri [ID76a,76b](#), M.T. Camerlingo [ID72a,72b](#), D. Cameron [ID36,h](#), C. Camincher [ID165](#),
 M. Campanelli [ID96](#), A. Camplani [ID42](#), V. Canale [ID72a,72b](#), A. Canesse [ID104](#), J. Cantero [ID163](#), Y. Cao [ID162](#),
 F. Capocasa [ID26](#), M. Capua [ID43b,43a](#), A. Carbone [ID71a,71b](#), R. Cardarelli [ID76a](#), J.C.J. Cardenas [ID8](#),
 F. Cardillo [ID163](#), G. Carducci [ID43b,43a](#), T. Carli [ID36](#), G. Carlino [ID72a](#), J.I. Carlotto [ID13](#), B.T. Carlson [ID129,x](#),
 E.M. Carlson [ID165,156a](#), J. Carmignani [ID92](#), L. Carminati [ID71a,71b](#), A. Carnelli [ID135](#), M. Carnesale [ID75a,75b](#),
 S. Caron [ID113](#), E. Carquin [ID137f](#), S. Carrá [ID71a,71b](#), G. Carratta [ID23b,23a](#), F. Carri Argos [ID33g](#),
 J.W.S. Carter [ID155](#), T.M. Carter [ID52](#), M.P. Casado [ID13,k](#), M. Caspar [ID48](#), F.L. Castillo [ID4](#),
 L. Castillo Garcia [ID13](#), V. Castillo Gimenez [ID163](#), N.F. Castro [ID130a,130e](#), A. Catinaccio [ID36](#),
 J.R. Catmore [ID125](#), V. Cavaliere [ID29](#), N. Cavalli [ID23b,23a](#), V. Cavasinni [ID74a,74b](#), Y.C. Cekmecelioglu [ID48](#),
 E. Celebi [ID21a](#), F. Celli [ID126](#), M.S. Centonze [ID70a,70b](#), V. Cepaitis [ID56](#), K. Cerny [ID122](#),
 A.S. Cerqueira [ID83a](#), A. Cerri [ID146](#), L. Cerrito [ID76a,76b](#), F. Cerutti [ID17a](#), B. Cervato [ID141](#), A. Cervelli [ID23b](#),
 G. Cesarini [ID53](#), S.A. Cetin [ID82](#), D. Chakraborty [ID115](#), J. Chan [ID170](#), W.Y. Chan [ID153](#), J.D. Chapman [ID32](#),
 E. Chapon [ID135](#), B. Chargeishvili [ID149b](#), D.G. Charlton [ID20](#), T.P. Charman [ID94](#), M. Chatterjee [ID19](#),
 C. Chauhan [ID133](#), S. Chekanov [ID6](#), S.V. Chekulaev [ID156a](#), G.A. Chelkov [ID38,a](#), A. Chen [ID106](#),
 B. Chen [ID151](#), B. Chen [ID165](#), H. Chen [ID14c](#), H. Chen [ID29](#), J. Chen [ID62c](#), J. Chen [ID142](#), M. Chen [ID126](#),
 S. Chen [ID153](#), S.J. Chen [ID14c](#), X. Chen [ID62c,135](#), X. Chen [ID14b,au](#), Y. Chen [ID62a](#), C.L. Cheng [ID170](#),
 H.C. Cheng [ID64a](#), S. Cheong [ID143](#), A. Cheplakov [ID38](#), E. Cheremushkina [ID48](#), E. Cherepanova [ID114](#),
 R. Cherkaoui El Moursli [ID35e](#), E. Cheu [ID7](#), K. Cheung [ID65](#), L. Chevalier [ID135](#), V. Chiarella [ID53](#),
 G. Chiarelli [ID74a](#), N. Chiedde [ID102](#), G. Chiodini [ID70a](#), A.S. Chisholm [ID20](#), A. Chitan [ID27b](#),

M. Chitishvili ¹⁶³, M.V. Chizhov ³⁸, K. Choi ¹¹, A.R. Chomont ^{75a,75b}, Y. Chou ¹⁰³,
E.Y.S. Chow ¹¹³, T. Chowdhury ^{33g}, K.L. Chu ¹⁶⁹, M.C. Chu ^{64a}, X. Chu ^{14a,14e}, J. Chudoba ¹³¹,
J.J. Chwastowski ⁸⁷, D. Cieri ¹¹⁰, K.M. Ciesla ^{86a}, V. Cindro ⁹³, A. Ciocio ^{17a}, F. Cirotto ^{72a,72b},
Z.H. Citron ^{169,o}, M. Citterio ^{71a}, D.A. Ciubotaru ^{27b}, A. Clark ⁵⁶, P.J. Clark ⁵², C. Clarry ¹⁵⁵,
J.M. Clavijo Columbie ⁴⁸, S.E. Clawson ⁴⁸, C. Clement ^{47a,47b}, J. Clercx ⁴⁸, Y. Coadou ¹⁰²,
M. Cobal ^{69a,69c}, A. Coccaro ^{57b}, R.F. Coelho Barrue ^{130a}, R. Coelho Lopes De Sa ¹⁰³,
S. Coelli ^{71a}, A.E.C. Coimbra ^{71a,71b}, B. Cole ⁴¹, J. Collot ⁶⁰, P. Conde Muiño ^{130a,130g},
M.P. Connell ^{33c}, S.H. Connell ^{33c}, I.A. Connelly ⁵⁹, E.I. Conroy ¹²⁶, F. Conventi ^{72a,aw},
H.G. Cooke ²⁰, A.M. Cooper-Sarkar ¹²⁶, A. Cordeiro Oudot Choi ¹²⁷, L.D. Corpe ⁴⁰,
M. Corradi ^{75a,75b}, F. Corriveau ^{104,ai}, A. Cortes-Gonzalez ¹⁸, M.J. Costa ¹⁶³, F. Costanza ⁴,
D. Costanzo ¹³⁹, B.M. Cote ¹¹⁹, G. Cowan ⁹⁵, K. Cranmer ¹⁷⁰, D. Cremonini ^{23b,23a},
S. Crépe-Renaudin ⁶⁰, F. Crescioli ¹²⁷, M. Cristinziani ¹⁴¹, M. Cristoforetti ^{78a,78b}, V. Croft ¹¹⁴,
J.E. Crosby ¹²¹, G. Crosetti ^{43b,43a}, A. Cueto ⁹⁹, T. Cuhadar Donszelmann ¹⁶⁰, H. Cui ^{14a,14e},
Z. Cui ⁷, W.R. Cunningham ⁵⁹, F. Curcio ^{43b,43a}, P. Czodrowski ³⁶, M.M. Czurylo ^{63b},
M.J. Da Cunha Sargedas De Sousa ^{57b,57a}, J.V. Da Fonseca Pinto ^{83b}, C. Da Via ¹⁰¹,
W. Dabrowski ^{86a}, T. Dado ⁴⁹, S. Dahbi ^{33g}, T. Dai ¹⁰⁶, D. Dal Santo ¹⁹, C. Dallapiccola ¹⁰³,
M. Dam ⁴², G. D'amen ²⁹, V. D'Amico ¹⁰⁹, J. Damp ¹⁰⁰, J.R. Dandoy ³⁴, M.F. Daneri ³⁰,
M. Danninger ¹⁴², V. Dao ³⁶, G. Darbo ^{57b}, S. Darmora ⁶, S.J. Das ^{29,ay}, S. D'Auria ^{71a,71b},
C. David ^{156b}, T. Davidek ¹³³, B. Davis-Purcell ³⁴, I. Dawson ⁹⁴, H.A. Day-hall ¹³², K. De ⁸,
R. De Asmundis ^{72a}, N. De Biase ⁴⁸, S. De Castro ^{23b,23a}, N. De Groot ¹¹³, P. de Jong ¹¹⁴,
H. De la Torre ¹¹⁵, A. De Maria ^{14c}, A. De Salvo ^{75a}, U. De Sanctis ^{76a,76b}, A. De Santo ¹⁴⁶,
J.B. De Vivie De Regie ⁶⁰, D.V. Dedovich ³⁸, J. Degens ¹¹⁴, A.M. Deiana ⁴⁴, F. Del Corso ^{23b,23a},
J. Del Peso ⁹⁹, F. Del Rio ^{63a}, F. Deliot ¹³⁵, C.M. Delitzsch ⁴⁹, M. Della Pietra ^{72a,72b},
D. Della Volpe ⁵⁶, A. Dell'Acqua ³⁶, L. Dell'Asta ^{71a,71b}, M. Delmastro ⁴, P.A. Delsart ⁶⁰,
S. Demers ¹⁷², M. Demichev ³⁸, S.P. Denisov ³⁷, L. D'Eramo ⁴⁰, D. Derendarz ⁸⁷, F. Derue ¹²⁷,
P. Dervan ⁹², K. Desch ²⁴, C. Deutsch ²⁴, F.A. Di Bello ^{57b,57a}, A. Di Ciaccio ^{76a,76b},
L. Di Ciaccio ⁴, A. Di Domenico ^{75a,75b}, C. Di Donato ^{72a,72b}, A. Di Girolamo ³⁶,
G. Di Gregorio ³⁶, A. Di Luca ^{78a,78b}, B. Di Micco ^{77a,77b}, R. Di Nardo ^{77a,77b}, C. Diaconu ¹⁰²,
M. Diamantopoulou ³⁴, F.A. Dias ¹¹⁴, T. Dias Do Vale ¹⁴², M.A. Diaz ^{137a,137b},
F.G. Diaz Capriles ²⁴, M. Didenko ¹⁶³, E.B. Diehl ¹⁰⁶, L. Diehl ⁵⁴, S. Díez Cornell ⁴⁸,
C. Díez Pardos ¹⁴¹, C. Dimitriadi ^{161,24}, A. Dimitrievska ^{17a}, J. Dingfelder ²⁴, I-M. Dinu ^{27b},
S.J. Dittmeier ^{63b}, F. Dittus ³⁶, F. Djama ¹⁰², T. Djobava ^{149b}, J.I. Djuvslund ¹⁶,
C. Doglioni ^{101,98}, A. Dohnalova ^{28a}, J. Dolejsi ¹³³, Z. Dolezal ¹³³, K.M. Dona ³⁹,
M. Donadelli ^{83c}, B. Dong ¹⁰⁷, J. Donini ⁴⁰, A. D'Onofrio ^{72a,72b}, M. D'Onofrio ⁹²,
J. Dopke ¹³⁴, A. Doria ^{72a}, N. Dos Santos Fernandes ^{130a}, P. Dougan ¹⁰¹, M.T. Dova ⁹⁰,
A.T. Doyle ⁵⁹, M.A. Dragnet ¹²⁶, E. Dreyer ¹⁶⁹, I. Drivas-koulouris ¹⁰, M. Drnevich ¹¹⁷,
A.S. Drobac ¹⁵⁸, M. Drozdova ⁵⁶, D. Du ^{62a}, T.A. du Pree ¹¹⁴, F. Dubinin ³⁷, M. Dubovsky ^{28a},
E. Duchovni ¹⁶⁹, G. Duckeck ¹⁰⁹, O.A. Ducu ^{27b}, D. Duda ⁵², A. Dudarev ³⁶, E.R. Duden ²⁶,
M. D'uffizi ¹⁰¹, L. Dufflot ⁶⁶, M. Dührssen ³⁶, C. Dülsen ¹⁷¹, A.E. Dumitriu ^{27b}, M. Dunford ^{63a},
S. Dungs ⁴⁹, K. Dunne ^{47a,47b}, A. Duperrin ¹⁰², H. Duran Yildiz ^{3a}, M. Düren ⁵⁸,
A. Durglishvili ^{149b}, B.L. Dwyer ¹¹⁵, G.I. Dyckes ^{17a}, M. Dyndal ^{86a}, B.S. Dziedzic ⁸⁷,
Z.O. Earnshaw ¹⁴⁶, G.H. Eberwein ¹²⁶, B. Eckerova ^{28a}, S. Eggebrecht ⁵⁵,
E. Egidio Purcino De Souza ¹²⁷, L.F. Ehrke ⁵⁶, G. Eigen ¹⁶, K. Einsweiler ^{17a}, T. Ekelof ¹⁶¹,
P.A. Ekman ⁹⁸, S. El Farkh ^{35b}, Y. El Ghazali ^{35b}, H. El Jarrari ³⁶, A. El Moussaouy ^{108,ab},
V. Ellajosyula ¹⁶¹, M. Ellert ¹⁶¹, F. Ellinghaus ¹⁷¹, N. Ellis ³⁶, J. Elmsheuser ²⁹, M. Elsing ³⁶,
D. Emelianov ¹³⁴, Y. Enari ¹⁵³, I. Ene ^{17a}, S. Epari ¹³, J. Erdmann ⁴⁹, P.A. Erland ⁸⁷,
M. Errenst ¹⁷¹, M. Escalier ⁶⁶, C. Escobar ¹⁶³, E. Etzion ¹⁵¹, G. Evans ^{130a}, H. Evans ⁶⁸,

L.S. Evans [ID⁹⁵](#), M.O. Evans [ID¹⁴⁶](#), A. Ezhilov [ID³⁷](#), S. Ezzarqtouni [ID^{35a}](#), F. Fabbri [ID⁵⁹](#), L. Fabbri [ID^{23b,23a}](#),
 G. Facini [ID⁹⁶](#), V. Fadeyev [ID¹³⁶](#), R.M. Fakhrutdinov [ID³⁷](#), S. Falciano [ID^{75a}](#), L.F. Falda Ulhoa Coelho [ID³⁶](#),
 P.J. Falke [ID²⁴](#), J. Faltova [ID¹³³](#), C. Fan [ID¹⁶²](#), Y. Fan [ID^{14a}](#), Y. Fang [ID^{14a,14e}](#), M. Fanti [ID^{71a,71b}](#),
 M. Faraj [ID^{69a,69b}](#), Z. Farazpay [ID⁹⁷](#), A. Farbin [ID⁸](#), A. Farilla [ID^{77a}](#), T. Farooque [ID¹⁰⁷](#), S.M. Farrington [ID⁵²](#),
 F. Fassi [ID^{35e}](#), D. Fassouliotis [ID⁹](#), M. Faucci Giannelli [ID^{76a,76b}](#), W.J. Fawcett [ID³²](#), L. Fayard [ID⁶⁶](#),
 P. Federic [ID¹³³](#), P. Federicova [ID¹³¹](#), O.L. Fedin [ID^{37,a}](#), G. Fedotov [ID³⁷](#), M. Feickert [ID¹⁷⁰](#),
 L. Feligioni [ID¹⁰²](#), D.E. Fellers [ID¹²³](#), C. Feng [ID^{62b}](#), M. Feng [ID^{14b}](#), Z. Feng [ID¹¹⁴](#), M.J. Fenton [ID¹⁶⁰](#),
 A.B. Fenyuk [ID³⁷](#), L. Ferencz [ID⁴⁸](#), R.A.M. Ferguson [ID⁹¹](#), S.I. Fernandez Luengo [ID^{137f}](#),
 P. Fernandez Martinez [ID¹³](#), M.J.V. Fernoux [ID¹⁰²](#), J. Ferrando [ID⁴⁸](#), A. Ferrari [ID¹⁶¹](#), P. Ferrari [ID^{114,113}](#),
 R. Ferrari [ID^{73a}](#), D. Ferrere [ID⁵⁶](#), C. Ferretti [ID¹⁰⁶](#), F. Fiedler [ID¹⁰⁰](#), P. Fiedler [ID¹³²](#), A. Filipčič [ID⁹³](#),
 E.K. Filmer [ID¹](#), F. Filthaut [ID¹¹³](#), M.C.N. Fiolhais [ID^{130a,130c,d}](#), L. Fiorini [ID¹⁶³](#), W.C. Fisher [ID¹⁰⁷](#),
 T. Fitschen [ID¹⁰¹](#), P.M. Fitzhugh [ID¹³⁵](#), I. Fleck [ID¹⁴¹](#), P. Fleischmann [ID¹⁰⁶](#), T. Flick [ID¹⁷¹](#), M. Flores [ID^{33d,ap}](#),
 L.R. Flores Castillo [ID^{64a}](#), L. Flores Sanz De Acedo [ID³⁶](#), F.M. Follega [ID^{78a,78b}](#), N. Fomin [ID¹⁶](#),
 J.H. Foo [ID¹⁵⁵](#), B.C. Forland [ID⁶⁸](#), A. Formica [ID¹³⁵](#), A.C. Forti [ID¹⁰¹](#), E. Fortin [ID³⁶](#), A.W. Fortman [ID⁶¹](#),
 M.G. Foti [ID^{17a}](#), L. Fountas [ID^{9,1}](#), D. Fournier [ID⁶⁶](#), H. Fox [ID⁹¹](#), P. Francavilla [ID^{74a,74b}](#), S. Francescato [ID⁶¹](#),
 S. Franchellucci [ID⁵⁶](#), M. Franchini [ID^{23b,23a}](#), S. Franchino [ID^{63a}](#), D. Francis [ID³⁶](#), L. Franco [ID¹¹³](#),
 V. Franco Lima [ID³⁶](#), L. Franconi [ID⁴⁸](#), M. Franklin [ID⁶¹](#), G. Frattari [ID²⁶](#), A.C. Freegard [ID⁹⁴](#),
 W.S. Freund [ID^{83b}](#), Y.Y. Frid [ID¹⁵¹](#), J. Friend [ID⁵⁹](#), N. Fritzsche [ID⁵⁰](#), A. Froch [ID⁵⁴](#), D. Froidevaux [ID³⁶](#),
 J.A. Frost [ID¹²⁶](#), Y. Fu [ID^{62a}](#), S. Fuenzalida Garrido [ID^{137f}](#), M. Fujimoto [ID¹⁰²](#), K.Y. Fung [ID^{64a}](#),
 E. Furtado De Simas Filho [ID^{83b}](#), M. Furukawa [ID¹⁵³](#), J. Fuster [ID¹⁶³](#), A. Gabrielli [ID^{23b,23a}](#),
 A. Gabrielli [ID¹⁵⁵](#), P. Gadow [ID³⁶](#), G. Gagliardi [ID^{57b,57a}](#), L.G. Gagnon [ID^{17a}](#), E.J. Gallas [ID¹²⁶](#),
 B.J. Gallop [ID¹³⁴](#), K.K. Gan [ID¹¹⁹](#), S. Ganguly [ID¹⁵³](#), Y. Gao [ID⁵²](#), F.M. Garay Walls [ID^{137a,137b}](#),
 B. Garcia [ID^{29,ay}](#), C. García [ID¹⁶³](#), A. Garcia Alonso [ID¹¹⁴](#), A.G. Garcia Caffaro [ID¹⁷²](#),
 J.E. García Navarro [ID¹⁶³](#), M. Garcia-Sciveres [ID^{17a}](#), G.L. Gardner [ID¹²⁸](#), R.W. Gardner [ID³⁹](#),
 N. Garelli [ID¹⁵⁸](#), D. Garg [ID⁸⁰](#), R.B. Garg [ID^{143,t}](#), J.M. Gargan [ID⁵²](#), C.A. Garner [ID¹⁵⁵](#), C.M. Garvey [ID^{33a}](#),
 P. Gaspar [ID^{83b}](#), V.K. Gassmann [ID¹⁵⁸](#), G. Gaudio [ID^{73a}](#), V. Gautam [ID¹³](#), P. Gauzzi [ID^{75a,75b}](#), I.L. Gavrilenko [ID³⁷](#),
 A. Gavrilyuk [ID³⁷](#), C. Gay [ID¹⁶⁴](#), G. Gaycken [ID⁴⁸](#), E.N. Gazis [ID¹⁰](#), A.A. Geanta [ID^{27b}](#), C.M. Gee [ID¹³⁶](#),
 A. Gekow [ID¹¹⁹](#), C. Gemme [ID^{57b}](#), M.H. Genest [ID⁶⁰](#), S. Gentile [ID^{75a,75b}](#), A.D. Gentry [ID¹¹²](#), S. George [ID⁹⁵](#),
 W.F. George [ID²⁰](#), T. Geralis [ID⁴⁶](#), P. Gessinger-Befurt [ID³⁶](#), M.E. Geyik [ID¹⁷¹](#), M. Ghani [ID¹⁶⁷](#),
 M. Ghneimat [ID¹⁴¹](#), K. Ghorbanian [ID⁹⁴](#), A. Ghosal [ID¹⁴¹](#), A. Ghosh [ID¹⁶⁰](#), A. Ghosh [ID⁷](#), B. Giacobbe [ID^{23b}](#),
 S. Giagu [ID^{75a,75b}](#), T. Giani [ID¹¹⁴](#), P. Giannetti [ID^{74a}](#), A. Giannini [ID^{62a}](#), S.M. Gibson [ID⁹⁵](#), M. Gignac [ID¹³⁶](#),
 D.T. Gil [ID^{86b}](#), A.K. Gilbert [ID^{86a}](#), B.J. Gilbert [ID⁴¹](#), D. Gillberg [ID³⁴](#), G. Gilles [ID¹¹⁴](#), N.E.K. Gillwald [ID⁴⁸](#),
 L. Ginabat [ID¹²⁷](#), D.M. Gingrich [ID^{2,av}](#), M.P. Giordani [ID^{69a,69c}](#), P.F. Giraud [ID¹³⁵](#), G. Giugliarelli [ID^{69a,69c}](#),
 D. Giugni [ID^{71a}](#), F. Giuli [ID³⁶](#), I. Gkialas [ID^{9,1}](#), L.K. Gladilin [ID³⁷](#), C. Glasman [ID⁹⁹](#), G.R. Gledhill [ID¹²³](#),
 G. Glemža [ID⁴⁸](#), M. Glisic [ID¹²³](#), I. Gnesi [ID^{43b,g}](#), Y. Go [ID^{29,ay}](#), M. Goblirsch-Kolb [ID³⁶](#), B. Gocke [ID⁴⁹](#),
 D. Godin [ID¹⁰⁸](#), B. Gokturk [ID^{21a}](#), S. Goldfarb [ID¹⁰⁵](#), T. Golling [ID⁵⁶](#), M.G.D. Gololo [ID^{33g}](#), D. Golubkov [ID³⁷](#),
 J.P. Gombas [ID¹⁰⁷](#), A. Gomes [ID^{130a,130b}](#), G. Gomes Da Silva [ID¹⁴¹](#), A.J. Gomez Delegido [ID¹⁶³](#),
 R. Gonçalves [ID^{130a,130c}](#), G. Gonella [ID¹²³](#), L. Gonella [ID²⁰](#), A. Gongadze [ID^{149c}](#), F. Gonnella [ID²⁰](#),
 J.L. Gonski [ID⁴¹](#), R.Y. González Andana [ID⁵²](#), S. González de la Hoz [ID¹⁶³](#), S. Gonzalez Fernandez [ID¹³](#),
 R. Gonzalez Lopez [ID⁹²](#), C. Gonzalez Renteria [ID^{17a}](#), M.V. Gonzalez Rodrigues [ID⁴⁸](#),
 R. Gonzalez Suarez [ID¹⁶¹](#), S. Gonzalez-Sevilla [ID⁵⁶](#), G.R. Gonzalvo Rodriguez [ID¹⁶³](#), L. Goossens [ID³⁶](#),
 B. Gorini [ID³⁶](#), E. Gorini [ID^{70a,70b}](#), A. Gorišek [ID⁹³](#), T.C. Gosart [ID¹²⁸](#), A.T. Goshaw [ID⁵¹](#), M.I. Gostkin [ID³⁸](#),
 S. Goswami [ID¹²¹](#), C.A. Gottardo [ID³⁶](#), S.A. Gotz [ID¹⁰⁹](#), M. Goughri [ID^{35b}](#), V. Goumarre [ID⁴⁸](#),
 A.G. Goussiou [ID¹³⁸](#), N. Govender [ID^{33c}](#), I. Grabowska-Bold [ID^{86a}](#), K. Graham [ID³⁴](#), E. Gramstad [ID¹²⁵](#),
 S. Grancagnolo [ID^{70a,70b}](#), M. Grandi [ID¹⁴⁶](#), C.M. Grant [ID^{1,135}](#), P.M. Gravila [ID^{27f}](#), F.G. Gravili [ID^{70a,70b}](#),
 H.M. Gray [ID^{17a}](#), M. Greco [ID^{70a,70b}](#), C. Grefe [ID²⁴](#), I.M. Gregor [ID⁴⁸](#), P. Grenier [ID¹⁴³](#), S.G. Grewe [ID¹¹⁰](#),
 C. Grieco [ID¹³](#), A.A. Grillo [ID¹³⁶](#), K. Grimm [ID³¹](#), S. Grinstein [ID^{13,ad}](#), J.-F. Grivaz [ID⁶⁶](#), E. Gross [ID¹⁶⁹](#),

J. Grosse-Knetter ⁵⁵, C. Grud ¹⁰⁶, J.C. Grundy ¹²⁶, L. Guan ¹⁰⁶, W. Guan ²⁹, C. Gubbels ¹⁶⁴,
 J.G.R. Guerrero Rojas ¹⁶³, G. Guerrieri ^{69a,69c}, F. Guescini ¹¹⁰, R. Gugel ¹⁰⁰, J.A.M. Guhit ¹⁰⁶,
 A. Guida ¹⁸, E. Guilloton ^{167,134}, S. Guindon ³⁶, F. Guo ^{14a,14e}, J. Guo ^{62c}, L. Guo ⁴⁸,
 Y. Guo ¹⁰⁶, R. Gupta ⁴⁸, R. Gupta ¹²⁹, S. Gurbuz ²⁴, S.S. Gurdasani ⁵⁴, G. Gustavino ³⁶,
 M. Guth ⁵⁶, P. Gutierrez ¹²⁰, L.F. Gutierrez Zagazeta ¹²⁸, M. Gutsche ⁵⁰, C. Gutschow ⁹⁶,
 C. Gwenlan ¹²⁶, C.B. Gwilliam ⁹², E.S. Haaland ¹²⁵, A. Haas ¹¹⁷, M. Habedank ⁴⁸,
 C. Haber ^{17a}, H.K. Hadavand ⁸, A. Hadeef ⁵⁰, S. Hadzic ¹¹⁰, A.I. Hagan ⁹¹, J.J. Hahn ¹⁴¹,
 E.H. Haines ⁹⁶, M. Haleem ¹⁶⁶, J. Haley ¹²¹, J.J. Hall ¹³⁹, G.D. Hallewell ¹⁰², L. Halser ¹⁹,
 K. Hamano ¹⁶⁵, M. Hamer ²⁴, G.N. Hamity ⁵², E.J. Hampshire ⁹⁵, J. Han ^{62b}, K. Han ^{62a},
 L. Han ^{14c}, L. Han ^{62a}, S. Han ^{17a}, Y.F. Han ¹⁵⁵, K. Hanagaki ⁸⁴, M. Hance ¹³⁶,
 D.A. Hangal ^{41,ao}, H. Hanif ¹⁴², M.D. Hank ¹²⁸, R. Hankache ¹⁰¹, J.B. Hansen ⁴²,
 J.D. Hansen ⁴², P.H. Hansen ⁴², K. Hara ¹⁵⁷, D. Harada ⁵⁶, T. Harenberg ¹⁷¹, S. Harkusha ³⁷,
 M.L. Harris ¹⁰³, Y.T. Harris ¹²⁶, J. Harrison ¹³, N.M. Harrison ¹¹⁹, P.F. Harrison ¹⁶⁷,
 N.M. Hartman ¹¹⁰, N.M. Hartmann ¹⁰⁹, Y. Hasegawa ¹⁴⁰, R. Hauser ¹⁰⁷, C.M. Hawkes ²⁰,
 R.J. Hawkings ³⁶, Y. Hayashi ¹⁵³, S. Hayashida ¹¹¹, D. Hayden ¹⁰⁷, C. Hayes ¹⁰⁶,
 R.L. Hayes ¹¹⁴, C.P. Hays ¹²⁶, J.M. Hays ⁹⁴, H.S. Hayward ⁹², F. He ^{62a}, M. He ^{14a,14e},
 Y. He ¹⁵⁴, Y. He ⁴⁸, N.B. Heatley ⁹⁴, V. Hedberg ⁹⁸, A.L. Heggelund ¹²⁵, N.D. Hehir ⁹⁴,
 C. Heidegger ⁵⁴, K.K. Heidegger ⁵⁴, W.D. Heidorn ⁸¹, J. Heilman ³⁴, S. Heim ⁴⁸, T. Heim ^{17a},
 J.G. Heinlein ¹²⁸, J.J. Heinrich ¹²³, L. Heinrich ^{110,at}, J. Hejbal ¹³¹, L. Helary ⁴⁸, A. Held ¹⁷⁰,
 S. Hellesund ¹⁶, C.M. Helling ¹⁶⁴, S. Hellman ^{47a,47b}, R.C.W. Henderson ⁹¹, L. Henkelmann ³²,
 A.M. Henriques Correia ³⁶, H. Herde ⁹⁸, Y. Hernández Jiménez ¹⁴⁵, L.M. Herrmann ²⁴,
 T. Herrmann ⁵⁰, G. Herten ⁵⁴, R. Hertenberger ¹⁰⁹, L. Hervas ³⁶, M.E. Hesping ¹⁰⁰,
 N.P. Hessey ^{156a}, H. Hibi ⁸⁵, E. Hill ¹⁵⁵, S.J. Hillier ²⁰, J.R. Hinds ¹⁰⁷, F. Hinterkeuser ²⁴,
 M. Hirose ¹²⁴, S. Hirose ¹⁵⁷, D. Hirschbuehl ¹⁷¹, T.G. Hitchings ¹⁰¹, B. Hiti ⁹³, J. Hobbs ¹⁴⁵,
 R. Hobincu ^{27e}, N. Hod ¹⁶⁹, M.C. Hodgkinson ¹³⁹, B.H. Hodgkinson ³², A. Hoecker ³⁶,
 D.D. Hofer ¹⁰⁶, J. Hofer ⁴⁸, T. Holm ²⁴, M. Holzbock ¹¹⁰, L.B.A.H. Hommels ³²,
 B.P. Honan ¹⁰¹, J. Hong ^{62c}, T.M. Hong ¹²⁹, B.H. Hooberman ¹⁶², W.H. Hopkins ⁶, Y. Horii ¹¹¹,
 S. Hou ¹⁴⁸, A.S. Howard ⁹³, J. Howarth ⁵⁹, J. Hoya ⁶, M. Hrabovsky ¹²², A. Hrynevich ⁴⁸,
 T. Hryn'ova ⁴, P.J. Hsu ⁶⁵, S.-C. Hsu ¹³⁸, Q. Hu ^{62a}, Y.F. Hu ^{14a,14e}, S. Huang ^{64b},
 X. Huang ^{14c}, X. Huang ^{14a,14e}, Y. Huang ^{139,m}, Y. Huang ^{14a}, Z. Huang ¹⁰¹, Z. Hubacek ¹³²,
 M. Huebner ²⁴, F. Hugging ²⁴, T.B. Huffman ¹²⁶, C.A. Hugli ⁴⁸, M. Huhtinen ³⁶,
 S.K. Huiberts ¹⁶, R. Hulsken ¹⁰⁴, N. Huseynov ¹², J. Huston ¹⁰⁷, J. Huth ⁶¹, R. Hyneman ¹⁴³,
 G. Iacobucci ⁵⁶, G. Iakovidis ²⁹, I. Ibragimov ¹⁴¹, L. Iconomidou-Fayard ⁶⁶, P. Iengo ^{72a,72b},
 R. Iguchi ¹⁵³, T. Iizawa ^{126,r}, Y. Ikegami ⁸⁴, N. Ilic ¹⁵⁵, H. Imam ^{35a}, M. Ince Lezki ⁵⁶,
 T. Ingebretsen Carlson ^{47a,47b}, G. Introzzi ^{73a,73b}, M. Iodice ^{77a}, V. Ippolito ^{75a,75b}, R.K. Irwin ⁹²,
 M. Ishino ¹⁵³, W. Islam ¹⁷⁰, C. Issever ^{18,48}, S. Istin ^{21a,ba}, H. Ito ¹⁶⁸, J.M. Iturbe Ponce ^{64a},
 R. Iuppa ^{78a,78b}, A. Ivina ¹⁶⁹, J.M. Izen ⁴⁵, V. Izzo ^{72a}, P. Jacka ^{131,132}, P. Jackson ¹,
 R.M. Jacobs ⁴⁸, B.P. Jaeger ¹⁴², C.S. Jagfeld ¹⁰⁹, G. Jain ^{156a}, P. Jain ⁵⁴, K. Jakobs ⁵⁴,
 T. Jakoubek ¹⁶⁹, J. Jamieson ⁵⁹, K.W. Janas ^{86a}, M. Javurkova ¹⁰³, F. Jeanneau ¹³⁵,
 L. Jeanty ¹²³, J. Jejelava ^{149a,al}, P. Jenni ^{54,i}, C.E. Jessiman ³⁴, S. Jézéquel ⁴, C. Jia ^{62b}, J. Jia ¹⁴⁵,
 X. Jia ⁶¹, X. Jia ^{14a,14e}, Z. Jia ^{14c}, S. Jiggins ⁴⁸, J. Jimenez Pena ¹³, S. Jin ^{14c}, A. Jinaru ^{27b},
 O. Jinnouchi ¹⁵⁴, P. Johansson ¹³⁹, K.A. Johns ⁷, J.W. Johnson ¹³⁶, D.M. Jones ³², E. Jones ⁴⁸,
 P. Jones ³², R.W.L. Jones ⁹¹, T.J. Jones ⁹², H.L. Joos ^{55,36}, R. Joshi ¹¹⁹, J. Jovicevic ¹⁵,
 X. Ju ^{17a}, J.J. Junggeburth ^{103,v}, T. Junkermann ^{63a}, A. Juste Rozas ^{13,ad}, M.K. Juzek ⁸⁷,
 S. Kabana ^{137e}, A. Kaczmarska ⁸⁷, M. Kado ¹¹⁰, H. Kagan ¹¹⁹, M. Kagan ¹⁴³, A. Kahn ⁴¹,
 A. Kahn ¹²⁸, C. Kahra ¹⁰⁰, T. Kaji ¹⁵³, E. Kajomovitz ¹⁵⁰, N. Kakati ¹⁶⁹, I. Kalaitzidou ⁵⁴,
 C.W. Kalderon ²⁹, A. Kamenshchikov ¹⁵⁵, N.J. Kang ¹³⁶, D. Kar ^{33g}, K. Karava ¹²⁶,

M.J. Kareem ^{156b}, E. Karentzos ⁵⁴, I. Karkanias ¹⁵², O. Karkout ¹¹⁴, S.N. Karpov ³⁸,
Z.M. Karpova ³⁸, V. Kartvelishvili ⁹¹, A.N. Karyukhin ³⁷, E. Kasimi ¹⁵², J. Katzy ⁴⁸,
S. Kaur ³⁴, K. Kawade ¹⁴⁰, M.P. Kawale ¹²⁰, C. Kawamoto ⁸⁸, T. Kawamoto ^{62a}, E.F. Kay ³⁶,
F.I. Kaya ¹⁵⁸, S. Kazakos ¹⁰⁷, V.F. Kazanin ³⁷, Y. Ke ¹⁴⁵, J.M. Keaveney ^{33a}, R. Keeler ¹⁶⁵,
G.V. Kehris ⁶¹, J.S. Keller ³⁴, A.S. Kelly ⁹⁶, J.J. Kempster ¹⁴⁶, K.E. Kennedy ⁴¹,
P.D. Kennedy ¹⁰⁰, O. Kepka ¹³¹, B.P. Kerridge ¹⁶⁷, S. Kersten ¹⁷¹, B.P. Kerševan ⁹³,
S. Keshri ⁶⁶, L. Keszeghova ^{28a}, S. Ketabchi Haghghat ¹⁵⁵, R.A. Khan ¹²⁹, M. Khandoga ¹²⁷,
A. Khanov ¹²¹, A.G. Kharlamov ³⁷, T. Kharlamova ³⁷, E.E. Khoda ¹³⁸, M. Kholodenko ³⁷,
T.J. Khoo ¹⁸, G. Khoraiuli ¹⁶⁶, J. Khubua ^{149b}, Y.A.R. Khwaira ⁶⁶, A. Kilgallon ¹²³,
D.W. Kim ^{47a,47b}, Y.K. Kim ³⁹, N. Kimura ⁹⁶, M.K. Kingston ⁵⁵, A. Kirchhoff ⁵⁵, C. Kirfel ²⁴,
F. Kirfel ²⁴, J. Kirk ¹³⁴, A.E. Kiryunin ¹¹⁰, C. Kitsaki ¹⁰, O. Kivernyk ²⁴, M. Klassen ^{63a},
C. Klein ³⁴, L. Klein ¹⁶⁶, M.H. Klein ¹⁰⁶, M. Klein ⁹², S.B. Klein ⁵⁶, U. Klein ⁹²,
P. Klimek ³⁶, A. Klimentov ²⁹, T. Klioutchnikova ³⁶, P. Kluit ¹¹⁴, S. Kluth ¹¹⁰, E. Kneringer ⁷⁹,
T.M. Knight ¹⁵⁵, A. Knue ⁴⁹, R. Kobayashi ⁸⁸, D. Kobylanski ¹⁶⁹, S.F. Koch ¹²⁶,
M. Kocian ¹⁴³, P. Kodyš ¹³³, D.M. Koeck ¹²³, P.T. Koenig ²⁴, T. Koffas ³⁴, O. Kolay ⁵⁰,
I. Koletsou ⁴, T. Komarek ¹²², K. Köneke ⁵⁴, A.X.Y. Kong ¹, T. Kono ¹¹⁸, N. Konstantinidis ⁹⁶,
P. Kontaxakis ⁵⁶, B. Konya ⁹⁸, R. Kopeliansky ⁶⁸, S. Koperny ^{86a}, K. Korcyl ⁸⁷, K. Kordas ^{152.f},
G. Koren ¹⁵¹, A. Korn ⁹⁶, S. Korn ⁵⁵, I. Korolkov ¹³, N. Korotkova ³⁷, B. Kortman ¹¹⁴,
O. Kortner ¹¹⁰, S. Kortner ¹¹⁰, W.H. Kostecka ¹¹⁵, V.V. Kostyukhin ¹⁴¹, A. Kotskechagia ¹³⁵,
A. Kotwal ⁵¹, A. Koulouris ³⁶, A. Kourkoumeli-Charalampidi ^{73a,73b}, C. Kourkoumelis ⁹,
E. Kourlitis ^{110.at}, O. Kovanda ¹⁴⁶, R. Kowalewski ¹⁶⁵, W. Kozanecki ¹³⁵, A.S. Kozhin ³⁷,
V.A. Kramarenko ³⁷, G. Kramberger ⁹³, P. Kramer ¹⁰⁰, M.W. Krasny ¹²⁷, A. Krasznahorkay ³⁶,
J.W. Kraus ¹⁷¹, J.A. Kremer ⁴⁸, T. Kresse ⁵⁰, J. Kretschmar ⁹², K. Kreul ¹⁸, P. Krieger ¹⁵⁵,
S. Krishnamurthy ¹⁰³, M. Krivos ¹³³, K. Krizka ²⁰, K. Kroeninger ⁴⁹, H. Kroha ¹¹⁰, J. Kroll ¹³¹,
J. Kroll ¹²⁸, K.S. Krowpman ¹⁰⁷, U. Kruchonak ³⁸, H. Krüger ²⁴, N. Krumnack ⁸¹, M.C. Kruse ⁵¹,
O. Kuchinskaia ³⁷, S. Kuday ^{3a}, S. Kuehn ³⁶, R. Kuesters ⁵⁴, T. Kuhl ⁴⁸, V. Kukhtin ³⁸,
Y. Kulchitsky ^{37.a}, S. Kuleshov ^{137d,137b}, M. Kumar ^{33g}, N. Kumari ⁴⁸, A. Kupco ¹³¹, T. Kupfer ⁴⁹,
A. Kupich ³⁷, O. Kuprash ⁵⁴, H. Kurashige ⁸⁵, L.L. Kurchaninov ^{156a}, O. Kurdysh ⁶⁶,
Y.A. Kurochkin ³⁷, A. Kurova ³⁷, M. Kuze ¹⁵⁴, A.K. Kvam ¹⁰³, J. Kvita ¹²², T. Kwan ¹⁰⁴,
N.G. Kyriacou ¹⁰⁶, L.A.O. Laatu ¹⁰², C. Lacasta ¹⁶³, F. Lacava ^{75a,75b}, H. Lacker ¹⁸,
D. Lacour ¹²⁷, N.N. Lad ⁹⁶, E. Ladygin ³⁸, B. Laforge ¹²⁷, T. Lagouri ^{137e}, F.Z. Lahbabi ^{35a},
S. Lai ⁵⁵, I.K. Lakomic ^{86a}, N. Lalloue ⁶⁰, J.E. Lambert ^{165.n}, S. Lammers ⁶⁸, W. Lampl ⁷,
C. Lampoudis ^{152.f}, A.N. Lancaster ¹¹⁵, E. Lançon ²⁹, U. Landgraf ⁵⁴, M.P.J. Landon ⁹⁴,
V.S. Lang ⁵⁴, R.J. Langenberg ¹⁰³, O.K.B. Langrekken ¹²⁵, A.J. Lankford ¹⁶⁰, F. Lanni ³⁶,
K. Lantzs ²⁴, A. Lanza ^{73a}, A. Lapertosa ^{57b,57a}, J.F. Laporte ¹³⁵, T. Lari ^{71a},
F. Lasagni Manghi ^{23b}, M. Lassnig ³⁶, V. Latonova ¹³¹, A. Laudrain ¹⁰⁰, A. Laurier ¹⁵⁰,
S.D. Lawlor ¹³⁹, Z. Lawrence ¹⁰¹, R. Lazaridou ¹⁶⁷, M. Lazzaroni ^{71a,71b}, B. Le ¹⁰¹,
E.M. Le Boulicaut ⁵¹, B. Leban ⁹³, A. Lebedev ⁸¹, M. LeBlanc ^{101.ar}, F. Ledroit-Guillon ⁶⁰,
A.C.A. Lee ⁹⁶, S.C. Lee ¹⁴⁸, S. Lee ^{47a,47b}, T.F. Lee ⁹², L.L. Leeuw ^{33c}, H.P. Lefebvre ⁹⁵,
M. Lefebvre ¹⁶⁵, C. Leggett ^{17a}, G. Lehmann Miotto ³⁶, M. Leigh ⁵⁶, W.A. Leight ¹⁰³,
W. Leinonen ¹¹³, A. Leisos ^{152.ac}, M.A.L. Leite ^{83c}, C.E. Leitgeb ⁴⁸, R. Leitner ¹³³,
K.J.C. Leney ⁴⁴, T. Lenz ²⁴, S. Leone ^{74a}, C. Leonidopoulos ⁵², A. Leopold ¹⁴⁴, C. Leroy ¹⁰⁸,
R. Les ¹⁰⁷, C.G. Lester ³², M. Levchenko ³⁷, J. Levêque ⁴, D. Levin ¹⁰⁶, L.J. Levinson ¹⁶⁹,
M.P. Lewicki ⁸⁷, D.J. Lewis ⁴, A. Li ⁵, B. Li ^{62b}, C. Li ^{62a}, C-Q. Li ¹¹⁰, H. Li ^{62a}, H. Li ^{62b},
H. Li ^{14c}, H. Li ^{14b}, H. Li ^{62b}, J. Li ^{62c}, K. Li ¹³⁸, L. Li ^{62c}, M. Li ^{14a,14e}, Q.Y. Li ^{62a},
S. Li ^{14a,14e}, S. Li ^{62d,62c.e}, T. Li ^{5.c}, X. Li ¹⁰⁴, Z. Li ¹²⁶, Z. Li ¹⁰⁴, Z. Li ⁹², Z. Li ^{14a,14e},
S. Liang ^{14a,14e}, Z. Liang ^{14a}, M. Liberatore ^{135.am}, B. Liberti ^{76a}, K. Lie ^{64c}, J. Lieber Marin ^{83b},

H. Lien ⁶⁸, K. Lin ¹⁰⁷, R.E. Lindley ⁷, J.H. Lindon ², E. Lipeles ¹²⁸, A. Lipniacka ¹⁶,
 A. Lister ¹⁶⁴, J.D. Little ⁴, B. Liu ^{14a}, B.X. Liu ¹⁴², D. Liu ^{62d,62c}, J.B. Liu ^{62a}, J.K.K. Liu ³²,
 K. Liu ^{62d,62c}, M. Liu ^{62a}, M.Y. Liu ^{62a}, P. Liu ^{14a}, Q. Liu ^{62d,138,62c}, X. Liu ^{62a}, Y. Liu ^{14d,14e},
 Y.L. Liu ^{62b}, Y.W. Liu ^{62a}, J. Llorente Merino ¹⁴², S.L. Lloyd ⁹⁴, E.M. Lobodzinska ⁴⁸,
 P. Loch ⁷, T. Lohse ¹⁸, K. Lohwasser ¹³⁹, E. Loiacono ⁴⁸, M. Lokajicek ^{131,*}, J.D. Lomas ²⁰,
 J.D. Long ¹⁶², I. Longarini ¹⁶⁰, L. Longo ^{70a,70b}, R. Longo ¹⁶², I. Lopez Paz ⁶⁷,
 A. Lopez Solis ⁴⁸, N. Lorenzo Martinez ⁴, A.M. Lory ¹⁰⁹, O. Loseva ³⁷, X. Lou ^{47a,47b},
 X. Lou ^{14a,14e}, A. Lounis ⁶⁶, J. Love ⁶, P.A. Love ⁹¹, G. Lu ^{14a,14e}, M. Lu ⁸⁰, S. Lu ¹²⁸,
 Y.J. Lu ⁶⁵, H.J. Lubatti ¹³⁸, C. Luci ^{75a,75b}, F.L. Lucio Alves ^{14c}, A. Lucotte ⁶⁰, F. Luehring ⁶⁸,
 I. Luise ¹⁴⁵, O. Lukianchuk ⁶⁶, O. Lundberg ¹⁴⁴, B. Lund-Jensen ¹⁴⁴, N.A. Luongo ⁶,
 M.S. Lutz ¹⁵¹, A.B. Lux ²⁵, D. Lynn ²⁹, H. Lyons ⁹², R. Lysak ¹³¹, E. Lytken ⁹⁸,
 V. Lyubushkin ³⁸, T. Lyubushkina ³⁸, M.M. Lyukova ¹⁴⁵, H. Ma ²⁹, K. Ma ^{62a}, L.L. Ma ^{62b},
 W. Ma ^{62a}, Y. Ma ¹²¹, D.M. Mac Donell ¹⁶⁵, G. Maccarrone ⁵³, J.C. MacDonald ¹⁰⁰,
 P.C. Machado De Abreu Farias ^{83b}, R. Madar ⁴⁰, W.F. Mader ⁵⁰, T. Madula ⁹⁶, J. Maeda ⁸⁵,
 T. Maeno ²⁹, H. Maguire ¹³⁹, V. Maiboroda ¹³⁵, A. Maio ^{130a,130b,130d}, K. Maj ^{86a},
 O. Majersky ⁴⁸, S. Majewski ¹²³, N. Makovec ⁶⁶, V. Maksimovic ¹⁵, B. Malaescu ¹²⁷,
 Pa. Malecki ⁸⁷, V.P. Maleev ³⁷, F. Malek ⁶⁰, M. Mali ⁹³, D. Malito ^{95,s}, U. Mallik ⁸⁰,
 S. Maltezos ¹⁰, S. Malyukov ³⁸, J. Mamuzic ¹³, G. Mancini ⁵³, G. Manco ^{73a,73b}, J.P. Mandalia ⁹⁴,
 I. Mandić ⁹³, L. Manhaes de Andrade Filho ^{83a}, I.M. Maniatis ¹⁶⁹, J. Manjarres Ramos ^{102,an},
 D.C. Mankad ¹⁶⁹, A. Mann ¹⁰⁹, B. Mansoulié ¹³⁵, S. Manzoni ³⁶, L. Mao ^{62c}, X. Mapekula ^{33c},
 A. Marantis ^{152,ac}, G. Marchiori ⁵, M. Marcisovsky ¹³¹, C. Marcon ^{71a,71b}, M. Marinescu ²⁰,
 S. Marium ⁴⁸, M. Marjanovic ¹²⁰, E.J. Marshall ⁹¹, Z. Marshall ^{17a}, S. Marti-Garcia ¹⁶³,
 T.A. Martin ¹⁶⁷, V.J. Martin ⁵², B. Martin dit Latour ¹⁶, L. Martinelli ^{75a,75b}, M. Martinez ^{13,ad},
 P. Martinez Agullo ¹⁶³, V.I. Martinez Outschoorn ¹⁰³, P. Martinez Suarez ¹³, S. Martin-Haugh ¹³⁴,
 V.S. Martoiu ^{27b}, A.C. Martyniuk ⁹⁶, A. Marzin ³⁶, D. Mascione ^{78a,78b}, L. Masetti ¹⁰⁰,
 T. Mashimo ¹⁵³, J. Masik ¹⁰¹, A.L. Maslennikov ³⁷, L. Massa ^{23b}, P. Massarotti ^{72a,72b},
 P. Mastrandrea ^{74a,74b}, A. Mastroberardino ^{43b,43a}, T. Masubuchi ¹⁵³, T. Mathisen ¹⁶¹,
 J. Matousek ¹³³, N. Matsuzawa ¹⁵³, J. Maurer ^{27b}, B. Maček ⁹³, D.A. Maximov ³⁷, R. Mazini ¹⁴⁸,
 I. Maznas ¹⁵², M. Mazza ¹⁰⁷, S.M. Mazza ¹³⁶, E. Mazzeo ^{71a,71b}, C. Mc Ginn ²⁹,
 J.P. Mc Gowan ¹⁰⁴, S.P. Mc Kee ¹⁰⁶, E.F. McDonald ¹⁰⁵, A.E. McDougall ¹¹⁴, J.A. Mcfayden ¹⁴⁶,
 R.P. McGovern ¹²⁸, G. Mchedlidze ^{149b}, R.P. Mckenzie ^{33g}, T.C. McLachlan ⁴⁸,
 D.J. McLaughlin ⁹⁶, S.J. McMahon ¹³⁴, C.M. Mcpartland ⁹², R.A. McPherson ^{165,ai},
 S. Mehlhase ¹⁰⁹, A. Mehta ⁹², D. Melini ¹⁵⁰, B.R. Mellado Garcia ^{33g}, A.H. Melo ⁵⁵,
 F. Meloni ⁴⁸, A.M. Mendes Jacques Da Costa ¹⁰¹, H.Y. Meng ¹⁵⁵, L. Meng ⁹¹, S. Menke ¹¹⁰,
 M. Mentink ³⁶, E. Meoni ^{43b,43a}, G. Mercado ¹¹⁵, C. Merlassino ^{69a,69c}, L. Merola ^{72a,72b},
 C. Meroni ^{71a,71b}, G. Merz ¹⁰⁶, O. Meshkov ³⁷, J. Metcalfe ⁶, A.S. Mete ⁶, C. Meyer ⁶⁸,
 J-P. Meyer ¹³⁵, R.P. Middleton ¹³⁴, L. Mijović ⁵², G. Mikenberg ¹⁶⁹, M. Mikestikova ¹³¹,
 M. Mikuž ⁹³, H. Mildner ¹⁰⁰, A. Milic ³⁶, C.D. Milke ⁴⁴, D.W. Miller ³⁹, L.S. Miller ³⁴,
 A. Milov ¹⁶⁹, D.A. Milstead ^{47a,47b}, T. Min ^{14c}, A.A. Minaenko ³⁷, I.A. Minashvili ^{149b}, L. Mince ⁵⁹,
 A.I. Mincer ¹¹⁷, B. Mindur ^{86a}, M. Mineev ³⁸, Y. Mino ⁸⁸, L.M. Mir ¹³, M. Miralles Lopez ¹⁶³,
 M. Mironova ^{17a}, A. Mishima ¹⁵³, M.C. Missio ¹¹³, A. Mitra ¹⁶⁷, V.A. Mitsou ¹⁶³,
 Y. Mitsumori ¹¹¹, O. Miu ¹⁵⁵, P.S. Miyagawa ⁹⁴, T. Mkrtchyan ^{63a}, M. Mlinarevic ⁹⁶,
 T. Mlinarevic ⁹⁶, M. Mlynarikova ³⁶, S. Mobius ¹⁹, P. Moder ⁴⁸, P. Mogg ¹⁰⁹,
 A.F. Mohammed ^{14a,14e}, S. Mohapatra ⁴¹, G. Mokgatitwane ^{33g}, L. Moleri ¹⁶⁹, B. Mondal ¹⁴¹,
 S. Mondal ¹³², G. Monig ¹⁴⁶, K. Mönig ⁴⁸, E. Monnier ¹⁰², L. Monsonis Romero ¹⁶³,
 J. Montejo Berlingen ¹³, M. Montella ¹¹⁹, F. Montekali ^{77a,77b}, F. Monticelli ⁹⁰,
 S. Monzani ^{69a,69c}, N. Morange ⁶⁶, A.L. Moreira De Carvalho ^{130a}, M. Moreno Llácer ¹⁶³,

C. Moreno Martinez ⁵⁶, P. Morettini ^{57b}, S. Morgenstern ³⁶, M. Morii ⁶¹, M. Morinaga ¹⁵³,
 A.K. Morley ³⁶, F. Morodei ^{75a,75b}, L. Morvaj ³⁶, P. Moschovakos ³⁶, B. Moser ³⁶,
 M. Mosidze ^{149b}, T. Moskalets ⁵⁴, P. Moskvitina ¹¹³, J. Moss ^{31,p}, E.J.W. Moyse ¹⁰³,
 O. Mtintsilana ^{33g}, S. Muanza ¹⁰², J. Mueller ¹²⁹, D. Muenstermann ⁹¹, R. Müller ¹⁹,
 G.A. Mullier ¹⁶¹, A.J. Mullin ³², J.J. Mullin ¹²⁸, D.P. Mungo ¹⁵⁵, D. Munoz Perez ¹⁶³,
 F.J. Munoz Sanchez ¹⁰¹, M. Murin ¹⁰¹, W.J. Murray ^{167,134}, A. Murrone ^{71a,71b}, M. Muškinja ^{17a},
 C. Mwewa ²⁹, A.G. Myagkov ^{37,a}, A.J. Myers ⁸, G. Myers ⁶⁸, M. Myska ¹³², B.P. Nachman ^{17a},
 O. Nackenhorst ⁴⁹, A. Nag ⁵⁰, K. Nagai ¹²⁶, K. Nagano ⁸⁴, J.L. Nagle ^{29,ay}, E. Nagy ¹⁰²,
 A.M. Nairz ³⁶, Y. Nakahama ⁸⁴, K. Nakamura ⁸⁴, K. Nakkalil ⁵, H. Nanjo ¹²⁴, R. Narayan ⁴⁴,
 E.A. Narayanan ¹¹², I. Naryshkin ³⁷, M. Naseri ³⁴, S. Nasri ¹⁵⁹, C. Nass ²⁴, G. Navarro ^{22a},
 J. Navarro-Gonzalez ¹⁶³, R. Nayak ¹⁵¹, A. Nayaz ¹⁸, P.Y. Nechaeva ³⁷, F. Nechansky ⁴⁸,
 L. Nedic ¹²⁶, T.J. Neep ²⁰, A. Negri ^{73a,73b}, M. Negrini ^{23b}, C. Nellist ¹¹⁴, C. Nelson ¹⁰⁴,
 K. Nelson ¹⁰⁶, S. Nemecek ¹³¹, M. Nessi ^{36,j}, M.S. Neubauer ¹⁶², F. Neuhaus ¹⁰⁰,
 J. Neundorff ⁴⁸, R. Newhouse ¹⁶⁴, P.R. Newman ²⁰, C.W. Ng ¹²⁹, Y.W.Y. Ng ⁴⁸, B. Ngair ^{35e},
 H.D.N. Nguyen ¹⁰⁸, R.B. Nickerson ¹²⁶, R. Nicolaidou ¹³⁵, J. Nielsen ¹³⁶, M. Niemeyer ⁵⁵,
 J. Niermann ^{55,36}, N. Nikiforou ³⁶, V. Nikolaenko ^{37,a}, I. Nikolic-Audit ¹²⁷, K. Nikolopoulos ²⁰,
 P. Nilsson ²⁹, I. Ninca ⁴⁸, H.R. Nindhito ⁵⁶, G. Ninio ¹⁵¹, A. Nisati ^{75a}, N. Nishu ²,
 R. Nisius ¹¹⁰, J-E. Nitschke ⁵⁰, E.K. Nkadimeng ^{33g}, T. Nobe ¹⁵³, D.L. Noel ³²,
 T. Nommensen ¹⁴⁷, M.B. Norfolk ¹³⁹, R.R.B. Norisam ⁹⁶, B.J. Norman ³⁴, M. Noury ^{35a},
 J. Novak ⁹³, T. Novak ⁴⁸, L. Novotny ¹³², R. Novotny ¹¹², L. Nozka ¹²², K. Ntekas ¹⁶⁰,
 N.M.J. Nunes De Moura Junior ^{83b}, E. Nurse ⁹⁶, J. Ocariz ¹²⁷, A. Ochi ⁸⁵, I. Ochoa ^{130a},
 S. Oerdek ^{48,y}, J.T. Offermann ³⁹, A. Ogrodnik ¹³³, A. Oh ¹⁰¹, C.C. Ohm ¹⁴⁴, H. Oide ⁸⁴,
 R. Oishi ¹⁵³, M.L. Ojeda ⁴⁸, M.W. O'Keefe ⁹², Y. Okumura ¹⁵³, L.F. Oleiro Seabra ^{130a},
 S.A. Olivares Pino ^{137d}, D. Oliveira Damazio ²⁹, D. Oliveira Goncalves ^{83a}, J.L. Oliver ¹⁶⁰,
 Ö.O. Öncel ⁵⁴, A.P. O'Neill ¹⁹, A. Onofre ^{130a,130e}, P.U.E. Onyisi ¹¹, M.J. Oreglia ³⁹,
 G.E. Orellana ⁹⁰, D. Orestano ^{77a,77b}, N. Orlando ¹³, R.S. Orr ¹⁵⁵, V. O'Shea ⁵⁹,
 L.M. Osojnak ¹²⁸, R. Ospanov ^{62a}, G. Otero y Garzon ³⁰, H. Otono ⁸⁹, P.S. Ott ^{63a},
 G.J. Ottino ^{17a}, M. Ouchrif ^{35d}, J. Ouellette ²⁹, F. Ould-Saada ¹²⁵, M. Owen ⁵⁹, R.E. Owen ¹³⁴,
 K.Y. Oyulmaz ^{21a}, V.E. Ozcan ^{21a}, F. Ozturk ⁸⁷, N. Ozturk ⁸, S. Ozturk ⁸², H.A. Pacey ¹²⁶,
 A. Pacheco Pages ¹³, C. Padilla Aranda ¹³, G. Padovano ^{75a,75b}, S. Pagan Griso ^{17a},
 G. Palacino ⁶⁸, A. Palazzo ^{70a,70b}, S. Palestini ³⁶, J. Pan ¹⁷², T. Pan ^{64a}, D.K. Panchal ¹¹,
 C.E. Pandini ¹¹⁴, J.G. Panduro Vazquez ⁹⁵, H.D. Pandya ¹, H. Pang ^{14b}, P. Pani ⁴⁸,
 G. Panizzo ^{69a,69c}, L. Paolozzi ⁵⁶, C. Papadatos ¹⁰⁸, S. Parajuli ⁴⁴, A. Paramonov ⁶,
 C. Paraskevopoulos ¹⁰, D. Paredes Hernandez ^{64b}, K.R. Park ⁴¹, T.H. Park ¹⁵⁵, M.A. Parker ³²,
 F. Parodi ^{57b,57a}, E.W. Parrish ¹¹⁵, V.A. Parrish ⁵², J.A. Parsons ⁴¹, U. Parzefall ⁵⁴,
 B. Pascual Dias ¹⁰⁸, L. Pascual Dominguez ¹⁵¹, E. Pasqualucci ^{75a}, S. Passaggio ^{57b}, F. Pastore ⁹⁵,
 P. Pasuwan ^{47a,47b}, P. Patel ⁸⁷, U.M. Patel ⁵¹, J.R. Pater ¹⁰¹, T. Pauly ³⁶, J. Pearkes ¹⁴³,
 M. Pedersen ¹²⁵, R. Pedro ^{130a}, S.V. Peleganchuk ³⁷, O. Penc ³⁶, E.A. Pender ⁵²,
 K.E. Pensi ¹⁰⁹, M. Penzin ³⁷, B.S. Peralva ^{83d}, A.P. Pereira Peixoto ⁶⁰, L. Pereira Sanchez ^{47a,47b},
 D.V. Perepelitsa ^{29,ay}, E. Perez Codina ^{156a}, M. Perganti ¹⁰, L. Perini ^{71a,71b,*}, H. Pernegger ³⁶,
 O. Perrin ⁴⁰, K. Peters ⁴⁸, R.F.Y. Peters ¹⁰¹, B.A. Petersen ³⁶, T.C. Petersen ⁴², E. Petit ¹⁰²,
 V. Petousis ¹³², C. Petridou ^{152,f}, A. Petrukhin ¹⁴¹, M. Pettee ^{17a}, N.E. Pettersson ³⁶,
 A. Petukhov ³⁷, K. Petukhova ¹³³, R. Pezoa ^{137f}, L. Pezzotti ³⁶, G. Pezzullo ¹⁷², T.M. Pham ¹⁷⁰,
 T. Pham ¹⁰⁵, P.W. Phillips ¹³⁴, G. Piacquadio ¹⁴⁵, E. Pianori ^{17a}, F. Piazza ¹²³, R. Piegai ³⁰,
 D. Pietreanu ^{27b}, A.D. Pilkington ¹⁰¹, M. Pinamonti ^{69a,69c}, J.L. Pinfold ²,
 B.C. Pinheiro Pereira ^{130a}, A.E. Pinto Pinoargote ^{100,135}, L. Pintucci ^{69a,69c}, K.M. Piper ¹⁴⁶,
 A. Pirttikoski ⁵⁶, D.A. Pizzi ³⁴, L. Pizzimento ^{64b}, A. Pizzini ¹¹⁴, M.-A. Pleier ²⁹, V. Plesanovs ⁵⁴,

V. Pleskot ¹³³, E. Plotnikova³⁸, G. Poddar ⁴, R. Poettgen ⁹⁸, L. Poggioli ¹²⁷, I. Pokharel ⁵⁵, S. Polacek ¹³³, G. Polesello ^{73a}, A. Poley ^{142,156a}, R. Polifka ¹³², A. Polini ^{23b}, C.S. Pollard ¹⁶⁷, Z.B. Pollock ¹¹⁹, V. Polychronakos ²⁹, E. Pompa Pacchi ^{75a,75b}, D. Ponomarenko ¹¹³, L. Pontecorvo ³⁶, S. Popa ^{27a}, G.A. Popeneciu ^{27d}, A. Poreba ³⁶, D.M. Portillo Quintero ^{156a}, S. Pospisil ¹³², M.A. Postill ¹³⁹, P. Postolache ^{27c}, K. Potamianos ¹⁶⁷, P.A. Potepa ^{86a}, I.N. Potrap ³⁸, C.J. Potter ³², H. Potti ¹, T. Poulsen ⁴⁸, J. Poveda ¹⁶³, M.E. Pozo Astigarraga ³⁶, A. Prades Ibanez ¹⁶³, J. Pretel ⁵⁴, D. Price ¹⁰¹, M. Primavera ^{70a}, M.A. Principe Martin ⁹⁹, R. Privara ¹²², T. Procter ⁵⁹, M.L. Proffitt ¹³⁸, N. Proklova ¹²⁸, K. Prokofiev ^{64c}, G. Proto ¹¹⁰, S. Protopopescu ²⁹, J. Proudfoot ⁶, M. Przybycien ^{86a}, W.W. Przygoda ^{86b}, J.E. Puddefoot ¹³⁹, D. Pudzha ³⁷, D. Pyatiizbyantseva ³⁷, J. Qian ¹⁰⁶, D. Qichen ¹⁰¹, Y. Qin ¹⁰¹, T. Qiu ⁵², A. Quadt ⁵⁵, M. Queitsch-Maitland ¹⁰¹, G. Quetant ⁵⁶, R.P. Quinn ¹⁶⁴, G. Rabanal Bolanos ⁶¹, D. Rafanoharana ⁵⁴, F. Ragusa ^{71a,71b}, J.L. Rainbolt ³⁹, J.A. Raine ⁵⁶, S. Rajagopalan ²⁹, E. Ramakoti ³⁷, I.A. Ramirez-Berend ³⁴, K. Ran ^{48,14e}, N.P. Rappheeha ^{33g}, H. Rasheed ^{27b}, V. Raskina ¹²⁷, D.F. Rassloff ^{63a}, S. Rave ¹⁰⁰, B. Ravina ⁵⁵, I. Ravinovich ¹⁶⁹, M. Raymond ³⁶, A.L. Read ¹²⁵, N.P. Readioff ¹³⁹, D.M. Rebutzi ^{73a,73b}, G. Redlinger ²⁹, A.S. Reed ¹¹⁰, K. Reeves ²⁶, J.A. Reidelsturz ^{171,aa}, D. Reikher ¹⁵¹, A. Rej ^{49,z}, C. Rembser ³⁶, A. Renardi ⁴⁸, M. Renda ^{27b}, M.B. Rendel¹¹⁰, F. Renner ⁴⁸, A.G. Rennie ¹⁶⁰, A.L. Rescia ⁴⁸, S. Resconi ^{71a}, M. Ressegotti ^{57b,57a}, S. Rettie ³⁶, J.G. Reyes Rivera ¹⁰⁷, E. Reynolds ^{17a}, O.L. Rezanova ³⁷, P. Reznicek ¹³³, N. Ribaric ⁹¹, E. Ricci ^{78a,78b}, R. Richter ¹¹⁰, S. Richter ^{47a,47b}, E. Richter-Was ^{86b}, M. Ridel ¹²⁷, S. Ridouani ^{35d}, P. Rieck ¹¹⁷, P. Riedler ³⁶, E.M. Riefel ^{47a,47b}, J.O. Rieger¹¹⁴, M. Rijssenbeek ¹⁴⁵, A. Rimoldi ^{73a,73b}, M. Rimoldi ³⁶, L. Rinaldi ^{23b,23a}, T.T. Rinn ²⁹, M.P. Rinnagel ¹⁰⁹, G. Ripellino ¹⁶¹, I. Riu ¹³, P. Rivadeneira ⁴⁸, J.C. Rivera Vergara ¹⁶⁵, F. Rizatdinova ¹²¹, E. Rizvi ⁹⁴, B.A. Roberts ¹⁶⁷, B.R. Roberts ^{17a}, S.H. Robertson ^{104,ai}, D. Robinson ³², C.M. Robles Gajardo^{137f}, M. Robles Manzano ¹⁰⁰, A. Robson ⁵⁹, A. Rocchi ^{76a,76b}, C. Roda ^{74a,74b}, S. Rodriguez Bosca ^{63a}, Y. Rodriguez Garcia ^{22a}, A. Rodriguez Rodriguez ⁵⁴, A.M. Rodríguez Vera ^{156b}, S. Roe³⁶, J.T. Roemer ¹⁶⁰, A.R. Roepe-Gier ¹³⁶, J. Roggel ¹⁷¹, O. Røhne ¹²⁵, R.A. Rojas ¹⁰³, C.P.A. Roland ¹²⁷, J. Roloff ²⁹, A. Romaniouk ³⁷, E. Romano ^{73a,73b}, M. Romano ^{23b}, A.C. Romero Hernandez ¹⁶², N. Rompotis ⁹², L. Roos ¹²⁷, S. Rosati ^{75a}, B.J. Rosser ³⁹, E. Rossi ¹²⁶, E. Rossi ^{72a,72b}, L.P. Rossi ^{57b}, L. Rossini ⁵⁴, R. Rosten ¹¹⁹, M. Rotaru ^{27b}, B. Rottler ⁵⁴, C. Rougier ^{102,an}, D. Rousseau ⁶⁶, D. Rousso ³², A. Roy ¹⁶², S. Roy-Garand ¹⁵⁵, A. Rozanov ¹⁰², Z.M.A. Rozario ⁵⁹, Y. Rozen ¹⁵⁰, X. Ruan ^{33g}, A. Rubio Jimenez ¹⁶³, A.J. Ruby ⁹², V.H. Ruelas Rivera ¹⁸, T.A. Ruggeri ¹, A. Ruggiero ¹²⁶, A. Ruiz-Martinez ¹⁶³, A. Rummeler ³⁶, Z. Rurikova ⁵⁴, N.A. Rusakovich ³⁸, H.L. Russell ¹⁶⁵, G. Russo ^{75a,75b}, J.P. Rutherford ⁷, S. Rutherford Colmenares ³², K. Rybacki⁹¹, M. Rybar ¹³³, E.B. Rye ¹²⁵, A. Ryzhov ⁴⁴, J.A. Sabater Iglesias ⁵⁶, P. Sabatini ¹⁶³, H.F-W. Sadrozinski ¹³⁶, F. Safai Tehrani ^{75a}, B. Safarzadeh Samani ¹³⁴, M. Safdari ¹⁴³, S. Saha ¹⁶⁵, M. Sahinsoy ¹¹⁰, A. Saibel ¹⁶³, M. Saimpert ¹³⁵, M. Saito ¹⁵³, T. Saito ¹⁵³, D. Salamani ³⁶, A. Salnikov ¹⁴³, J. Salt ¹⁶³, A. Salvador Salas ¹⁵¹, D. Salvatore ^{43b,43a}, F. Salvatore ¹⁴⁶, A. Salzburger ³⁶, D. Sammel ⁵⁴, D. Sampsonidis ^{152,f}, D. Sampsonidou ¹²³, J. Sánchez ¹⁶³, A. Sanchez Pineda ⁴, V. Sanchez Sebastian ¹⁶³, H. Sandaker ¹²⁵, C.O. Sander ⁴⁸, J.A. Sandesara ¹⁰³, M. Sandhoff ¹⁷¹, C. Sandoval ^{22b}, D.P.C. Sankey ¹³⁴, T. Sano ⁸⁸, A. Sansoni ⁵³, L. Santi ^{75a,75b}, C. Santoni ⁴⁰, H. Santos ^{130a,130b}, S.N. Santpur ^{17a}, A. Santra ¹⁶⁹, K.A. Saoucha ^{116b}, J.G. Saraiva ^{130a,130d}, J. Sardain ⁷, O. Sasaki ⁸⁴, K. Sato ¹⁵⁷, C. Sauer^{63b}, F. Sauerburger ⁵⁴, E. Sauvan ⁴, P. Savard ^{155,av}, R. Sawada ¹⁵³, C. Sawyer ¹³⁴, L. Sawyer ⁹⁷, I. Sayago Galvan¹⁶³, C. Sbarra ^{23b}, A. Sbrizzi ^{23b,23a}, T. Scanlon ⁹⁶, J. Schaarschmidt ¹³⁸, P. Schacht ¹¹⁰, U. Schäfer ¹⁰⁰, A.C. Schaffer ^{66,44}, D. Schaile ¹⁰⁹, R.D. Schamberger ¹⁴⁵, C. Scharf ¹⁸, M.M. Schefer ¹⁹,

V.A. Schegelsky [id](#)³⁷, D. Scheirich [id](#)¹³³, F. Schenck [id](#)¹⁸, M. Schernau [id](#)¹⁶⁰, C. Scheulen [id](#)⁵⁵, C. Schiavi [id](#)^{57b,57a}, E.J. Schioppa [id](#)^{70a,70b}, M. Schioppa [id](#)^{43b,43a}, B. Schlag [id](#)^{143,t}, K.E. Schleicher [id](#)⁵⁴, S. Schlenker [id](#)³⁶, J. Schmeing [id](#)¹⁷¹, M.A. Schmidt [id](#)¹⁷¹, K. Schmieden [id](#)¹⁰⁰, C. Schmitt [id](#)¹⁰⁰, N. Schmitt [id](#)¹⁰⁰, S. Schmitt [id](#)⁴⁸, L. Schoeffel [id](#)¹³⁵, A. Schoening [id](#)^{63b}, P.G. Scholer [id](#)⁵⁴, E. Schopf [id](#)¹²⁶, M. Schott [id](#)¹⁰⁰, J. Schovancova [id](#)³⁶, S. Schramm [id](#)⁵⁶, F. Schroeder [id](#)¹⁷¹, T. Schroer [id](#)⁵⁶, H-C. Schultz-Coulon [id](#)^{63a}, M. Schumacher [id](#)⁵⁴, B.A. Schumm [id](#)¹³⁶, Ph. Schune [id](#)¹³⁵, A.J. Schuy [id](#)¹³⁸, H.R. Schwartz [id](#)¹³⁶, A. Schwartzman [id](#)¹⁴³, T.A. Schwarz [id](#)¹⁰⁶, Ph. Schwemling [id](#)¹³⁵, R. Schwienhorst [id](#)¹⁰⁷, A. Sciandra [id](#)¹³⁶, G. Sciolla [id](#)²⁶, F. Scuri [id](#)^{74a}, C.D. Sebastiani [id](#)⁹², K. Sedlaczek [id](#)¹¹⁵, P. Seema [id](#)¹⁸, S.C. Seidel [id](#)¹¹², A. Seiden [id](#)¹³⁶, B.D. Seidlitz [id](#)⁴¹, C. Seitz [id](#)⁴⁸, J.M. Seixas [id](#)^{83b}, G. Sekhniaidze [id](#)^{72a}, S.J. Sekula [id](#)⁴⁴, L. Selem [id](#)⁶⁰, N. Semprini-Cesari [id](#)^{23b,23a}, D. Sengupta [id](#)⁵⁶, V. Senthilkumar [id](#)¹⁶³, L. Serin [id](#)⁶⁶, L. Serkin [id](#)^{69a,69b}, M. Sessa [id](#)^{76a,76b}, H. Severini [id](#)¹²⁰, F. Sforza [id](#)^{57b,57a}, A. Sfyrta [id](#)⁵⁶, E. Shabalina [id](#)⁵⁵, R. Shaheen [id](#)¹⁴⁴, J.D. Shahinian [id](#)¹²⁸, D. Shaked Renous [id](#)¹⁶⁹, L.Y. Shan [id](#)^{14a}, M. Shapiro [id](#)^{17a}, A. Sharma [id](#)³⁶, A.S. Sharma [id](#)¹⁶⁴, P. Sharma [id](#)⁸⁰, S. Sharma [id](#)⁴⁸, P.B. Shatalov [id](#)³⁷, K. Shaw [id](#)¹⁴⁶, S.M. Shaw [id](#)¹⁰¹, A. Shcherbakova [id](#)³⁷, Q. Shen [id](#)^{62c,5}, D.J. Sheppard [id](#)¹⁴², P. Sherwood [id](#)⁹⁶, L. Shi [id](#)⁹⁶, X. Shi [id](#)^{14a}, C.O. Shimmin [id](#)¹⁷², J.D. Shinner [id](#)⁹⁵, I.P.J. Shipsey [id](#)¹²⁶, S. Shirabe [id](#)^{56,j}, M. Shiyakova [id](#)^{38,ag}, J. Shlomi [id](#)¹⁶⁹, M.J. Shochet [id](#)³⁹, J. Shojaii [id](#)¹⁰⁵, D.R. Shope [id](#)¹²⁵, B. Shrestha [id](#)¹²⁰, S. Shrestha [id](#)^{119,az}, E.M. Shrif [id](#)^{33g}, M.J. Shroff [id](#)¹⁶⁵, P. Sicho [id](#)¹³¹, A.M. Sickles [id](#)¹⁶², E. Sideras Haddad [id](#)^{33g}, A. Sidoti [id](#)^{23b}, F. Siegert [id](#)⁵⁰, Dj. Sijacki [id](#)¹⁵, F. Sili [id](#)⁹⁰, J.M. Silva [id](#)²⁰, M.V. Silva Oliveira [id](#)²⁹, S.B. Silverstein [id](#)^{47a}, S. Simion [id](#)⁶⁶, R. Simoniello [id](#)³⁶, E.L. Simpson [id](#)⁵⁹, H. Simpson [id](#)¹⁴⁶, L.R. Simpson [id](#)¹⁰⁶, N.D. Simpson [id](#)⁹⁸, S. Simsek [id](#)⁸², S. Sindhu [id](#)⁵⁵, P. Sinervo [id](#)¹⁵⁵, S. Singh [id](#)¹⁵⁵, S. Sinha [id](#)⁴⁸, S. Sinha [id](#)¹⁰¹, M. Sioli [id](#)^{23b,23a}, I. Siral [id](#)³⁶, E. Sitnikova [id](#)⁴⁸, S.Yu. Sivoklov [id](#)^{37,*}, J. Sjölin [id](#)^{47a,47b}, A. Skaf [id](#)⁵⁵, E. Skorda [id](#)^{20,aq}, P. Skubic [id](#)¹²⁰, M. Slawinska [id](#)⁸⁷, V. Smakhtin [id](#)¹⁶⁹, B.H. Smart [id](#)¹³⁴, J. Smiesko [id](#)³⁶, S.Yu. Smirnov [id](#)³⁷, Y. Smirnov [id](#)³⁷, L.N. Smirnova [id](#)^{37,a}, O. Smirnova [id](#)⁹⁸, A.C. Smith [id](#)⁴¹, E.A. Smith [id](#)³⁹, H.A. Smith [id](#)¹²⁶, J.L. Smith [id](#)⁹², R. Smith [id](#)¹⁴³, M. Smizanska [id](#)⁹¹, K. Smolek [id](#)¹³², A.A. Snesev [id](#)³⁷, S.R. Snider [id](#)¹⁵⁵, H.L. Snoek [id](#)¹¹⁴, S. Snyder [id](#)²⁹, R. Sobie [id](#)^{165,ai}, A. Soffer [id](#)¹⁵¹, C.A. Solans Sanchez [id](#)³⁶, E.Yu. Soldatov [id](#)³⁷, U. Soldevila [id](#)¹⁶³, A.A. Solodkov [id](#)³⁷, S. Solomon [id](#)²⁶, A. Soloshenko [id](#)³⁸, K. Solovieva [id](#)⁵⁴, O.V. Solovyanov [id](#)⁴⁰, V. Solovyev [id](#)³⁷, P. Sommer [id](#)³⁶, A. Sonay [id](#)¹³, W.Y. Song [id](#)^{156b}, J.M. Sonneveld [id](#)¹¹⁴, A. Sopczak [id](#)¹³², A.L. Soppio [id](#)⁹⁶, F. Sopkova [id](#)^{28b}, I.R. Sotarriva Alvarez [id](#)¹⁵⁴, V. Sothilingam [id](#)^{63a}, O.J. Soto Sandoval [id](#)^{137c,137b}, S. Sottocornola [id](#)⁶⁸, R. Soualah [id](#)^{116b}, Z. Soumami [id](#)^{35e}, D. South [id](#)⁴⁸, N. Soybelman [id](#)¹⁶⁹, S. Spagnolo [id](#)^{70a,70b}, M. Spalla [id](#)¹¹⁰, D. Sperlich [id](#)⁵⁴, G. Spigo [id](#)³⁶, S. Spinali [id](#)⁹¹, D.P. Spiteri [id](#)⁵⁹, M. Spousta [id](#)¹³³, E.J. Staats [id](#)³⁴, A. Stabile [id](#)^{71a,71b}, R. Stamen [id](#)^{63a}, A. Stampekis [id](#)²⁰, M. Standke [id](#)²⁴, E. Stanecka [id](#)⁸⁷, M.V. Stange [id](#)⁵⁰, B. Stanislaus [id](#)^{17a}, M.M. Stanitzki [id](#)⁴⁸, B. Stapf [id](#)⁴⁸, E.A. Starchenko [id](#)³⁷, G.H. Stark [id](#)¹³⁶, J. Stark [id](#)^{102,an}, D.M. Starko [id](#)^{156b}, P. Staroba [id](#)¹³¹, P. Starovoitov [id](#)^{63a}, S. Stärz [id](#)¹⁰⁴, R. Staszewski [id](#)⁸⁷, G. Stavropoulos [id](#)⁴⁶, J. Steentoft [id](#)¹⁶¹, P. Steinberg [id](#)²⁹, B. Stelzer [id](#)^{142,156a}, H.J. Stelzer [id](#)¹²⁹, O. Stelzer-Chilton [id](#)^{156a}, H. Stenzel [id](#)⁵⁸, T.J. Stevenson [id](#)¹⁴⁶, G.A. Stewart [id](#)³⁶, J.R. Stewart [id](#)¹²¹, M.C. Stockton [id](#)³⁶, G. Stoicea [id](#)^{27b}, M. Stolarski [id](#)^{130a}, S. Stonjek [id](#)¹¹⁰, A. Straessner [id](#)⁵⁰, J. Strandberg [id](#)¹⁴⁴, S. Strandberg [id](#)^{47a,47b}, M. Stratmann [id](#)¹⁷¹, M. Strauss [id](#)¹²⁰, T. Streblner [id](#)¹⁰², P. Strizenc [id](#)^{28b}, R. Ströhmer [id](#)¹⁶⁶, D.M. Strom [id](#)¹²³, R. Stroynowski [id](#)⁴⁴, A. Strubig [id](#)^{47a,47b}, S.A. Stucci [id](#)²⁹, B. Stugu [id](#)¹⁶, J. Stupak [id](#)¹²⁰, N.A. Styles [id](#)⁴⁸, D. Su [id](#)¹⁴³, S. Su [id](#)^{62a}, W. Su [id](#)^{62d}, X. Su [id](#)^{62a,66}, K. Sugizaki [id](#)¹⁵³, V.V. Sulin [id](#)³⁷, M.J. Sullivan [id](#)⁹², D.M.S. Sultan [id](#)^{78a,78b}, L. Sultanaliev [id](#)³⁷, S. Sultansoy [id](#)^{3b}, T. Sumida [id](#)⁸⁸, S. Sun [id](#)¹⁰⁶, S. Sun [id](#)¹⁷⁰, O. Sunneborn Gudnadottir [id](#)¹⁶¹, N. Sur [id](#)¹⁰², M.R. Sutton [id](#)¹⁴⁶, H. Suzuki [id](#)¹⁵⁷, M. Svatos [id](#)¹³¹, M. Swiatlowski [id](#)^{156a}, T. Swirski [id](#)¹⁶⁶, I. Sykora [id](#)^{28a}, M. Sykora [id](#)¹³³, T. Sykora [id](#)¹³³, D. Ta [id](#)¹⁰⁰, K. Tackmann [id](#)^{48,ae}, A. Taffard [id](#)¹⁶⁰, R. Tafirout [id](#)^{156a}, J.S. Tafuya Vargas [id](#)⁶⁶, E.P. Takeva [id](#)⁵²,

Y. Takubo ¹⁸⁴, M. Talby ¹⁰², A.A. Talyshev ³⁷, K.C. Tam ^{64b}, N.M. Tamir ¹⁵¹, A. Tanaka ¹⁵³,
 J. Tanaka ¹⁵³, R. Tanaka ⁶⁶, M. Tanasini ^{57b,57a}, Z. Tao ¹⁶⁴, S. Tapia Araya ^{137f},
 S. Tapprogge ¹⁰⁰, A. Tarek Abouelfadl Mohamed ¹⁰⁷, S. Tarem ¹⁵⁰, K. Tariq ^{14a}, G. Tarna ^{102,27b},
 G.F. Tartarelli ^{71a}, P. Tas ¹³³, M. Tasevsky ¹³¹, E. Tassi ^{43b,43a}, A.C. Tate ¹⁶², G. Tateno ¹⁵³,
 Y. Tayalati ^{35e,ah}, G.N. Taylor ¹⁰⁵, W. Taylor ^{156b}, A.S. Tee ¹⁷⁰, R. Teixeira De Lima ¹⁴³,
 P. Teixeira-Dias ⁹⁵, J.J. Teoh ¹⁵⁵, K. Terashi ¹⁵³, J. Terron ⁹⁹, S. Terzo ¹³, M. Testa ⁵³,
 R.J. Teuscher ^{155,ai}, A. Thaler ⁷⁹, O. Theiner ⁵⁶, N. Themistokleous ⁵², T. Thevenaux-Pelzer ¹⁰²,
 O. Thielmann ¹⁷¹, D.W. Thomas ⁹⁵, J.P. Thomas ²⁰, E.A. Thompson ^{17a}, P.D. Thompson ²⁰,
 E. Thomson ¹²⁸, Y. Tian ⁵⁵, V. Tikhomirov ^{37,a}, Yu.A. Tikhonov ³⁷, S. Timoshenko ³⁷,
 D. Timoshyn ¹³³, E.X.L. Ting ¹, P. Tipton ¹⁷², S.H. Tlou ^{33g}, A. Tnourji ⁴⁰, K. Todome ¹⁵⁴,
 S. Todorova-Nova ¹³³, S. Todt ⁵⁰, M. Togawa ⁸⁴, J. Tojo ⁸⁹, S. Tokár ^{28a}, K. Tokushuku ⁸⁴,
 O. Toldaiev ⁶⁸, R. Tombs ³², M. Tomoto ^{84,111}, L. Tompkins ^{143,t}, K.W. Topolnicki ^{86b},
 E. Torrence ¹²³, H. Torres ^{102,an}, E. Torró Pastor ¹⁶³, M. Toscani ³⁰, C. Tosciri ³⁹, M. Tost ¹¹,
 D.R. Tovey ¹³⁹, A. Traeet ¹⁶, I.S. Trandafir ^{27b}, T. Trefzger ¹⁶⁶, A. Tricoli ²⁹, I.M. Trigger ^{156a},
 S. Trincaz-Duvoid ¹²⁷, D.A. Trischuk ²⁶, B. Trocmé ⁶⁰, C. Troncon ^{71a}, L. Truong ^{33c},
 M. Trzebinski ⁸⁷, A. Trzuppek ⁸⁷, F. Tsai ¹⁴⁵, M. Tsai ¹⁰⁶, A. Tsiamis ^{152,f}, P.V. Tsiareshka ³⁷,
 S. Tsigaridas ^{156a}, A. Tsigotis ^{152,ac}, V. Tsiskaridze ¹⁵⁵, E.G. Tskhadadze ^{149a},
 M. Tsopoulou ^{152,f}, Y. Tsujikawa ⁸⁸, I.I. Tsukerman ³⁷, V. Tsulaia ^{17a}, S. Tsuno ⁸⁴, K. Tsuru ¹¹⁸,
 D. Tsybychev ¹⁴⁵, Y. Tu ^{64b}, A. Tudorache ^{27b}, V. Tudorache ^{27b}, A.N. Tuna ⁶¹,
 S. Turchikhin ^{57b,57a}, I. Turk Cakir ^{3a}, R. Turra ^{71a}, T. Turtuvshin ^{38,aj}, P.M. Tuts ⁴¹,
 S. Tzamarias ^{152,f}, P. Tzanis ¹⁰, E. Tzovara ¹⁰⁰, F. Ukegawa ¹⁵⁷, P.A. Ulloa Poblete ^{137c,137b},
 E.N. Umaka ²⁹, G. Unal ³⁶, M. Unal ¹¹, A. Undrus ²⁹, G. Unel ¹⁶⁰, J. Urban ^{28b},
 P. Urquijo ¹⁰⁵, P. Urrejola ^{137a}, G. Usai ⁸, R. Ushioda ¹⁵⁴, M. Usman ¹⁰⁸, Z. Uysal ^{21b},
 V. Vacek ¹³², B. Vachon ¹⁰⁴, K.O.H. Vadla ¹²⁵, T. Vafeiadis ³⁶, A. Vaitkus ⁹⁶, C. Valderanis ¹⁰⁹,
 E. Valdes Santurio ^{47a,47b}, M. Valente ^{156a}, S. Valentinetti ^{23b,23a}, A. Valero ¹⁶³,
 E. Valiente Moreno ¹⁶³, A. Vallier ^{102,an}, J.A. Valls Ferrer ¹⁶³, D.R. Van Arneman ¹¹⁴,
 T.R. Van Daalen ¹³⁸, A. Van Der Graaf ⁴⁹, P. Van Gemmeren ⁶, M. Van Rijnbach ^{125,36},
 S. Van Stroud ⁹⁶, I. Van Vulpen ¹¹⁴, M. Vanadia ^{76a,76b}, W. Vandelli ³⁶, M. Vandenbroucke ¹³⁵,
 E.R. Vandewall ¹²¹, D. Vannicola ¹⁵¹, L. Vannoli ^{57b,57a}, R. Vari ^{75a}, E.W. Varnes ⁷,
 C. Varni ^{17b}, T. Varol ¹⁴⁸, D. Varouchas ⁶⁶, L. Varriale ¹⁶³, K.E. Varvell ¹⁴⁷, M.E. Vasile ^{27b},
 L. Vaslin ⁸⁴, G.A. Vasquez ¹⁶⁵, A. Vasyukov ³⁸, F. Vazeille ⁴⁰, T. Vazquez Schroeder ³⁶,
 J. Veatch ³¹, V. Vecchio ¹⁰¹, M.J. Veen ¹⁰³, I. Veliscek ¹²⁶, L.M. Veloce ¹⁵⁵, F. Veloso ^{130a,130c},
 S. Veneziano ^{75a}, A. Ventura ^{70a,70b}, S. Ventura Gonzalez ¹³⁵, A. Verbytskyi ¹¹⁰,
 M. Verducci ^{74a,74b}, C. Vergis ²⁴, M. Verissimo De Araujo ^{83b}, W. Verkerke ¹¹⁴,
 J.C. Vermeulen ¹¹⁴, C. Vernieri ¹⁴³, M. Vessella ¹⁰³, M.C. Vetterli ^{142,av}, A. Vgenopoulos ^{152,f},
 N. Viaux Maira ^{137f}, T. Vickey ¹³⁹, O.E. Vickey Boeriu ¹³⁹, G.H.A. Viehhauser ¹²⁶, L. Vigani ^{63b},
 M. Villa ^{23b,23a}, M. Villaplana Perez ¹⁶³, E.M. Villhauer ⁵², E. Vilucchi ⁵³, M.G. Vinciter ³⁴,
 G.S. Virdee ²⁰, A. Vishwakarma ⁵², A. Visibile ¹¹⁴, C. Vittori ³⁶, I. Vivarelli ¹⁴⁶,
 E. Voevodina ¹¹⁰, F. Vogel ¹⁰⁹, J.C. Voigt ⁵⁰, P. Vokac ¹³², Yu. Volkotrub ^{86a}, J. Von Ahnen ⁴⁸,
 E. Von Toerne ²⁴, B. Vormwald ³⁶, V. Vorobel ¹³³, K. Vorobev ³⁷, M. Vos ¹⁶³, K. Voss ¹⁴¹,
 J.H. Vossebeld ⁹², M. Vozak ¹¹⁴, L. Vozdecky ⁹⁴, N. Vranjes ¹⁵, M. Vranjes Milosavljevic ¹⁵,
 M. Vreeswijk ¹¹⁴, R. Vuillermet ³⁶, O. Vujanovic ¹⁰⁰, I. Vukotic ³⁹, S. Wada ¹⁵⁷, C. Wagner ¹⁰³,
 J.M. Wagner ^{17a}, W. Wagner ¹⁷¹, S. Wahdan ¹⁷¹, H. Wahlberg ⁹⁰, M. Wakida ¹¹¹, J. Walder ¹³⁴,
 R. Walker ¹⁰⁹, W. Walkowiak ¹⁴¹, A. Wall ¹²⁸, T. Wamorkar ⁶, A.Z. Wang ¹³⁶, C. Wang ¹⁰⁰,
 C. Wang ^{62c}, H. Wang ^{17a}, J. Wang ^{64a}, R.-J. Wang ¹⁰⁰, R. Wang ⁶¹, R. Wang ⁶,
 S.M. Wang ¹⁴⁸, S. Wang ^{62b}, T. Wang ^{62a}, W.T. Wang ⁸⁰, W. Wang ^{14a}, X. Wang ^{14c},
 X. Wang ¹⁶², X. Wang ^{62c}, Y. Wang ^{62d}, Y. Wang ^{14c}, Z. Wang ¹⁰⁶, Z. Wang ^{62d,51,62c},

Z. Wang ¹⁰⁶, A. Warburton ¹⁰⁴, R.J. Ward ²⁰, N. Warrack ⁵⁹, A.T. Watson ²⁰, H. Watson ⁵⁹, M.F. Watson ²⁰, E. Watton ^{59,134}, G. Watts ¹³⁸, B.M. Waugh ⁹⁶, C. Weber ²⁹, H.A. Weber ¹⁸, M.S. Weber ¹⁹, S.M. Weber ^{63a}, C. Wei ^{62a}, Y. Wei ¹²⁶, A.R. Weidberg ¹²⁶, E.J. Weik ¹¹⁷, J. Weingarten ⁴⁹, M. Weirich ¹⁰⁰, C. Weiser ⁵⁴, C.J. Wells ⁴⁸, T. Wenaus ²⁹, B. Wendland ⁴⁹, T. Wengler ³⁶, N.S. Wenke ¹¹⁰, N. Wermes ²⁴, M. Wessels ^{63a}, A.M. Wharton ⁹¹, A.S. White ⁶¹, A. White ⁸, M.J. White ¹, D. Whiteson ¹⁶⁰, L. Wickremasinghe ¹²⁴, W. Wiedenmann ¹⁷⁰, C. Wiel ⁵⁰, M. Wielers ¹³⁴, C. Wiglesworth ⁴², D.J. Wilbern ¹²⁰, H.G. Wilkens ³⁶, D.M. Williams ⁴¹, H.H. Williams ¹²⁸, S. Williams ³², S. Willocq ¹⁰³, B.J. Wilson ¹⁰¹, P.J. Windischhofer ³⁹, F.I. Winkel ³⁰, F. Winklmeier ¹²³, B.T. Winter ⁵⁴, J.K. Winter ¹⁰¹, M. Wittgen ¹⁴³, M. Wobisch ⁹⁷, Z. Wolffs ¹¹⁴, J. Wollrath ¹⁶⁰, M.W. Wolter ⁸⁷, H. Wolters ^{130a,130c}, A.F. Wongel ⁴⁸, E.L. Woodward ⁴¹, S.D. Worm ⁴⁸, B.K. Wosiek ⁸⁷, K.W. Woźniak ⁸⁷, S. Wozniowski ⁵⁵, K. Wraight ⁵⁹, C. Wu ²⁰, J. Wu ^{14a,14e}, M. Wu ^{64a}, M. Wu ¹¹³, S.L. Wu ¹⁷⁰, X. Wu ⁵⁶, Y. Wu ^{62a}, Z. Wu ¹³⁵, J. Wuerzinger ^{110,at}, T.R. Wyatt ¹⁰¹, B.M. Wynne ⁵², S. Xella ⁴², L. Xia ^{14c}, M. Xia ^{14b}, J. Xiang ^{64c}, M. Xie ^{62a}, X. Xie ^{62a}, S. Xin ^{14a,14e}, A. Xiong ¹²³, J. Xiong ^{17a}, D. Xu ^{14a}, H. Xu ^{62a}, L. Xu ^{62a}, R. Xu ¹²⁸, T. Xu ¹⁰⁶, Y. Xu ^{14b}, Z. Xu ⁵², Z. Xu ^{14c}, B. Yabsley ¹⁴⁷, S. Yacoob ^{33a}, Y. Yamaguchi ¹⁵⁴, E. Yamashita ¹⁵³, H. Yamauchi ¹⁵⁷, T. Yamazaki ^{17a}, Y. Yamazaki ⁸⁵, J. Yan ^{62c}, S. Yan ¹²⁶, Z. Yan ²⁵, H.J. Yang ^{62c,62d}, H.T. Yang ^{62a}, S. Yang ^{62a}, T. Yang ^{64c}, X. Yang ³⁶, X. Yang ^{14a}, Y. Yang ⁴⁴, Y. Yang ^{62a}, Z. Yang ^{62a}, W.-M. Yao ^{17a}, Y.C. Yap ⁴⁸, H. Ye ^{14c}, H. Ye ⁵⁵, J. Ye ^{14a}, S. Ye ²⁹, X. Ye ^{62a}, Y. Yeh ⁹⁶, I. Yeletsikh ³⁸, B.K. Yeo ^{17b}, M.R. Yexley ⁹⁶, P. Yin ⁴¹, K. Yorita ¹⁶⁸, S. Younas ^{27b}, C.J.S. Young ³⁶, C. Young ¹⁴³, C. Yu ^{14a,14e,ax}, Y. Yu ^{62a}, M. Yuan ¹⁰⁶, R. Yuan ^{62b}, L. Yue ⁹⁶, M. Zaazoua ^{62a}, B. Zabinski ⁸⁷, E. Zaid ⁵², T. Zakareishvili ^{149b}, N. Zakharchuk ³⁴, S. Zambito ⁵⁶, J.A. Zamora Saa ^{137d,137b}, J. Zang ¹⁵³, D. Zanzi ⁵⁴, O. Zaplatilek ¹³², C. Zeitnitz ¹⁷¹, H. Zeng ^{14a}, J.C. Zeng ¹⁶², D.T. Zenger Jr ²⁶, O. Zenin ³⁷, T. Ženiš ^{28a}, S. Zenz ⁹⁴, S. Zerradi ^{35a}, D. Zerwas ⁶⁶, M. Zhai ^{14a,14e}, B. Zhang ^{14c}, D.F. Zhang ¹³⁹, J. Zhang ^{62b}, J. Zhang ⁶, K. Zhang ^{14a,14e}, L. Zhang ^{14c}, P. Zhang ^{14a,14e}, R. Zhang ¹⁷⁰, S. Zhang ¹⁰⁶, S. Zhang ⁴⁴, T. Zhang ¹⁵³, X. Zhang ^{62c}, X. Zhang ^{62b}, Y. Zhang ^{62c,5}, Y. Zhang ⁹⁶, Y. Zhang ^{14c}, Z. Zhang ^{17a}, Z. Zhang ⁶⁶, H. Zhao ¹³⁸, T. Zhao ^{62b}, Y. Zhao ¹³⁶, Z. Zhao ^{62a}, A. Zhemchugov ³⁸, J. Zheng ^{14c}, K. Zheng ¹⁶², X. Zheng ^{62a}, Z. Zheng ¹⁴³, D. Zhong ¹⁶², B. Zhou ¹⁰⁶, H. Zhou ⁷, N. Zhou ^{62c}, Y. Zhou ⁷, C.G. Zhu ^{62b}, J. Zhu ¹⁰⁶, Y. Zhu ^{62c}, Y. Zhu ^{62a}, X. Zhuang ^{14a}, K. Zhukov ³⁷, V. Zhulanov ³⁷, N.I. Zimine ³⁸, J. Zinsser ^{63b}, M. Ziolkowski ¹⁴¹, L. Živković ¹⁵, A. Zoccoli ^{23b,23a}, K. Zoch ⁶¹, T.G. Zorbas ¹³⁹, O. Zormpa ⁴⁶, W. Zou ⁴¹, L. Zwalinski ³⁶.

¹Department of Physics, University of Adelaide, Adelaide; Australia.

²Department of Physics, University of Alberta, Edmonton AB; Canada.

^{3(a)}Department of Physics, Ankara University, Ankara; ^(b)Division of Physics, TOBB University of Economics and Technology, Ankara; Türkiye.

⁴LAPP, Université Savoie Mont Blanc, CNRS/IN2P3, Annecy; France.

⁵APC, Université Paris Cité, CNRS/IN2P3, Paris; France.

⁶High Energy Physics Division, Argonne National Laboratory, Argonne IL; United States of America.

⁷Department of Physics, University of Arizona, Tucson AZ; United States of America.

⁸Department of Physics, University of Texas at Arlington, Arlington TX; United States of America.

⁹Physics Department, National and Kapodistrian University of Athens, Athens; Greece.

¹⁰Physics Department, National Technical University of Athens, Zografou; Greece.

¹¹Department of Physics, University of Texas at Austin, Austin TX; United States of America.

¹²Institute of Physics, Azerbaijan Academy of Sciences, Baku; Azerbaijan.

- ¹³Institut de Física d'Altes Energies (IFAE), Barcelona Institute of Science and Technology, Barcelona; Spain.
- ¹⁴(^a)Institute of High Energy Physics, Chinese Academy of Sciences, Beijing; (^b)Physics Department, Tsinghua University, Beijing; (^c)Department of Physics, Nanjing University, Nanjing; (^d)School of Science, Shenzhen Campus of Sun Yat-sen University; (^e)University of Chinese Academy of Science (UCAS), Beijing; China.
- ¹⁵Institute of Physics, University of Belgrade, Belgrade; Serbia.
- ¹⁶Department for Physics and Technology, University of Bergen, Bergen; Norway.
- ¹⁷(^a)Physics Division, Lawrence Berkeley National Laboratory, Berkeley CA; (^b)University of California, Berkeley CA; United States of America.
- ¹⁸Institut für Physik, Humboldt Universität zu Berlin, Berlin; Germany.
- ¹⁹Albert Einstein Center for Fundamental Physics and Laboratory for High Energy Physics, University of Bern, Bern; Switzerland.
- ²⁰School of Physics and Astronomy, University of Birmingham, Birmingham; United Kingdom.
- ²¹(^a)Department of Physics, Bogazici University, Istanbul; (^b)Department of Physics Engineering, Gaziantep University, Gaziantep; (^c)Department of Physics, Istanbul University, Istanbul; Türkiye.
- ²²(^a)Facultad de Ciencias y Centro de Investigaciones, Universidad Antonio Nariño, Bogotá; (^b)Departamento de Física, Universidad Nacional de Colombia, Bogotá; (^c)Pontificia Universidad Javeriana, Bogota; Colombia.
- ²³(^a)Dipartimento di Fisica e Astronomia A. Righi, Università di Bologna, Bologna; (^b)INFN Sezione di Bologna; Italy.
- ²⁴Physikalisches Institut, Universität Bonn, Bonn; Germany.
- ²⁵Department of Physics, Boston University, Boston MA; United States of America.
- ²⁶Department of Physics, Brandeis University, Waltham MA; United States of America.
- ²⁷(^a)Transilvania University of Brasov, Brasov; (^b)Horia Hulubei National Institute of Physics and Nuclear Engineering, Bucharest; (^c)Department of Physics, Alexandru Ioan Cuza University of Iasi, Iasi; (^d)National Institute for Research and Development of Isotopic and Molecular Technologies, Physics Department, Cluj-Napoca; (^e)University Politehnica Bucharest, Bucharest; (^f)West University in Timisoara, Timisoara; (^g)Faculty of Physics, University of Bucharest, Bucharest; Romania.
- ²⁸(^a)Faculty of Mathematics, Physics and Informatics, Comenius University, Bratislava; (^b)Department of Subnuclear Physics, Institute of Experimental Physics of the Slovak Academy of Sciences, Kosice; Slovak Republic.
- ²⁹Physics Department, Brookhaven National Laboratory, Upton NY; United States of America.
- ³⁰Universidad de Buenos Aires, Facultad de Ciencias Exactas y Naturales, Departamento de Física, y CONICET, Instituto de Física de Buenos Aires (IFIBA), Buenos Aires; Argentina.
- ³¹California State University, CA; United States of America.
- ³²Cavendish Laboratory, University of Cambridge, Cambridge; United Kingdom.
- ³³(^a)Department of Physics, University of Cape Town, Cape Town; (^b)iThemba Labs, Western Cape; (^c)Department of Mechanical Engineering Science, University of Johannesburg, Johannesburg; (^d)National Institute of Physics, University of the Philippines Diliman (Philippines); (^e)University of South Africa, Department of Physics, Pretoria; (^f)University of Zululand, KwaDlangezwa; (^g)School of Physics, University of the Witwatersrand, Johannesburg; South Africa.
- ³⁴Department of Physics, Carleton University, Ottawa ON; Canada.
- ³⁵(^a)Faculté des Sciences Ain Chock, Réseau Universitaire de Physique des Hautes Energies - Université Hassan II, Casablanca; (^b)Faculté des Sciences, Université Ibn-Tofail, Kénitra; (^c)Faculté des Sciences Semlalia, Université Cadi Ayyad, LPHEA-Marrakech; (^d)LPMR, Faculté des Sciences, Université Mohamed Premier, Oujda; (^e)Faculté des sciences, Université Mohammed V, Rabat; (^f)Institute of Applied

Physics, Mohammed VI Polytechnic University, Ben Guerir; Morocco.

³⁶CERN, Geneva; Switzerland.

³⁷Affiliated with an institute covered by a cooperation agreement with CERN.

³⁸Affiliated with an international laboratory covered by a cooperation agreement with CERN.

³⁹Enrico Fermi Institute, University of Chicago, Chicago IL; United States of America.

⁴⁰LPC, Université Clermont Auvergne, CNRS/IN2P3, Clermont-Ferrand; France.

⁴¹Nevis Laboratory, Columbia University, Irvington NY; United States of America.

⁴²Niels Bohr Institute, University of Copenhagen, Copenhagen; Denmark.

⁴³(^a)Dipartimento di Fisica, Università della Calabria, Rende; (^b)INFN Gruppo Collegato di Cosenza, Laboratori Nazionali di Frascati; Italy.

⁴⁴Physics Department, Southern Methodist University, Dallas TX; United States of America.

⁴⁵Physics Department, University of Texas at Dallas, Richardson TX; United States of America.

⁴⁶National Centre for Scientific Research "Demokritos", Agia Paraskevi; Greece.

⁴⁷(^a)Department of Physics, Stockholm University; (^b)Oskar Klein Centre, Stockholm; Sweden.

⁴⁸Deutsches Elektronen-Synchrotron DESY, Hamburg and Zeuthen; Germany.

⁴⁹Fakultät Physik , Technische Universität Dortmund, Dortmund; Germany.

⁵⁰Institut für Kern- und Teilchenphysik, Technische Universität Dresden, Dresden; Germany.

⁵¹Department of Physics, Duke University, Durham NC; United States of America.

⁵²SUPA - School of Physics and Astronomy, University of Edinburgh, Edinburgh; United Kingdom.

⁵³INFN e Laboratori Nazionali di Frascati, Frascati; Italy.

⁵⁴Physikalisches Institut, Albert-Ludwigs-Universität Freiburg, Freiburg; Germany.

⁵⁵II. Physikalisches Institut, Georg-August-Universität Göttingen, Göttingen; Germany.

⁵⁶Département de Physique Nucléaire et Corpusculaire, Université de Genève, Genève; Switzerland.

⁵⁷(^a)Dipartimento di Fisica, Università di Genova, Genova; (^b)INFN Sezione di Genova; Italy.

⁵⁸II. Physikalisches Institut, Justus-Liebig-Universität Giessen, Giessen; Germany.

⁵⁹SUPA - School of Physics and Astronomy, University of Glasgow, Glasgow; United Kingdom.

⁶⁰LPSC, Université Grenoble Alpes, CNRS/IN2P3, Grenoble INP, Grenoble; France.

⁶¹Laboratory for Particle Physics and Cosmology, Harvard University, Cambridge MA; United States of America.

⁶²(^a)Department of Modern Physics and State Key Laboratory of Particle Detection and Electronics, University of Science and Technology of China, Hefei; (^b)Institute of Frontier and Interdisciplinary Science and Key Laboratory of Particle Physics and Particle Irradiation (MOE), Shandong University, Qingdao; (^c)School of Physics and Astronomy, Shanghai Jiao Tong University, Key Laboratory for Particle Astrophysics and Cosmology (MOE), SKLPPC, Shanghai; (^d)Tsung-Dao Lee Institute, Shanghai; (^e)School of Physics and Microelectronics, Zhengzhou University; China.

⁶³(^a)Kirchhoff-Institut für Physik, Ruprecht-Karls-Universität Heidelberg, Heidelberg; (^b)Physikalisches Institut, Ruprecht-Karls-Universität Heidelberg, Heidelberg; Germany.

⁶⁴(^a)Department of Physics, Chinese University of Hong Kong, Shatin, N.T., Hong Kong; (^b)Department of Physics, University of Hong Kong, Hong Kong; (^c)Department of Physics and Institute for Advanced Study, Hong Kong University of Science and Technology, Clear Water Bay, Kowloon, Hong Kong; China.

⁶⁵Department of Physics, National Tsing Hua University, Hsinchu; Taiwan.

⁶⁶IJCLab, Université Paris-Saclay, CNRS/IN2P3, 91405, Orsay; France.

⁶⁷Centro Nacional de Microelectrónica (IMB-CNM-CSIC), Barcelona; Spain.

⁶⁸Department of Physics, Indiana University, Bloomington IN; United States of America.

⁶⁹(^a)INFN Gruppo Collegato di Udine, Sezione di Trieste, Udine; (^b)ICTP, Trieste; (^c)Dipartimento Politecnico di Ingegneria e Architettura, Università di Udine, Udine; Italy.

⁷⁰(^a)INFN Sezione di Lecce; (^b)Dipartimento di Matematica e Fisica, Università del Salento, Lecce; Italy.

- 71^(a) INFN Sezione di Milano;^(b) Dipartimento di Fisica, Università di Milano, Milano; Italy.
- 72^(a) INFN Sezione di Napoli;^(b) Dipartimento di Fisica, Università di Napoli, Napoli; Italy.
- 73^(a) INFN Sezione di Pavia;^(b) Dipartimento di Fisica, Università di Pavia, Pavia; Italy.
- 74^(a) INFN Sezione di Pisa;^(b) Dipartimento di Fisica E. Fermi, Università di Pisa, Pisa; Italy.
- 75^(a) INFN Sezione di Roma;^(b) Dipartimento di Fisica, Sapienza Università di Roma, Roma; Italy.
- 76^(a) INFN Sezione di Roma Tor Vergata;^(b) Dipartimento di Fisica, Università di Roma Tor Vergata, Roma; Italy.
- 77^(a) INFN Sezione di Roma Tre;^(b) Dipartimento di Matematica e Fisica, Università Roma Tre, Roma; Italy.
- 78^(a) INFN-TIFPA;^(b) Università degli Studi di Trento, Trento; Italy.
- 79 Universität Innsbruck, Department of Astro and Particle Physics, Innsbruck; Austria.
- 80 University of Iowa, Iowa City IA; United States of America.
- 81 Department of Physics and Astronomy, Iowa State University, Ames IA; United States of America.
- 82 Istinye University, Sariyer, Istanbul; Türkiye.
- 83^(a) Departamento de Engenharia Elétrica, Universidade Federal de Juiz de Fora (UFJF), Juiz de Fora;^(b) Universidade Federal do Rio De Janeiro COPPE/EE/IF, Rio de Janeiro;^(c) Instituto de Física, Universidade de São Paulo, São Paulo;^(d) Rio de Janeiro State University, Rio de Janeiro; Brazil.
- 84 KEK, High Energy Accelerator Research Organization, Tsukuba; Japan.
- 85 Graduate School of Science, Kobe University, Kobe; Japan.
- 86^(a) AGH University of Krakow, Faculty of Physics and Applied Computer Science, Krakow;^(b) Marian Smoluchowski Institute of Physics, Jagiellonian University, Krakow; Poland.
- 87 Institute of Nuclear Physics Polish Academy of Sciences, Krakow; Poland.
- 88 Faculty of Science, Kyoto University, Kyoto; Japan.
- 89 Research Center for Advanced Particle Physics and Department of Physics, Kyushu University, Fukuoka ; Japan.
- 90 Instituto de Física La Plata, Universidad Nacional de La Plata and CONICET, La Plata; Argentina.
- 91 Physics Department, Lancaster University, Lancaster; United Kingdom.
- 92 Oliver Lodge Laboratory, University of Liverpool, Liverpool; United Kingdom.
- 93 Department of Experimental Particle Physics, Jožef Stefan Institute and Department of Physics, University of Ljubljana, Ljubljana; Slovenia.
- 94 School of Physics and Astronomy, Queen Mary University of London, London; United Kingdom.
- 95 Department of Physics, Royal Holloway University of London, Egham; United Kingdom.
- 96 Department of Physics and Astronomy, University College London, London; United Kingdom.
- 97 Louisiana Tech University, Ruston LA; United States of America.
- 98 Fysiska institutionen, Lunds universitet, Lund; Sweden.
- 99 Departamento de Física Teórica C-15 and CIAFF, Universidad Autónoma de Madrid, Madrid; Spain.
- 100 Institut für Physik, Universität Mainz, Mainz; Germany.
- 101 School of Physics and Astronomy, University of Manchester, Manchester; United Kingdom.
- 102 CPPM, Aix-Marseille Université, CNRS/IN2P3, Marseille; France.
- 103 Department of Physics, University of Massachusetts, Amherst MA; United States of America.
- 104 Department of Physics, McGill University, Montreal QC; Canada.
- 105 School of Physics, University of Melbourne, Victoria; Australia.
- 106 Department of Physics, University of Michigan, Ann Arbor MI; United States of America.
- 107 Department of Physics and Astronomy, Michigan State University, East Lansing MI; United States of America.
- 108 Group of Particle Physics, University of Montreal, Montreal QC; Canada.
- 109 Fakultät für Physik, Ludwig-Maximilians-Universität München, München; Germany.

- ¹¹⁰Max-Planck-Institut für Physik (Werner-Heisenberg-Institut), München; Germany.
- ¹¹¹Graduate School of Science and Kobayashi-Maskawa Institute, Nagoya University, Nagoya; Japan.
- ¹¹²Department of Physics and Astronomy, University of New Mexico, Albuquerque NM; United States of America.
- ¹¹³Institute for Mathematics, Astrophysics and Particle Physics, Radboud University/Nikhef, Nijmegen; Netherlands.
- ¹¹⁴Nikhef National Institute for Subatomic Physics and University of Amsterdam, Amsterdam; Netherlands.
- ¹¹⁵Department of Physics, Northern Illinois University, DeKalb IL; United States of America.
- ¹¹⁶(^a)New York University Abu Dhabi, Abu Dhabi;(^b)University of Sharjah, Sharjah; United Arab Emirates.
- ¹¹⁷Department of Physics, New York University, New York NY; United States of America.
- ¹¹⁸Ochanomizu University, Otsuka, Bunkyo-ku, Tokyo; Japan.
- ¹¹⁹Ohio State University, Columbus OH; United States of America.
- ¹²⁰Homer L. Dodge Department of Physics and Astronomy, University of Oklahoma, Norman OK; United States of America.
- ¹²¹Department of Physics, Oklahoma State University, Stillwater OK; United States of America.
- ¹²²Palacký University, Joint Laboratory of Optics, Olomouc; Czech Republic.
- ¹²³Institute for Fundamental Science, University of Oregon, Eugene, OR; United States of America.
- ¹²⁴Graduate School of Science, Osaka University, Osaka; Japan.
- ¹²⁵Department of Physics, University of Oslo, Oslo; Norway.
- ¹²⁶Department of Physics, Oxford University, Oxford; United Kingdom.
- ¹²⁷LPNHE, Sorbonne Université, Université Paris Cité, CNRS/IN2P3, Paris; France.
- ¹²⁸Department of Physics, University of Pennsylvania, Philadelphia PA; United States of America.
- ¹²⁹Department of Physics and Astronomy, University of Pittsburgh, Pittsburgh PA; United States of America.
- ¹³⁰(^a)Laboratório de Instrumentação e Física Experimental de Partículas - LIP, Lisboa;(^b)Departamento de Física, Faculdade de Ciências, Universidade de Lisboa, Lisboa;(^c)Departamento de Física, Universidade de Coimbra, Coimbra;(^d)Centro de Física Nuclear da Universidade de Lisboa, Lisboa;(^e)Departamento de Física, Universidade do Minho, Braga;(^f)Departamento de Física Teórica y del Cosmos, Universidad de Granada, Granada (Spain);(^g)Departamento de Física, Instituto Superior Técnico, Universidade de Lisboa, Lisboa; Portugal.
- ¹³¹Institute of Physics of the Czech Academy of Sciences, Prague; Czech Republic.
- ¹³²Czech Technical University in Prague, Prague; Czech Republic.
- ¹³³Charles University, Faculty of Mathematics and Physics, Prague; Czech Republic.
- ¹³⁴Particle Physics Department, Rutherford Appleton Laboratory, Didcot; United Kingdom.
- ¹³⁵IRFU, CEA, Université Paris-Saclay, Gif-sur-Yvette; France.
- ¹³⁶Santa Cruz Institute for Particle Physics, University of California Santa Cruz, Santa Cruz CA; United States of America.
- ¹³⁷(^a)Departamento de Física, Pontificia Universidad Católica de Chile, Santiago;(^b)Millennium Institute for Subatomic physics at high energy frontier (SAPHIR), Santiago;(^c)Instituto de Investigación Multidisciplinario en Ciencia y Tecnología, y Departamento de Física, Universidad de La Serena;(^d)Universidad Andres Bello, Department of Physics, Santiago;(^e)Instituto de Alta Investigación, Universidad de Tarapacá, Arica;(^f)Departamento de Física, Universidad Técnica Federico Santa María, Valparaíso; Chile.
- ¹³⁸Department of Physics, University of Washington, Seattle WA; United States of America.
- ¹³⁹Department of Physics and Astronomy, University of Sheffield, Sheffield; United Kingdom.

- ¹⁴⁰Department of Physics, Shinshu University, Nagano; Japan.
- ¹⁴¹Department Physik, Universität Siegen, Siegen; Germany.
- ¹⁴²Department of Physics, Simon Fraser University, Burnaby BC; Canada.
- ¹⁴³SLAC National Accelerator Laboratory, Stanford CA; United States of America.
- ¹⁴⁴Department of Physics, Royal Institute of Technology, Stockholm; Sweden.
- ¹⁴⁵Departments of Physics and Astronomy, Stony Brook University, Stony Brook NY; United States of America.
- ¹⁴⁶Department of Physics and Astronomy, University of Sussex, Brighton; United Kingdom.
- ¹⁴⁷School of Physics, University of Sydney, Sydney; Australia.
- ¹⁴⁸Institute of Physics, Academia Sinica, Taipei; Taiwan.
- ¹⁴⁹^(a)E. Andronikashvili Institute of Physics, Iv. Javakhishvili Tbilisi State University, Tbilisi;^(b)High Energy Physics Institute, Tbilisi State University, Tbilisi;^(c)University of Georgia, Tbilisi; Georgia.
- ¹⁵⁰Department of Physics, Technion, Israel Institute of Technology, Haifa; Israel.
- ¹⁵¹Raymond and Beverly Sackler School of Physics and Astronomy, Tel Aviv University, Tel Aviv; Israel.
- ¹⁵²Department of Physics, Aristotle University of Thessaloniki, Thessaloniki; Greece.
- ¹⁵³International Center for Elementary Particle Physics and Department of Physics, University of Tokyo, Tokyo; Japan.
- ¹⁵⁴Department of Physics, Tokyo Institute of Technology, Tokyo; Japan.
- ¹⁵⁵Department of Physics, University of Toronto, Toronto ON; Canada.
- ¹⁵⁶^(a)TRIUMF, Vancouver BC;^(b)Department of Physics and Astronomy, York University, Toronto ON; Canada.
- ¹⁵⁷Division of Physics and Tomonaga Center for the History of the Universe, Faculty of Pure and Applied Sciences, University of Tsukuba, Tsukuba; Japan.
- ¹⁵⁸Department of Physics and Astronomy, Tufts University, Medford MA; United States of America.
- ¹⁵⁹United Arab Emirates University, Al Ain; United Arab Emirates.
- ¹⁶⁰Department of Physics and Astronomy, University of California Irvine, Irvine CA; United States of America.
- ¹⁶¹Department of Physics and Astronomy, University of Uppsala, Uppsala; Sweden.
- ¹⁶²Department of Physics, University of Illinois, Urbana IL; United States of America.
- ¹⁶³Instituto de Física Corpuscular (IFIC), Centro Mixto Universidad de Valencia - CSIC, Valencia; Spain.
- ¹⁶⁴Department of Physics, University of British Columbia, Vancouver BC; Canada.
- ¹⁶⁵Department of Physics and Astronomy, University of Victoria, Victoria BC; Canada.
- ¹⁶⁶Fakultät für Physik und Astronomie, Julius-Maximilians-Universität Würzburg, Würzburg; Germany.
- ¹⁶⁷Department of Physics, University of Warwick, Coventry; United Kingdom.
- ¹⁶⁸Waseda University, Tokyo; Japan.
- ¹⁶⁹Department of Particle Physics and Astrophysics, Weizmann Institute of Science, Rehovot; Israel.
- ¹⁷⁰Department of Physics, University of Wisconsin, Madison WI; United States of America.
- ¹⁷¹Fakultät für Mathematik und Naturwissenschaften, Fachgruppe Physik, Bergische Universität Wuppertal, Wuppertal; Germany.
- ¹⁷²Department of Physics, Yale University, New Haven CT; United States of America.
- ^a Also Affiliated with an institute covered by a cooperation agreement with CERN.
- ^b Also at An-Najah National University, Nablus; Palestine.
- ^c Also at APC, Université Paris Cité, CNRS/IN2P3, Paris; France.
- ^d Also at Borough of Manhattan Community College, City University of New York, New York NY; United States of America.
- ^e Also at Center for High Energy Physics, Peking University; China.
- ^f Also at Center for Interdisciplinary Research and Innovation (CIRI-AUTH), Thessaloniki; Greece.

- ^g Also at Centro Studi e Ricerche Enrico Fermi; Italy.
- ^h Also at CERN Tier-0; Switzerland.
- ⁱ Also at CERN, Geneva; Switzerland.
- ^j Also at Département de Physique Nucléaire et Corpusculaire, Université de Genève, Genève; Switzerland.
- ^k Also at Departament de Física de la Universitat Autònoma de Barcelona, Barcelona; Spain.
- ^l Also at Department of Financial and Management Engineering, University of the Aegean, Chios; Greece.
- ^m Also at Department of Physics and Astronomy, University of Sheffield, Sheffield; United Kingdom.
- ⁿ Also at Department of Physics and Astronomy, University of Victoria, Victoria BC; Canada.
- ^o Also at Department of Physics, Ben Gurion University of the Negev, Beer Sheva; Israel.
- ^p Also at Department of Physics, California State University, Sacramento; United States of America.
- ^q Also at Department of Physics, King's College London, London; United Kingdom.
- ^r Also at Department of Physics, Oxford University, Oxford; United Kingdom.
- ^s Also at Department of Physics, Royal Holloway University of London, Egham; United Kingdom.
- ^t Also at Department of Physics, Stanford University, Stanford CA; United States of America.
- ^u Also at Department of Physics, University of Fribourg, Fribourg; Switzerland.
- ^v Also at Department of Physics, University of Massachusetts, Amherst MA; United States of America.
- ^w Also at Department of Physics, University of Thessaly; Greece.
- ^x Also at Department of Physics, Westmont College, Santa Barbara; United States of America.
- ^y Also at Deutsches Elektronen-Synchrotron DESY, Hamburg and Zeuthen; Germany.
- ^z Also at Fakultät Physik , Technische Universität Dortmund, Dortmund; Germany.
- ^{aa} Also at Fakultät für Mathematik und Naturwissenschaften, Fachgruppe Physik, Bergische Universität Wuppertal, Wuppertal; Germany.
- ^{ab} Also at Group of Particle Physics, University of Montreal, Montreal QC; Canada.
- ^{ac} Also at Hellenic Open University, Patras; Greece.
- ^{ad} Also at Institutio Catalana de Recerca i Estudis Avancats, ICREA, Barcelona; Spain.
- ^{ae} Also at Institut für Experimentalphysik, Universität Hamburg, Hamburg; Germany.
- ^{af} Also at Institut für Physik, Universität Mainz, Mainz; Germany.
- ^{ag} Also at Institute for Nuclear Research and Nuclear Energy (INRNE) of the Bulgarian Academy of Sciences, Sofia; Bulgaria.
- ^{ah} Also at Institute of Applied Physics, Mohammed VI Polytechnic University, Ben Guerir; Morocco.
- ^{ai} Also at Institute of Particle Physics (IPP); Canada.
- ^{aj} Also at Institute of Physics and Technology, Ulaanbaatar; Mongolia.
- ^{ak} Also at Institute of Physics, Azerbaijan Academy of Sciences, Baku; Azerbaijan.
- ^{al} Also at Institute of Theoretical Physics, Ilia State University, Tbilisi; Georgia.
- ^{am} Also at IRFU, CEA, Université Paris-Saclay, Gif-sur-Yvette; France.
- ^{an} Also at L2IT, Université de Toulouse, CNRS/IN2P3, UPS, Toulouse; France.
- ^{ao} Also at Lawrence Livermore National Laboratory, Livermore; United States of America.
- ^{ap} Also at National Institute of Physics, University of the Philippines Diliman (Philippines); Philippines.
- ^{aq} Also at School of Physics and Astronomy, University of Birmingham, Birmingham; United Kingdom.
- ^{ar} Also at School of Physics and Astronomy, University of Manchester, Manchester; United Kingdom.
- ^{as} Also at SUPA - School of Physics and Astronomy, University of Glasgow, Glasgow; United Kingdom.
- ^{at} Also at Technical University of Munich, Munich; Germany.
- ^{au} Also at The Collaborative Innovation Center of Quantum Matter (CICQM), Beijing; China.
- ^{av} Also at TRIUMF, Vancouver BC; Canada.
- ^{aw} Also at Università di Napoli Parthenope, Napoli; Italy.
- ^{ax} Also at University of Chinese Academy of Sciences (UCAS), Beijing; China.

ay Also at University of Colorado Boulder, Department of Physics, Colorado; United States of America.

az Also at Washington College, Chestertown, MD; United States of America.

ba Also at Yeditepe University, Physics Department, Istanbul; Türkiye.

* Deceased